The Color of Lobsters

Wijk, A. van

The Color of Lobsters

The Bathochromic Shift of Astaxanthin in α-Crustacyanin

Arjan van Wijk

The Color of Lobsters

The Bathochromic Shift of Astaxanthin in α-Crustacyanin

Proefschrift

Ter verkrijging van de graad van Doctor aan de Universiteit Leiden,
op gezag van de Rector Magnificus Dr. D.D. Breimer,
hoogleraar in de faculteit der Wiskunde en Natuurwetenschappen en die der Geneeskunde,
volgens besluit van het College voor Promoties te verdedigen op
woensdag 15 juni 2005
klokke 15.15 uur

door

Adrianus Antonius Cornelius van Wijk
geboren te Bunnik
in 1976

PROMOTIECOMMISSIE

Promotores:	Prof. dr. J. Lugtenburg
	Prof. dr. H.J.M. de Groot
Referent:	Prof. dr. J. Cornelisse
Overige Leden:	Prof. dr. J. Brouwer
	Prof. dr. A.P.G. Kieboom
	Prof. dr. H.S. Overkleeft
	Dr. F. Buda

CONTENTS

CHAPTER 1

GENERAL INTRODUCTION

1.1 CAROTENOIDS

Carotenoids constitute a class of widespread unsaturated tetraterpenes with important biological functions. Over 600 carotenoids with different structures have been isolated from natural sources.[1] Carotenoids are well-known as natural colorants, ranging in color from yellow, orange and red to deep purple.[2,3] The color and other properties of carotenoids are closely related to their structure. The long conjugated polyene chain of the carotenoids is responsible for the absorption of visible light, giving carotenoids their vivid colors. Some examples of carotenoids are given in Figure 1.

The ability to produce carotenoids *de novo* was developed at an early stage in evolution. Only the chloroplasts in plant cells, algae, cyanobacteria and some other micro-organisms have this capability.[4,5] Isopentenyl diphosphate is the universal precursor of all isoprenoids, including carotenoids. Recently it was found that the biosynthetic route of carotenoids in many bacteria, some unicellular green algae and in the plant chloroplasts is different from the route for all other isoprenoids.[4,6]

Carotenes are a subclass of carotenoids that are built from carbon and hydrogen only. Lycopene, the red pigment of the tomato, is the first deeply colored carotene resulting from biosynthesis. Enzymatic conversion of lycopene results in β-carotene with two six-membered ring end groups. Via enzymatic reactions various oxygen containing groups may be introduced leading to the subclass of carotenoids called xanthophylls, of which canthaxanthin and astaxanthin are examples.

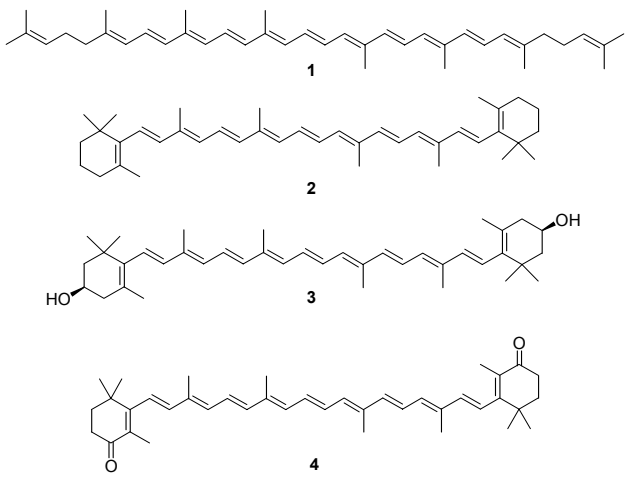

Figure 1. *Examples of carotenoids; lycopene (**1**), β-carotene (**2**), (3R,3R')-zeaxanthin (**3**) and canthaxanthin (**4**).*

In plants further chemical conversion takes place leading to apocarotenoids that have shorter carbon skeletons. Many aroma compounds of flowers and fruit are apocarotenoids derived from carotenoids.[7]

An essential function of carotenoids in plants is related to the conjugated polyene chain, which makes carotenoids effective quenchers of excited triplet states and traps of radicals.[8,9] Both the photosynthetic reaction centers I and II in plants and the reaction centers in bacteria contain a tightly bound carotenoid that quenches the triplet states that are formed as side products during photosynthesis and prevents the formation of destructive singlet oxygen. Without this protection the photosynthetic reaction centers are destroyed and photosynthesis, essential for life on earth, will not take place. This is demonstrated when plants are treated with herbicides that prevent carotenoid biosynthesis. Exposure to light leads to complete destruction of these plants.[10]

Animals and man cannot produce carotenoids *de novo* and depend on carotenoids present in their diet. Knowledge of the role of carotenoids in various aspects of the life processes in man and animals is increasing at a rapid rate. Observational studies have shown quite consistently a reduced risk of cancer in individuals with a high intake of carotenoids or high carotenoid concentrations in blood.[11,12] β-Carotene has been the most studied carotenoid for its role in cancer prevention, but recently also other carotenoids that are present in our daily food are investigated.[13-19] Since carotenoids play a role in the protection against reactive oxygen, carotenoids, mainly β-carotene, are studied for their role in prevention of damaging effects of UV-light on the skin, such as sunburn, skin aging and skin cancer.[20-23] In recent epidemiological studies, an inverse correlation was found between β-carotene concentrations in serum and the risk of developing cardiovascular disease. Even though several risk factors play a role in the mechanism leading to this disease, it appears that carotenoids play a role in the prevention of cardiovascular disease, and these compounds are therefore of great interest for further study.[11]

In animals and humans, carotenoids play an important role as vitamin A precursors. Vitamin A, also known as retinol, is vital for growth, development and vision.[24] The daily advised intake of vitamin A is about 1.2 mg per day. Insufficient vitamin A intake leads very rapidly to health problems. This is dramatically demonstrated by the fact that annually about 10 million children in developing countries become blind and subsequently die due to vitamin A deficiency.[25-27] Furthermore, recent research suggests that carotenoids reduce the risk of age-related macular degeneration and cataract, the leading causes of blindness in the western world. [11,28-34]

Another role of carotenoids is found in reproduction and fertility. Although the precise role and actions of carotenoids in reproduction is not clear yet, there have been many reports over the years of a positive effect of carotenoids on fertility and reproductive capacity in animals, such as chickens and flamingos.[35]

Since carotenoids have a beneficial effect on health, but cannot be produced *de novo* in humans and animals, carotenoids are of great commercial interest as food and feed additives.

Many carotenoids are commercially available and are industrially produced at multi-ton scale via total organic synthesis by DSM and BASF,[36-39] or made by algae or yeasts in large-scale bioreactors.[40-42] For example, *Haematococcus pluvialis,* which is responsible for the striking red color of so-called 'blood rain', and *Haematococcus nivalis,* the red color of 'blood snow', are cultivated in large-scale bioreactors for the isolation of astaxanthin as a source for salmon and trout farming.[43-46]

Carotenoids are also widely used as human food colorants, for which their non-toxicity and bright colors make them well suitable. Examples of carotenoids as food colorants are β-carotene in margarine, snacks, juices, cheese and ice cream.

1.2 STUDY OF THE BLUE LOBSTER CAROTENOPROTEIN α-CRUSTACYANIN

In nature, many carotenoids are non-covalently bound to proteins. Proteins with stoichiometrically bound carotenoids are known as carotenoproteins.[47,48] A large class of carotenoproteins is found in marine animals, particularly the crustacea.[49] Most of these colored protein complexes contain an astaxanthin chromophore which is shown in Figure 2. This C_{40}-carotenoid has the same carbon skeleton as β-carotene, with two six-membered end-rings. In addition astaxanthin contains two carbonyl groups at the 4,4-positions and two hydroxyl groups at the 3,3'-positions. The hydroxyl groups induce chirality of the molecule. In nature all stereoisomers (*RR*', *SS*' and *RS*') have been found, although (3*S*,3'*S*)-astaxanthin is most common.[50] The presence of the carbonyl and hydroxyl groups in conjugation with the polyene chain cause a shift of color of astaxanthin relative to β-carotene. β-Carotene is orange with λ_{max} = 450 nm in *n*-hexane whereas astaxanthine has a deep red color with λ_{max} = 469 nm in *n*-hexane.[51]

Binding of carotenoids to proteins can also induce a shift in the absorption maximum of the bound carotenoid. Protein complexes with colors ranging from yellow to deep blue have been described.[48] A widely studied protein complex is α-crustacyanin, the carotenoprotein that is responsible for the dark blue color of the carapace of the lobster *Homarus gammarus*, also known as the European or North Sea lobster. Upon heat treatment the dark blue protein complex, with a λ_{max} of 632 nm, denatures and astaxanthin is released, resulting in a color change of the lobster from dark blue to deep red. The large bathochromic shift in the absorption

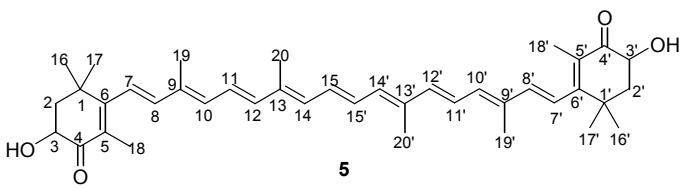

5

Figure 2. *Structure and numbering of astaxanthin.*

spectrum of astaxanthin upon binding (163 nm; 5500 cm^{-1}) is the largest shift known to occur upon binding of a chromophore with a protein.

A similar shift as for α-crustacyanin can be seen for the slightly grey colored North Sea shrimp *Crangon crangon*, which appears almost colorless to humans, as the λ_{max} of the carotenoprotein is outside the spectrum that can be detected by the human eye. Upon heating, the protein denatures and the carotenoid is released, yielding the familiar reddish color.

The original interest in α-crustacyanin arose from the similarity of the spectral shift of astaxanthin in α-crustacyanin to that of retinal in the rod visual pigment rhodopsin.[52] Rhodopsin serves as a paradigm for the superfamily of seven transmembrane helix G-protein coupled receptors (GPCRs).[53] The GPCRs mediate a broad array of important physiological and pharmaceutical signal transduction processes that involve signaling by neurotransmitters, hormones and neuropeptides.[54] In rhodopsin the retinal ligand is covalently bound by a protonated Schiff base linkage, and the magnitude of the spectral shift is regulated by side-chain counterions.[55,56]

α-Crustacyanin belongs to the lipocalin superfamily, comprising over 20 different proteins which bind small lipophilic ligands.[57,58] In contrast to rhodopsin, the carotenoids in α-crustacyanin are attached non-covalently. Furthermore, α-crustacyanin contains a β-barrel formed from β-pleated sheets with apolar amino acid residues, instead of the trans-membrane seven-helix structure in the retinal-binding proteins.

Understanding the mechanism of the color shift and the interactions between the carotenoid and the protein will give information on how the proteins of the lipocalin superfamily specifically bind their ligands. This information can be compared with the binding of retinal in rhodopsins.

It is now known that α-crustacyanin is a 320 kDa water-soluble carotenoprotein complex which consists of an octamer of dimers. Each dimer consists of two polypeptide subunits of about 20 kDa, containing two astaxanthins.[48-60] The dimer is also known as β-crustacyanin, and has a purple color, with λ_{max} = 586 nm. The absorption spectra of α-crustacyanin, β-crustacyanin and astaxanthin are shown in Figure 3.

A model for the dimer was proposed by Zagalsky et al.[61-63] and recently refined by X-ray studies, as shown in Figure 4.[64] No X-ray analysis of α-crustacyanin is known as yet, but the study of β-crustacyanin gave useful information on the structure of the subunits and the binding site of the carotenoid.[65]

It was found that the subunits have a tertiary structure resembling other members of the lipocalin superfamily. Both subunits of the dimer contain a β-barrel, consisting of two distinct β-sheets. The β-barrel has a calyx shape, with the open ends of each calyx facing each other, forming a cavity that contains the chromophore. The two bound astaxanthins interpenetrate the interface between the subunits, each subunit containing half of each carotenoid.[66]

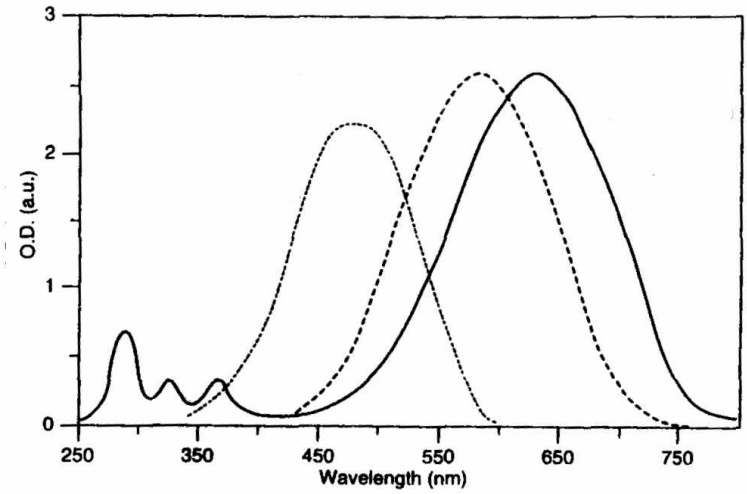

Figure 3. *UV-Vis absorption spectra of astaxanthin (·····), β-crustacyanin (-----) and α-crustacyanin (——). (after Britton et al.[69]).*

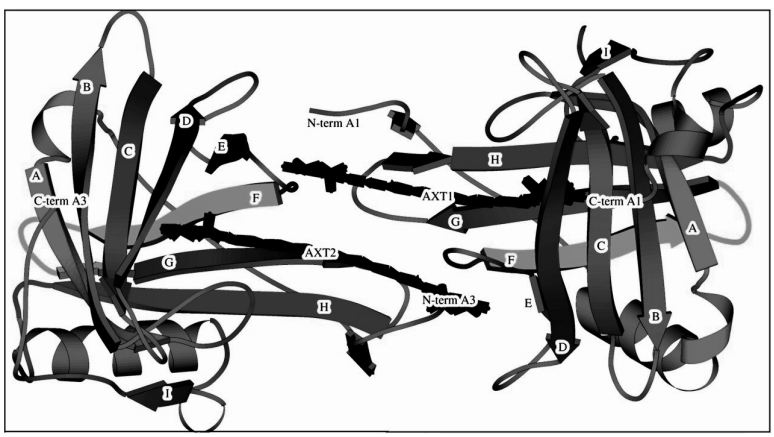

Figure 4. *X-ray model of β-crustacyanin with the chromophores (AXT1 and AXT2) located in the central cavity between the subunits.*

Astaxanthin can be extracted from the purified protein complex and the colorless apoprotein can be reconstituted with chemically modified astaxanthins.[67,68] Reconstitution studies with modified chromophores have established essential structural characteristics required for binding.[69] In general, only a minor variation in the overall shape and size of the chromophore is tolerated for binding. It was found that the presence of both 20 and 20'-methyl groups is essential for reconstitution. Also the two 4,4'-carbonyl groups are necessary for binding. Only if both carbonyl groups are in conjugation with the polyene chain a blue protein complex can be formed.

In contrast, the hydroxyl groups at positions 3 and 3′ are not essential for binding. In particular, canthaxanthin (**4**) also binds to give a blue carotenoprotein.[50]

For over 50 years scientists have devoted their attention to understanding the fundamental basis of the bathochromic shift, but the precise mechanism that could account for such a large color shift is still a matter of debate.

In a seminal paper, Buchwald and Jencks reported that α-crustacyanin can be irreversibly dissociated in eight β-crustacyanin units.[49,70] Every β-crustacyanin consists of two apoprotein units and two bound astaxanthin units. The visible, optical rotary dispersion and circular dichroism (CD) spectra of α- and β-crustacyanin show evidence for a splitting of the excitation which is in line with exciton theory. Among the possible mechanisms for the perturbed optical properties of astaxanthin in α-crustacyanin it was suggested that intermolecular interactions of the π-electron systems and/or distortion such as twisted double bonds induced by the protein may play a role.[49]

The subsequent resonance Raman spectroscopy of α-crustacyanin by Carey et al. indicated that the astaxanthin chromophore shows no distortion due to twists in the double bonds of the conjugated system and is in agreement with free relaxed carotenes.[49] On the basis of this resonance Raman study the hypothesis of the exciton mechanism was discarded and it was concluded that the bathochromic shift is caused by a charge polarization mechanism possibly induced by charged groups and/or by hydrogen bonds in the binding site.[49]

Weesie et al. used the combination of selective isotope enrichment, ^{13}C magic angle spinning (MAS) solid-state NMR and semi-empirical quantum chemical modeling to analyze the ligand-protein interactions, associated with the bathochromic shift of astaxanthin in α-crustacyanin. In this work, ^{13}C-enriched astaxanthins were prepared by total organic synthesis,[71,72] reconstituted into the protein and analyzed by ^{13}C CP/MAS NMR. Although α-crustacyanin is a water-soluble protein, it is too large to be analyzed by solution NMR techniques. Solution NMR spectra show broad and diffuse signals, due to relatively slow movement of the large protein in solution.

The presence of ^{13}C labels at specific positions in astaxanthin, increases the NMR signal of these C-atoms by a factor 90. This makes it possible to distinguish these signals from protein background response, and to obtain the chemical shifts for the enriched ^{13}C nuclei.

Spectra of α-crustacyanin were obtained after reconstitution with $^{13}C_2$-labeled astaxanthins with ^{13}C enrichment at positions 4,4′, 12,12′, 13,13′, 14,14′, 15,15′ or 20,20′.[73] The chemical shift data were compared with the ^{13}C NMR data of astaxanthin in solution. The ^{13}C MAS NMR studies reveal substantial downfield shifts at C-atoms 12,12′ and 14,14′ when astaxanthin is bound in α-crustacyanin. Small upfield shifts were observed at 13,13′ and 15,15′. The results show an unequal perturbation of both halves of the chromophore after binding. However, the main perturbation is of symmetrical origin, since the chemical shift differences show a symmetrical pattern in both halves of the chromophore.[74,75]

These experiments provide a strong indication that, when excitonic interactions are excluded, charge polarization is essential to explain the observed bathochromic shift. The NMR shifts and

color shift were compared with calculated charge densities of several protein-ligand models. The initial NMR results could be reconciled with a mechanism in which astaxanthin is considerably charged and subject to electrostatic polarization originating from both keto groups. This hypothesis was in line with computational studies[76,77] and Stark spectroscopy.[78]

Specific ^{13}C labeling of the chromophore gives information on the contribution of distinct vibrations to the vibrational lines in the Raman spectrum and on the geometry of the electronic ground state and excited states of the chromophore in α-crustacyanin.[76,77,79] Resonance Raman spectroscopy is an important technique for probing the vibrational properties of carotenoids. The frequency of the vibrational bands is a property of the electronic ground state of the system, while the intensity of the bands is a property of the geometry of both the ground state and the excited electronic states. Resonance Raman spectroscopy can be applied to dilute samples and is therefore very suitable for the study of a chromophore in a biological system. By using a laser excitation wavelength that corresponds to the electronic transition of the molecule in the visible absorption region, the vibrational levels of the molecule are dramatically increased. Some Raman lines can be enhanced by a factor of about 10^5.

The effect of ^{13}C labeling in resonance Raman experiments is visible by a shift of the vibrational bands. Since the vibration depends on the mass of the atoms, the substitution of ^{12}C by ^{13}C shifts the vibrational frequencies. In addition, coupled modes can be decoupled due to ^{13}C enrichment.

The resonance Raman studies of ^{13}C-labeled astaxanthins and the corresponding ^{13}C-labeled crustacyanins show that upon binding to the protein the Raman spectrum of astaxanthin is changed. Bands are shifted, intensity is redistributed and new lines appear. Since the position of the bands is determined by the electronic ground state and the intensity of the bands by both the electronic ground state and excited states of the chromophore, the spectra indicate that the geometries of both the electronic ground state and the excited state of astaxanthin change upon binding.[76,77]

In spite of the considerable progress made in structural and spectroscopic studies, a clear converging picture on the dominant mechanism for the bathochromic shift in crustacyanin is still missing. There are two main hypotheses that are still debated: (i) the "on-site" (intramolecular) mechanism involving protein induced conformational changes and/or charge-polarization effects modifying the electronic ground state of the chromophore; (ii) the aggregation (intermolecular) mechanism due to the interaction of the chromophores in the subunits of crustacyanin inducing an exciton coupling of the transition dipole moments in the excited state.

In order to resolve the precise molecular basis of the coloration mechanism of α-crustacyanin we used ^{13}C-labeled astaxanthins as chromophores for solid-state ^{13}C NMR and resonance Raman spectroscopy of [6,6′,7,7′]-$^{13}C_4$ α-crustacyanin and [8,8',9,9',10,10',11,11',20,20']-$^{13}C_{10}$ α-crustacyanin, establishing the electronic charge distribution and vibrational contribution of the remaining sp^2-carbon atoms. Figure 5 shows the structure and numbering of the all-*E*

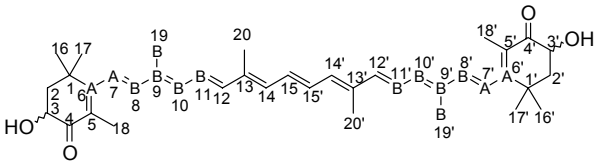

Figure 5. *Molecular structure and IUPAC numbering of synthetic all-E astaxanthin as a mixture of 25% (3R,3'R), 25% (3S,3'S) and 50% (3R,3'S).*

A = ^{13}C for [6,6',7,7']-$^{13}C_4$ all-E astaxanthin
B = ^{13}C for [8,8',9,9',10,10',11,11',19,19']-$^{13}C_{10}$ all-E astaxanthin.

astaxanthin chromophore. The position of the ^{13}C enrichment is marked with (A) for [6,6',7,7']-$^{13}C_4$ astaxanthin and with (B) for [8,8',9,9',10,10',11,11',19,19']-$^{13}C_{10}$ astaxanthin.

We complement the spectroscopic data with quantum mechanical calculations of the electronic ground state and excitation energies of various astaxanthin models based on the structural information available for β-crustacyanin. The theoretical investigation is crucial in identifying the relative importance of different mechanisms that can contribute to the total bathochromic shift.

1.3 SYNTHESIS OF ^{13}C-LABELED CAROTENOIDS AND RETINOIDS

As demonstrated in the earlier study of the blue lobster carotenoprotein α-crustacyanin, the use of ^{13}C-labeled carotenoids is essential for the isotope-sensitive analysis of carotenoids in biological systems. This requires the development of appropriate synthetic methods for the preparation of these compounds.

The synthesis of many carotenoids is well known and published in the literature, but the synthesis of ^{13}C-labeled carotenoids and retinoids is subject to limitations.[80] The ^{13}C labels have to be introduced using ^{13}C-labeled compounds. Only relatively small uniformly or selectively ^{13}C-labeled compounds are commercially available at reasonable price, e.g. acetone, methyl iodide, acetic acid, acetonitrile and ethyl acetoacetate. These small synthons have to be used to obtain ^{13}C enrichment at the desired position(s) in the final product. These compounds are all derived from natural abundant 1.1% ^{13}CO, which is separated from ^{12}CO via several distillations until >99% ^{13}CO is obtained. This is the reason that ^{13}C-labeled compounds are relatively expensive. For example, $^{13}C_2$-acetonitrile costs about € 1000 /g, while the unlabeled acetonitrile costs about € 0.20 /g. Therefore, large-scale synthesis, for which most synthetic schemes of carotenoids are developed, would be very expensive. To prevent loss of expensive ^{13}C-labeled material, a short synthetic route is essential, with high overall yield based on the ^{13}C-labeled starting compounds. Very efficient is the use of a convergent modular synthetic scheme, in which the desired compound is built from smaller synthons that are coupled at the final stages

of the synthesis. A modular synthetic strategy was developed in our group for the synthesis of uniformly ^{13}C-labeled retinal,[81] and a similar approach could be used for the synthesis of ^{13}C-labeled carotenoids.

1.4 OUTLINE OF THE THESIS

The introduction gives the background of the research and explains the research strategy. First synthetic schemes will be developed for the preparation of ^{13}C-enriched retinoids and carotenoids. The synthesized ^{13}C-labeled carotenoids are used for the analysis of retinoids and carotenoids in their natural systems in a second step.

A modular scheme for the synthesis of ^{13}C-labeled carotenoids is described in **Chapter 2**, and the synthesis of $^{13}C_4$ astaxanthin and $^{13}C_{10}$ astaxanthin is discussed in detail.

The application of ^{13}C-labeled carotenoids for study of biological systems is described in **Chapter 3**, where the binding of astaxanthin in the carotenoprotein α-crustacyanin is discussed. The ^{13}C-labeled astaxanthin was reconstituted into the natural system, and analyzed in a non-invasive way by SSNMR spectroscopy and resonance Raman spectroscopy. The results of the SSNMR and Raman analysis are interpreted with the help of quantum chemical calculations, giving pronounced insight into the binding of astaxanthin in α-crustacyanin and the accompanying color change.

In **Chapter 4** the introduction of ^{13}C labels in the central part of carotenoids is discussed. A method was developed for the synthesis of ^{13}C-labeled 2,7-dimethylocta-2,4,6-triene-1,8-dial, the C_{10}-dialdehyde that is used as the central part of carotenoids in synthetic schemes. Introduction of ^{13}C labels in the central part of carotenoids makes them suitable for *in vivo* studies in the human body, via LC-MS or resonance Raman spectroscopy. This way useful information about the health effects of carotenoids in the human body can be obtained.

Synthetic schemes for the preparation of ^{13}C-labeled retinal derivatives, 3,4-didehydroretinal, 3-hydroxyretinal and 4-hydroxyretinal, are described in **Chapter 5**. These retinal analogues are the chromophores of the visual pigments of animals like amphibians and fresh-water fish, flies and butterflies, and squid. The ^{13}C-labeled compounds can be used to study the visual systems of these animals. This also gives possibilities to study the effect of substituents on the end-ring of retinal in bovine or human rhodopsin via ^{13}C SSNMR. The ^{13}C-labeled retinal derivatives can be used for the synthesis of ^{13}C-enriched carotenoids, via the McMurry dimerization. This gives another route to a short and efficient synthesis of ^{13}C-labeled carotenoids.

Finally, general conclusions and prospects are given in **Chapter 6**. Ideas for future research, both for organic synthesis as well as for the application of ^{13}C-labeled carotenoids in the study of biological systems, are discussed here.

REFERENCES

[1] *Key to Carotenoids*; Pfander HP; Ed. Birkäuser Verlag: Basel, 1987.
[2] Weedon BCL, Moss GP in *Carotenoids, Volume 1A: Isolation and Analysis*; Britton G, Liaaen-Jensen S, Pfander HP; Eds. Birkhäuser Verlag: Basel, 1995.
[3] Britton G, Liaaen-Jensen S, Pfander HP in *Carotenoids, Volume 1A: Isolation and Analysis*; Britton G, Liaaen-Jensen S, Pfander HP; Eds. Birkhäuser Verlag: Basel, 1995.
[4] Rohmer M, *Pure Appl. Chem.* **1999**, *71*(12), 2279-2284.
[5] Britton G in *Carotenoids, Volume 3: Biosynthesis and Metabolism*; Britton G, Liaaen-Jensen S, Pfander HP; Eds. Birkhäuser Verlag: Basel, 1998.
[6] Cunningham FX, *Pure Appl. Chem.* **2002**, *74*(8), 1409-1417.
[7] Winterhalter P, Rouseff RL in *Carotenoid-Derived Aroma Compounds*; ACS Publishers: Washington, 2001.
[8] Schrott EL, *Pure Appl. Chem.* **1985**, *57*, 729.
[9] Van Döring WE, Kitagawa T, *J. Am. Chem. Soc.* **1994**, *113*, 4288.
[10] Ridley SM in *Carotenoid Chemistry and Biochemistry*; Britton G, Doodwin TW; Eds. Pergamon Press: Oxford, 1982.
[11] Broekmans WMR, *PhD. Thesis*, Wageningen University, 2002.
[12] Van Poppel G, Goldbohm RA, *Am. J. Clin. Nutr.* **1995**, *62*, 1393S-1402S.
[13] Van den Berg H, Faulks R, Granado HF et al. *J. Sci. Food. Agric.* **2000**, *80*, 880-912.
[14] Murakoshi M, Nishino H, Satomi Y, Takayasu J, Hasegawa T, Tokuda H, Iwashima A, Okuzumi J, Okabe H, Kitano H, Iwasaki R, *Cancer Res.* **1995**, *52*, 6583-6587.
[15] Narisawa T, Fukaura Y, Hasebe M, Ito M, Aizawa R, Murakoshi M, Uemura S, Khachik F, Nishino H, *Cancer Lett*. **1996**, *107*, 137-142.
[16] Franceschi S, Bidoli E, La Veccia C, Talamini R, D'Avanzo B, Negri E, *Int. J. Cancer* **1994**, *59*, 181-184.
[17] Giovanucci E, Ascherio A, Rimm EB, Stampfer MJ, Colditz GA, Willett WC, *J. Natl. Cancer Inst.* **1995**, *87*, 1767-1776.
[18] Nagasawa K, Mitamura T, Sakamoto S, Yamamoto K, *Anticancer Res.* **1995**, *15*, 1173-1178.
[19] Nishino H, Tokuda H, Satomi Y, Masuda M, Bu P, Onozuka M, Yamaguchi S, Okuda Y, Takaysu J, Tsuruta J, Okadu M, Ichiishi E, Murakoshi M, Kato T, Misawa N, Narisawa T, Takasuka N, Yano M, *Pure Appl. Chem.* **1999**, *71*(12), 2273-2278.
[20] Frieling U M, Schaumberg DA, Kupper TS, Muntwyler J, Hennekens CH, *Arch. Dermatol.* **2000**, *136*, 179-184.
[21] Mathews-Roth MM, *Ann. N. Y. Acad. Sci.* **1993**, *691*, 127-138.
[22] Kune GA, Bannerman S, Field B, Watson LF, Cleland H, Merenstein D, Vitetta L, *Nutr. Cancer* **1992**, *129*, 5-8.
[23] Wei Q, Matanoski GM, Farmer ER, Strickland P, Grossman L, *J. Clin. Epidemiol.* **1994**, *47*, 829-836.
[24] Isler O in *Carotenoids*; Birkhäuser Verlag: Basel, 1971.
[25] Van Lieshout M, West CE, Permaesih MD, Wang Y, Xu X, VanBreemen RB, Creemers AFL, Verhoeven MA, Lugtenburg J, *Am. J. Clin. Nutr.* **2001**, *73*, 949-958.
[26] Wang Y, Xu X, Van Lieshout M, West CE, Lugtenburg J, Verhoeven MA, Creemers AFL, Muhilal, VanBreemen RB, *Anal. Chem.* **2000**, *72*, 4999-5003.
[27] FAO/WHO, *Fao Food and Nutrition Series* **1985**, *23*, 17.
[28] Chasan-Taber L, Willett WC, Seddon JM, Stampfer MJ, Rosner B, Colditz GA, Hankinson SE, *Epidemiology* **1999**, *10*, 679-684.
[29] Brown L, Rimm EB, Seddon JM et al. *Am. J. Clin. Nutr.* **1999**, *129*, 1135-1139.
[30] Lyle BJ, Mares-Perlman JA, Klein BE, Klein R, Greger JL, *Am. J. Epidemiol.* **1999**, *149*, 801-809.
[31] Hankinson SE, Stampfer MJ, Seddon JM, Colditz GA, Rosner B, Speizer FE, Willett WC, *BMJ* **1992**, *305*, 335-339.
[32] Jacques PF, Chylack LT, *Am. J. Clin. Nutr.* **1991**, *53*, 352s-355s.
[33] Landrum JT, Bone RA, Kilburn MD, *Adv. Pharmacol.* **1997**, *38*, 537-556.
[34] Taylor A in *Nutritional and environmental influences on the eye*; CRC Press: New York, 1999.
[35] Kläui H in *Carotenoid Chemistry and Biochemistry*; Britton G, Goodwin TW; Eds. Pergamon Press: Oxford, 1982, 309-317.
[36] Paust J in *Carotenoids, Volume 2: Synthesis*; Britton G, Liaaen-Jensen S, Pfander HP; Eds. Birkhäuser Verlag: Basel, 1996, 259.

[37] Isler O, Lindlar H, Montavon M, Rüegg R, Zeller P, *Helv. Chim. Acta* **1956**, *39*, 249.
[38] Pommer H, *Angew. Chem.* **1960**, *72*, 911.
[39] Kläui H, Bauernfeind JC in *Carotenoids as colorants and vitamin A precursors*; Bauerfeind JC; Ed. Academic Press: New York, 1981, 309-328.
[40] Sandmann G, *Trends in Plant Science* **2001**, *6*(1), 14-17.
[41] Tripathi U, Sarada R, Ravishankar GA, *World Journal of Microbiology & Biotechnology* **2001**, *17*, 325-239.
[42] Boussiba S, *Physiol. Plantarum.* **2000**, *108*(2), 111-117.
[43] Simpson KL, Katayama T, Chichester CO in *Carotenoids as colorants and vitamin A precursors*; Bauerfeind JC; Ed. Academic Press: New York, 1981, 463
[44] Marusich WL, Bauernfield JC in *Carotenoids as colorants and vitamin A precursors*; Bauerfeind JC; Ed. Academic Press: New York, 1981, 319.
[45] Meyers SP, *Pure Appl. Chem.* **1994**, *66*(5), 1069-1076.
[46] Ausich RL, *Pure Appl. Chem.* **1994**, *66*(5), 1057-1068.
[47] Thommen H in *Carotenoids*; Isler O; Ed. Birkhäuser Verlag: Basel, 1971, 656.
[48] Britton G, Armitt GM, Lau SYM, Patel AK, Shone CC in *Carotenoid Chemistry and Biochemistry*; Britton G, Goodwin TW; Eds. Pergamon Press: Oxford, 1982, 237.
[49] Buchwald M, Jencks WP, *Biochemistry* **1968**, *7*, 844-859.
[50] Renström B, Rönneberg H, Borch G, Liaaen-Jensen S, *Comp. Biochem. Phsyiol.* **1982**, *71B*, 249-252.
[51] Jansen FJHM, *PhD. Thesis*, 1996, 112-113.
[52] Wald G, Nathanson N, Jencks WP, Tarr E, *Biol. Bull.* **1948**, *95*, 249-250.
[53] Baldwin JM, Schertler GFX, Unger VM, *J. Mol. Biol.* **1997**, *272*, 144-164.
[54] Ji TH, Grossmann M, Ji I, *J. Mol. Biol.* **1998**, *273*, 17299-17302.
[55] Bourne HR, Meng EC, *Science* **2000**, *289,* 733-738.
[56] Palczewski K, Kumasaka T, Hori T, Behnke CA, Motoshima H, Fox BA, Le Trong I, Teller D, Okada T, Stenkamp RE et al. *Science* **2000**, *289*, 739-745.
[57] North ACT, *Int. J. Biol. Macromol.***1989**, *11*, 56-58.
[58] North ACT, *J. Mol. Graphics* **1989**, *7*, 67-70.
[59] Zagalsky PF, *Pure Appl. Chem.* **1994**, *66*, 973-980.
[60] Zagalsky PF, Mummery RS, Eliopoulos EE, Findlay JBC, *Comp. Biochem. Physiol.* **1991**, *79B*, 837-848.
[61] Keen JN, Caceres I, Eliopoulos EE, Zagalsky PF, Findlay JBC, *Eur. J. Biochem.* **1991**, *197*, 407-417.
[62] Keen JN, Caceres I, Eliopoulos EE, Zagalsky PF, Findlay JBC, *Eur. J. Biochem.* **1991**, *201*, 31-40.
[63] Clarke JB, Eliopoulos EE, Findlay JBC, Zagalsky PF, *Biochem. J.* **1990**, *265*, 919-921.
[64] Cianci M, Rizkallah PJ, Olczak A, Raftery J, Chayen NE, Zagalsky PF, Helliwell JR, *Proc. Natl. Acad. Sci.U.S.A.* **2002**, *99(15)*, 9795-9800.
[65] Chayen NE, Cianci M, Grossmann JG, Habash J, Helliwell JR, Nneji GA, Raftery J, Rizkallah PJ, Zagalsky PF, *Acta Cryst. D* **2003**, *D59*, 2072-2082.
[66] Gordon EJ, Leonard GA, McSweeney S, Zagalsky PF, *Acta Cryst. D* **2001**, *D57*, 1230-1237.
[67] Warburton JD, *PhD. Thesis*, 1986.
[68] Zagalsky PF in *Methods in Enzymology 111B*; Law JH, Riling HC; Eds. Academic Press: London, 1985, 216.
[69] Britton G, Weesie RJ, Askin D, Warburton JD, Gallardo-Guerrero L, Jansen FJHM, De Groot HJM, Lugtenburg J, Cornard JP, Merlin JC, *Pure Appl. Chem.* **1997**, *69*, 2075-2084.
[70] Buchwald M, Jencks WP, *Biochemistry* **1968**, *7*, 834-843.
[71] Jansen FJHM, Lugtenburg J, *Eur. J. Org. Chem.* **2000**, 829-836.
[72] Jansen FJHM, Kwestro M, Schmitt D, Lugtenburg J, *Recl. Trav. Chim. Pays-Bas* **1994**, *113*, 552-562.
[73] Weesie RJ, Verel R, Jansen FJHM, Britton G, Lugtenburg J, De Groot HJM, *Pure Appl. Chem.* **1997**, *69*, 2085-2090.
[74] Weesie RJ, Jansen FJHM, Merlin JC, Lugtenburg J, Britton G, De Groot HJM, *Biochemistry* **1997**, *36*, 7288-7296.
[75] Weesie RJ, Askin D, Jansen FJHM, De Groot HJM, Britton G, *FEBS Lett.* **1995**, *362*, 34-38.
[76] Weesie RJ, Merlin JC, De Groot HJM, Lugtenburg J, Jansen FJHM, Cornard JP, *Biospectroscopy* **1999**, *5*, 358-370.
[77] Weesie RJ, Merlin JC, Lugtenburg J, Britton G, Jansen FJHM, Cornard JP, *Biospectroscopy* **1999**, *5*, 19-33.
[78] Krawczyk S, Britton G, *Biochim. Biophys. Acta* **2001**, *1544*, 301-310.
[79] Dokter AM, Van Hemert MC, In 't Velt CM, Van der Hoef K, Lugtenburg J, Frank HA, Groenen EJJ, *J. Phys. Chem. A* **2002**, *106*, 9463-9469

[80] Pfander HP, Liaaen-Jensen S, Britton G, in *Carotenoids, Volume 2, Synthesis*; Britton G, Liaaen-Jensen S, Pfander HP; Eds. Birkhäuser Verlag: Basel, 1996.
[81] Creemers AFL, Lugtenburg J, *J. Am. Chem. Soc.* **2002**, *124*, 6324-6334.

CHAPTER 2

SYNTHESIS OF ^{13}C-LABELED ASTAXANTHIN

2.1 INTRODUCTION

The synthesis of ^{13}C-labeled compounds has to be efficient, because enriched compounds have to be made from a limited number of commercially available, small building blocks that are expensive. Synthetic schemes for the preparation of ^{13}C-labeled astaxanthin have been developed by Jansen et al. and have been applied for the synthesis of several $^{13}C_2$-labeled astaxanthins. Via these schemes, astaxanthins with symmetrical $^{13}C_2$ labels at the central positions 12-15, 20 and at the carbonyl at position 4 were made.[1-4] The $^{13}C_2$-labeled astaxanthins were incorporated in the lobster carotenoprotein α-crustacyanin and analyzed with SSNMR and resonance Raman spectroscopy. These studies indicated that a protonation at the carbonyl groups of astaxanthin upon binding to the protein may be responsible for the blue color of α-crustacyanin.[5,6] We prepared ^{13}C-labeled astaxanthins with ^{13}C labels at the positions close to the C6-ring, where the effects of a protonation at the carbonyl group would yield a considerable NMR chemical shift. By incorporation of the ^{13}C-labeled astaxanthins in α-crustacyanin and subsequent SSNMR and resonance Raman analysis it can be determined if protonation of astaxanthin is the basis of the color shift that occurs upon binding to the protein.

Using the modular synthetic scheme that was developed for the synthesis of uniformly ^{13}C-labeled ([U-^{13}C]) retinal by Creemers et al.[7], multifold ^{13}C-labeled astaxanthin can be prepared in more efficient manner and in higher yield than in the earlier work. The preparation of [6,6′,7,7′]-$^{13}C_4$ and [8,8′,9′,9,10,10′,11,11′,19,19′]-$^{13}C_{10}$ astaxanthin, as depicted in Figure 1, was optimized and applied to prepare both isotopomers on a 100 mg scale.

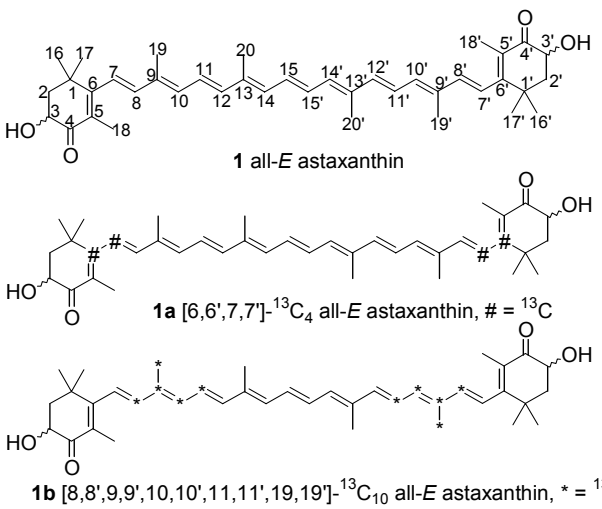

Figure 1. *Structure, numbering and position of ^{13}C labeling of synthetic all-E astaxanthin as a mixture of 25% (3R,3′R), 50% (3R,3′S) and 25% (3S,3′S).*

This chapter will give detailed information on the recent improvements in the synthesis of ^{13}C-labeled astaxanthin, providing essential knowledge for reproduction of the synthetic steps. Also the NMR characterization and the effect of the ^{13}C labeling on the NMR spectra is discussed in this chapter. It is concluded with a section providing experimental details and the NMR data of the intermediates that are produced in the synthesis.

2.2 MODULAR SYNTHETIC STRATEGY

Astaxanthin is synthesized via the modular $C_{15}+C_{10}+C_{15} \rightarrow C_{40}$ scheme, which is based on the final step in which a suitable C_{15}-Wittig compound is linked to both sides of the central C_{10}-dialdehyde, as shown in Scheme 1. This $C_{15}+C_{10}+C_{15} \rightarrow C_{40}$ scheme is generally used for the synthesis of C_{40}-carotenoids.[4]

In Chapter 4 the strategy to introduce ^{13}C labels in the central part of carotenoids is discussed, describing an efficient method for ^{13}C labeling of the central C_{10}-dialdehyde. The C_{15}-Wittig compound is built from a C_{10}-synthon and a C_5-synthon. Jansen et al. have described a route for the synthesis of astaxanthin with ^{13}C labels in the C_{10}-synthon of the C_{15}-part.[2,3] This method could be improved by using the scheme developed for the synthesis of [U-^{13}C]-retinal, by Creemers et al.[7] Introduction of ^{13}C labels at positions 8,9,10,11 and 19 is effected via triethyl 3-methyl-4-phosphonocrotonate (**17**), as shown in Scheme 2.

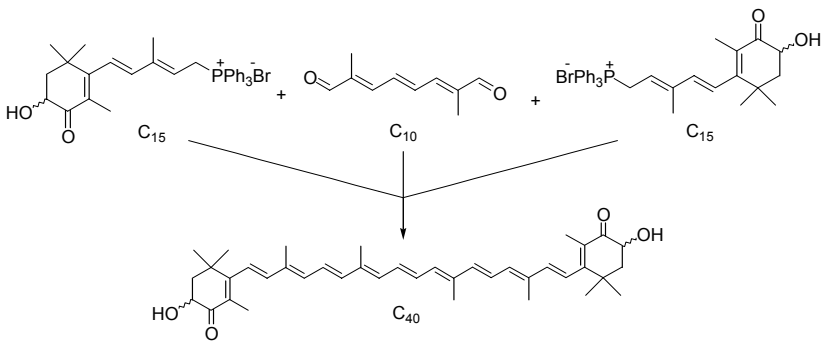

Scheme 1. *$C_{15} + C_{10} + C_{15} \rightarrow C_{40}$ scheme for the synthesis of astaxanthin.*

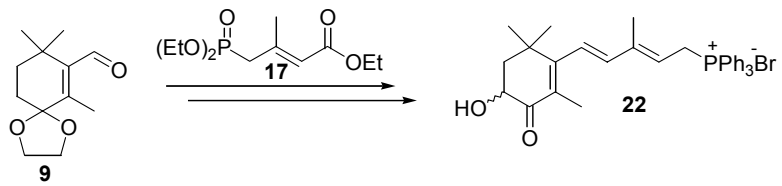

Scheme 2. *$C_{10} + C_5 \rightarrow C_{15}$ scheme for the synthesis of the C_{15}-Wittig compound (**22**).*

2.3 SYNTHESIS OF THE C_{10}-SYNTHON

The synthesis of [6,6′,7,7′]-$^{13}C_4$ astaxanthin had to be optimized for the introduction of ^{13}C labels in the C_{10}-aldehyde **9**. Scheme 3 shows the synthesis of 2,10,10-trimethyl-4,7-dioxaspiro[4,5]dex-1-enecarbaldehyde **9a**, with ^{13}C labels at positions 6 and 7.

The synthesis starts with the commercially available 6-methyl-5-hepten-2-one (**2**), which can also be prepared with ^{13}C labels at any position or combination of positions.[1,7,9] The ^{13}C labels are introduced by a Horner-Wadsworth-Emmons (HWE) reaction of ketone **2** with $^{13}C_2$ diethyl cyanomethylphosphonate, which was made *in situ* from commercially available $^{13}C_2$ acetonitrile and diethyl chlorophosphate. After purification on a silica-gel column, [1,2]-$^{13}C_2$ 3,7-dimethyl-2,6-octadienenitrile (**3a**) was obtained in 96% yield. It was found that purification on a silica column (20% diethyl ether/light petroleum (PE)) is essential, since low yields for the next reaction were obtained, even when small amounts of side-products were still present. Nitrile **3a** was treated with sulfuric acid, to give [1,2]-$^{13}C_2$ α-cyclonitrile (**4a**) in 83% yield. When the reaction mixture is kept at 0˚C and workup is performed under non-basic conditions, more than 95% of the product is the desired α-cyclonitrile. A small amount of the thermodynamically more stable β-cyclonitrile, with the double bond between C-5 and C-6, is formed. α-Cyclonitrile (**4a**) reacts with *meta*-chloroperbenzoic acid (*m*CPBA) to form epoxide **5a**, while β-cyclonitrile does not react. The epoxide **5a** is converted to alcohol **6a** with lithium diisopropylamide (LDA). The allylic alcohol is oxidized to compound **7a** with pyridinium chlorochromate (PCC). Workup of this reaction is troubled by the PCC-tar formed during the reaction, and yields improve from 60% to 73% when PCC on basic alumina is used, which is easily removed by filtration over silica

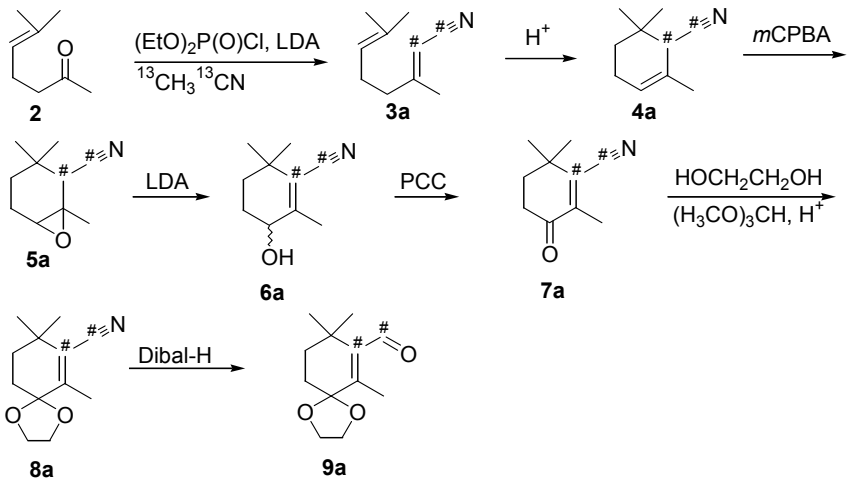

Scheme 3. *Synthesis of the C_{10}-synthon (**9a**) leading to astaxanthin with ^{13}C labels at positions 6,6′ and 7,7′ (# = ^{13}C).*

gel. The resulting β-cyclonitrile can be separated from ketone **7** after the PCC-oxidation by silica-gel chromatography. Subsequently, the ketone is protected by ethylene glycol to form acetal **8a** in 98% yield. With diisobutylaluminium hydride (Dibal-H) the nitrile group of **8a** is reduced to an aldehyde, to give **9a** in 86% yield. It is important to follow this reaction closely with thin layer chromatography (TLC, 50% diethyl ether/PE), to verify if complete conversion to **9a** is achieved. Traces of unreacted nitrile are difficult to remove via column chromatography, and their presence in the reaction mixture leads to significant lower yields in the next step of the reaction scheme.

2.4 SYNTHESIS OF [U-^{13}C] C_5-PHOSPHONATE

The C_{15}-Wittig salts that are used in the synthesis of astaxanthin were prepared by coupling of the C_{10}-ring **9** to C_5-phosphonate **17**. The suitable Wittig salts for the synthesis of astaxanthin with ^{13}C labels at positions 8,9,10,11 and 19 were made using [U-^{13}C]-C_5 phosphonate. The synthesis of [U-^{13}C] 4-(diethylphosphono)-3-methyl-2-butenenitrile was developed by Creemers et al.[7] and the same scheme, with small modifications, could be used for the synthesis of $^{13}C_5$ triethyl 3-methyl-4-phosphonocrotonate (**17b**), shown in Scheme 4. Starting compounds for this synthesis are the commercially available $^{13}C_2$ acetic acid (**10b**) and $^{13}C_4$ ethyl acetoacetate (**13b**).

Acetic acid is quantitatively converted into ethyl bromoacetate (**11b**) with the Hell-Vollhardt-Zelinsky reaction.[8] Bromoacetate is converted into triethyl phosphonoacetate (**12b**) via an Arbuzov reaction, in 90% yield after distillation. The commercially obtained [1,2,3,4]-$^{13}C_4$ ethyl acetoacetate (**13b**) was chlorinated at the α-position with sulfuryl chloride to obtain ethyl 2-chloroacetoacetate (**14b**) in 99% yield. By adding sulfuric acid and water and refluxing for

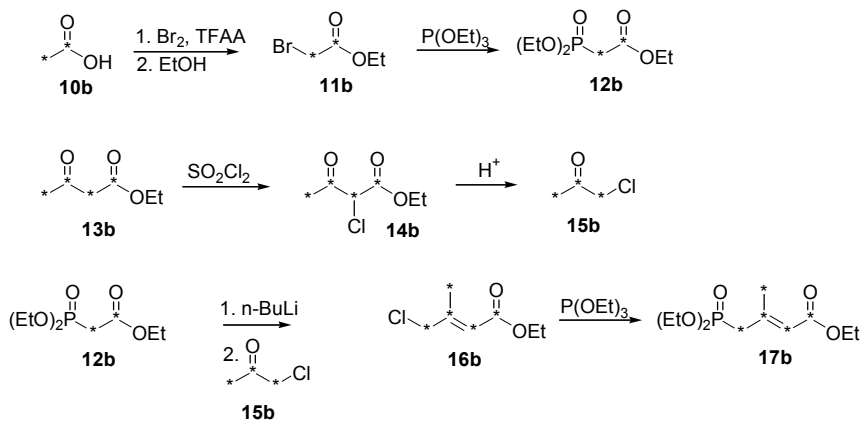

Scheme 4. *Synthesis of $^{13}C_5$ triethyl 3-methyl-4-phosphonocrotonate (**17b**) (* = ^{13}C).*

2 days in tetrahydrofuran (THF) the compound was saponificated and decarboxylated, to give $^{13}C_3$ chloroacetone (**15b**). In this step one ^{13}C label is lost, but since $^{13}C_4$ ethyl acetoacetate is less expensive than [2,3,4]-$^{13}C_3$ ethyl acetoacetate, this is acceptable. After workup, the relatively unstable chloroacetone was kept in a THF-solution, dried with molecular sieves, and directly used in the next reaction. After a HWE-coupling reaction, $^{13}C_3$ chloroacetone (**15b**) and $^{13}C_2$ triethyl phosphonoacetate (**12b**) gave $^{13}C_5$ ethyl 4-chloro-3-methylcrotonate (**16b**), as a mixture of *E/Z*-isomers, in 72% yield (over 2 steps). Subsequent Arbuzov reaction with triethyl phosphite gave the desired C_5-synthon $^{13}C_5$ triethyl 3-methyl-4-phosphonocrotonate (**17b**) in 89% yield.

2.5 SYNTHESIS OF C_{15}-WITTIG SALTS

The final steps leading to $^{13}C_4$ astaxanthin and $^{13}C_{10}$ astaxanthin are the same, which is an advantage of this modular scheme for the synthesis of these compounds. By introducing the ^{13}C labels in the desired synthon, the same route can be used for the synthesis of astaxanthins with ^{13}C labels at different positions, and a limited number of reactions with the expensive ^{13}C-labeled compound have to be performed, increasing the yield and reducing the risk of loss of material.

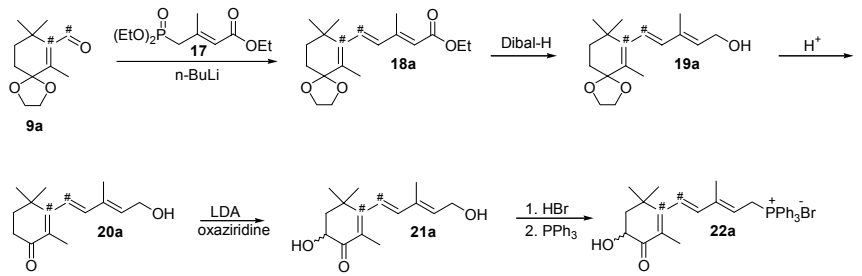

Scheme 5a. *Synthesis of C_{15}-Wittig compound **22a** for the synthesis of $^{13}C_4$-labeled astaxanthin **1a**.*

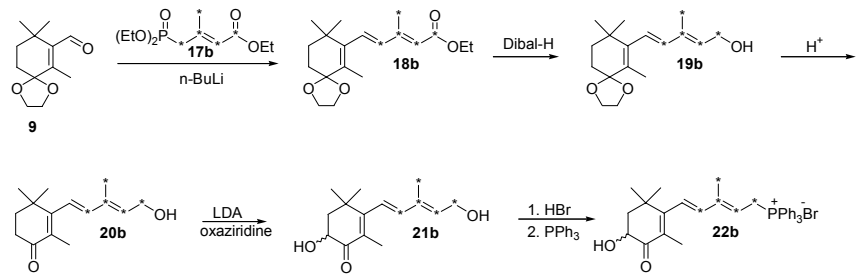

Scheme 5b. *Synthesis of C_{15}-Wittig compound **22b** for the synthesis of $^{13}C_{10}$-labeled astaxanthin **1b**.*

From here, the route is the same for $^{13}C_4$-labeled and $^{13}C_{10}$-labeled astaxanthin, as shown in Scheme 5. The ^{13}C labels of $^{13}C_4$ astaxanthin (**1a**) are marked with (#), the ^{13}C labels of $^{13}C_{10}$ astaxanthin (**1b**) are marked with (*).

The C_{10}-aldehyde **9** was coupled in HWE-coupling to C_5-phosphonate **17**, to give the C_{15}-ester **18** in 85% yield. The ester was dissolved in PE and reduced to the corresponding alcohol **19** with 2.2 equivalent of Dibal-H. Reproducibility of this reaction is poor, and yields vary between 40% and 80%. This is partly caused by the reduction of the acetal to the corresponding ether which occurs as a side-reaction.[9] We tried to optimize this step by changing conditions such as temperature, scale, amount of Dibal-H and reaction times. Best yields were obtained when Dibal-H was added at -80˚C and the solution was allowed to slowly warm up. The reaction was quenched just after all the starting material was converted, as shown by TLC (50% diethyl ether/PE), usually at about -40˚C. The starting compound needs to be well purified. In particular, it is of importance that no C_{10}-nitrile **8** is present, since this compound is reduced to the corresponding aldehyde **9**, this way interfering with the reduction of the ester. The acetal group of **19** was hydrolyzed to ketone **20** with a trace of acid in acetone in 93% yield. At this stage the hydroxyl group at position 3 was introduced. With 2.2 equivalent of LDA the dianion of **20** was made, and reacted with (+)-(dichlorocamphorylsulforyl)oxaziridine to give diol **21** in 53% yield. Higher yields for this reaction have been reported in the literature.[9] Purification of the desired product **21** is difficult, since this product and the reduced reagent, (+)-(8,8-dichlorocamphorylsulfonyl)imine, have similar retention times on silica-gel chromatography. When the reaction is performed on larger scale (>1 g of **20**), most of the side-product can be removed by recrystallization of the imine in dichloromethane/diethyl ether, followed by a silica-gel column purification (50% diethyl ether/PE).

When the reaction mixture is allowed to warm to room temperature, a mixture of 3*R* and 3*S* isomers is obtained. Stereoselectivity can be obtained when the reaction is kept at low temperature. The configuration at the 3-position can be manipulated by choosing the desired combination of (+)- or (-)-oxaziridine and base.[10,11] The relatively expensive oxaziridine can be recycled by oxidation of the formed imine back to the original oxaziridine with OXONE.[12]

Subsequently, the allylic hydroxyl group of **21** is converted to a bromide with hydrogen bromide, and the resulting product reacts with triphenylphosphine (PPh_3) to form the desired C_{15}-Wittig salt **22** with ^{13}C labels at the desired positions, in 50% yield.

2.6 SYNTHESIS OF ASTAXANTHIN

In the final step, 2.2 equivalents of the C_{15}-Wittig compound and 1 equivalent C_{10}-dialdehyde **23** were suspended in 1,2-epoxybutane and refluxed overnight, under dim red light. This double Wittig reaction gives the desired [6,6′,7,7′]-$^{13}C_4$ astaxanthin **1a** and [8,8′,9,9′,10,10′,11,11′,19,19′]-$^{13}C_{10}$ astaxanthin **1b** in one step, as shown in Schemes 6a and 6b. Astaxanthin was precipitated in

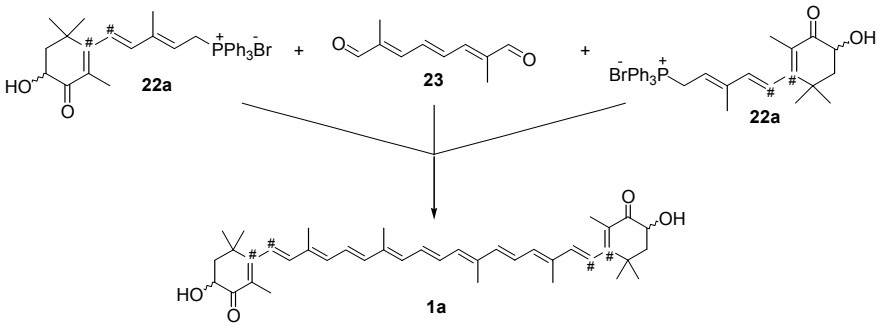

Scheme 6a. *Double coupling of C_{15}-Wittig compound **22a** to the central C_{10}-dialdehyde **23** to synthesize all-E [6,6′,7,7′]-$^{13}C_4$ astaxanthin **1a** as mixture of 25% (3R,3′R), 50% (3R,3′S) and 25% (3S,3′S).*

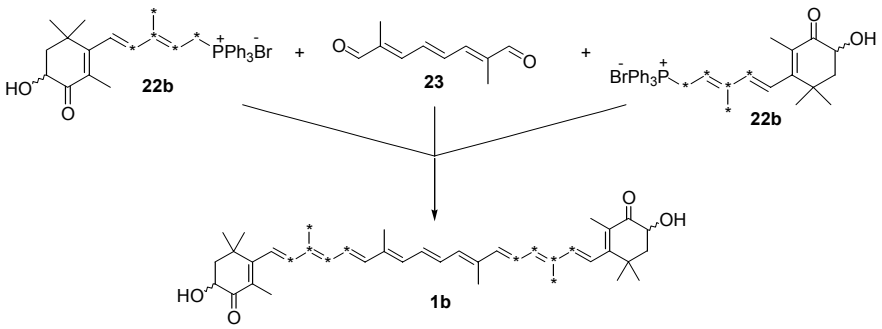

Scheme 6b. *Double coupling of C_{15}-Wittig compound **22b** to the central C_{10}-dialdehyde **23** to synthesize all-E [8,8′,9,9′,10,10′,11,11′,19,19′]-$^{13}C_{10}$ astaxanthin **1b** as mixture of 25% (3R,3′R), 50% (3R,3′S) and 25% (3S,3′S).*

ethanol, collected by filtration and isomerized to the all-*E* configuration by refluxing overnight in *n*-heptane. After cooling, the crystals of all-*trans* astaxanthin were collected by filtration, and further purified by crystallization in DCM/MeOH and DCM/*n*-hexane. This way, [6,6′,7,7′]-$^{13}C_4$ all-*E* astaxanthin **1a** and [8,8′,9,9′,10,10′,11,11′,19,19′]-$^{13}C_{10}$ all-*E* astaxanthin **1b** were prepared, with >99% ^{13}C enrichment at the desired positions. Yields of the final reaction are usually about 30%, although higher yields, up to 70%, have been reported in the literature for similar Wittig reactions.[13]

The main reason for the lower yields that were obtained compared to the literature, is the relatively small scale on which the reactions were performed.[14-16] During the crystallization steps, a considerable amount of product is lost when working at 100 mg-scale. The use of expensive ^{13}C labels demands a small synthetic scale. For the reconstitution of astaxanthin to the lobster protein α-crustacyanin, less than 1 mg is sufficient, so the aim was to develop a synthetic route that would give sufficient amounts of the final product for structural analysis. Working at too small scale (<100 mg) makes the final crystallization step of the product a difficult challenge.

The total yield of the synthesis of $^{13}C_{10}$ astaxanthin is 1.6% starting from $^{13}C_2$ acetic acid or $^{13}C_4$ ethyl acetoacetate (13 steps, 73% average), and 1.5% for the synthesis of $^{13}C_4$ astaxanthin, starting from $^{13}C_2$ acetonitrile (10 steps, 66% average).

2.7 ^{1}H NMR SPECTROSCOPY

[6,6′,7,7′]-$^{13}C_4$ all-*E* astaxanthin (**1a**), [8,8′,9,9′,10,10′,11,11′,19,19′]-$^{13}C_{10}$ all-*E* astaxanthin (**1b**) and natural abundance all-*E* astaxanthin (**1**) were characterized with 600 MHz ^{1}H NMR, to determine the structure and purity of the compounds, the position of the ^{13}C labels and the label incorporation.

The NMR data are given in the experimental details at the end of the chapter, and will briefly be discussed here. Figure 2 shows the 600 MHz ^{1}H NMR spectrum and the assignment of the all-*E* astaxanthin NMR response.

The spectral values are well in line with the published data for all-*E* astaxanthin of Englert et al.[17] The spectrum confirms a high purity and the all-*E* structure; within experimental error, no *Z*-isomers could be detected. The synthetic astaxanthin consists as a mixture of 25% (3*R*,3′*R*), 50% (3*R*,3′*S*) and 25% (3*S*,3′*S*). No differences between these stereoisomers are observed.

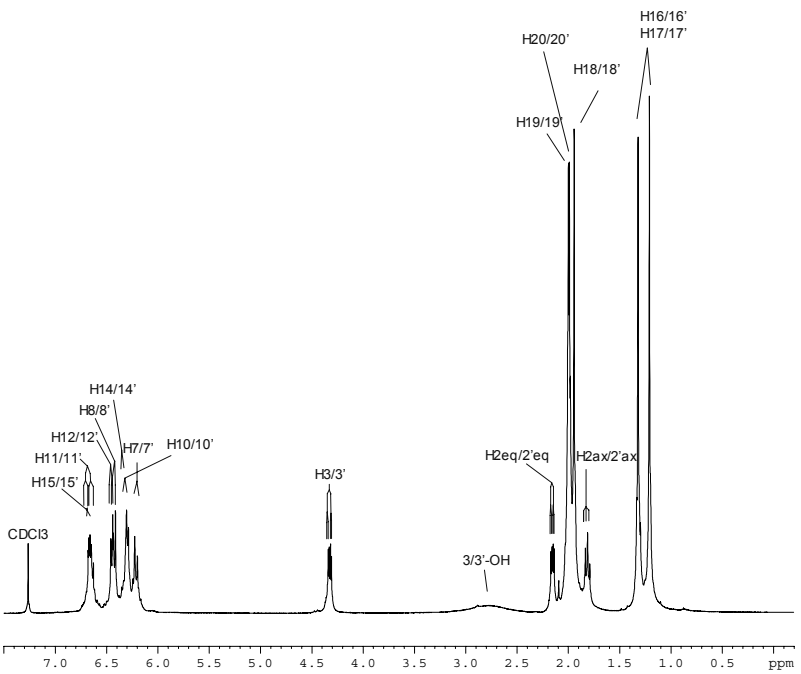

Figure 2. *600 MHz ^{1}H NMR spectrum and assignment of all-E astaxanthin in $CDCl_3$.*

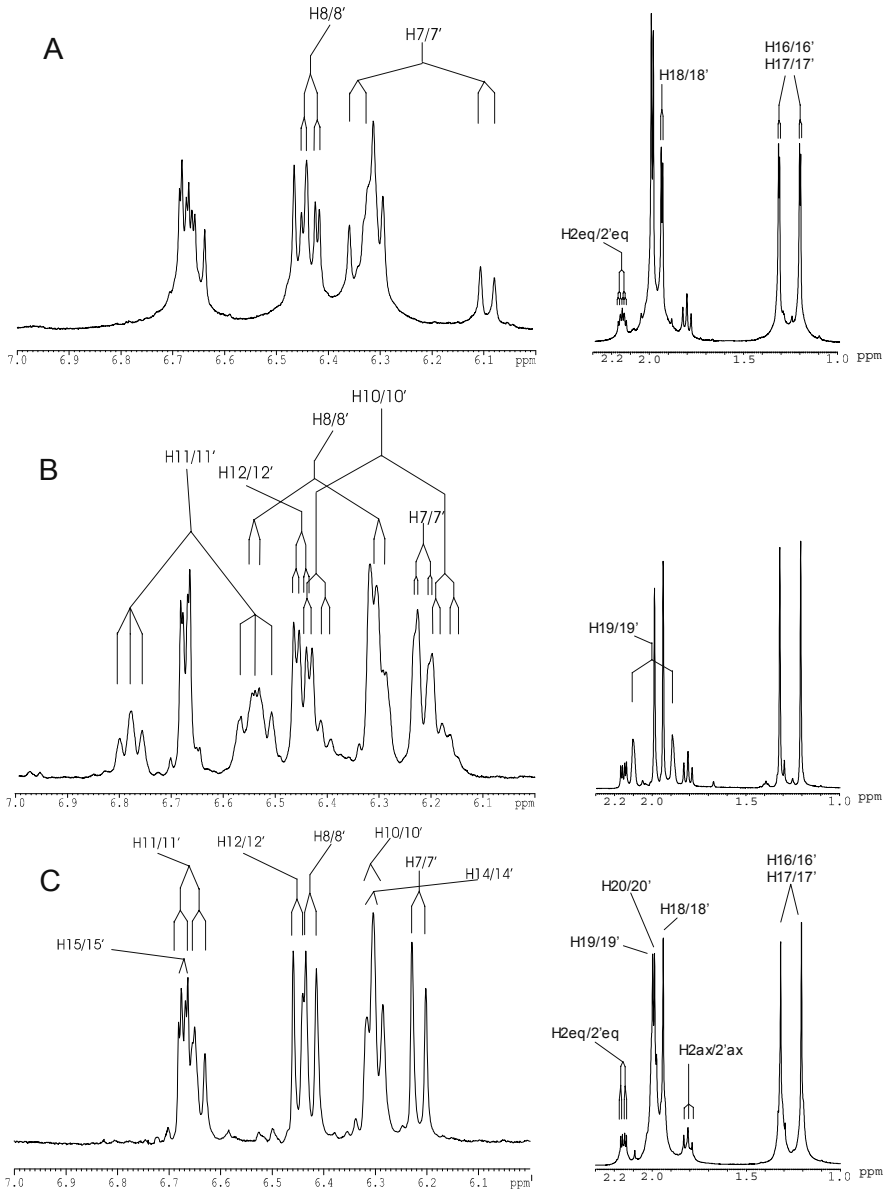

Figure 3. *The vinylic region (7.0 - 6.0 ppm) and aliphatic region (2.2 – 1.0 ppm) of the 600 MHz ^{1}H NMR spectrum of [6,6',7,7']-$^{13}C_4$ all-E astaxanthin (A), [8,8',9,9',10,10',11,11',19,19']-$^{13}C_{10}$ all-E astaxanthin (B) and natural abundance all-E astaxanthin (C). In C the assignment of the resonances is indicated. For A and B only the additional splitting due to the incorporation of ^{13}C isotopes is given.*

Figure 3 shows the significant regions of the 600 MHz ^{1}H NMR spectrum of [6,6′,7,7′]-$^{13}C_4$ all-*E* astaxanthin (**1a**), [8,8′,9,9′,10,10′,11,11′,19,19′]-$^{13}C_{10}$ all-*E* astaxanthin (**1b**) and natural abundance all-*E* astaxanthin (**1**). The ^{1}H NMR chemical shifts of $^{13}C_4$ astaxanthin **1a** and $^{13}C_{10}$ astaxanthin **1b** are the same as for natural abundance all-*E* astaxanthin **1**, confirming the purity and all-*E* structure of $^{13}C_4$ astaxanthin **1a** and $^{13}C_{10}$ astaxanthin **1b**. However, at specific positions additional splitting of signals is observed in the ^{1}H NMR spectra of the ^{13}C-labeled astaxanthins, due to the presence of ^{13}C labels. Compared to the ^{1}H NMR spectrum of all-*E* astaxanthin, the spectrum of [6,6′,7,7′]-$^{13}C_4$ astaxanthin (Figure 3A) shows a large additional splitting of the signal of H7/7′ ($^{1}J_{C7H7}$ = 151.8 Hz) and a smaller splitting of 4.7 Hz of H8/8′. According to Courtin et al.[18] this should be assigned to either $^{2}J_{C7H8}$ or $^{3}J_{C6H8}$. Doublets are observed for H16/16′, H17/17′ ($^{3}J_{C6H16/17}$ = 3.4/3.7 Hz) and H18/18′ ($^{3}J_{C6H18}$ = 4.8 Hz) and an additional splitting is observed for $H2_{eq}$/$H2'_{eq}$ ($^{3}J_{C6H2eq}$ = 6.0 Hz). The other signals are unperturbed compared to natural abundance all-*E* astaxanthin. The observed ^{13}C-^{1}H couplings confirm the selective ^{13}C labeling at 6,6′ and 7,7′. No peaks at the original position of H7/7′ can be observed, which shows the high ^{13}C enrichment of >99%.

The ^{1}H NMR spectrum of [8,8′,9,9′,10,10′,11,11′,19,19′]-$^{13}C_{10}$ astaxanthin (Figure 3B) shows a complex splitting pattern in the vinylic region due to ^{13}C-^{1}H couplings. The chemical shift values and J-couplings could not be determined directly or via a simulation.

In the vinylic region of the spectrum, only H14/14′ and H15/15′ are unperturbed compared to natural abundance all-*E* astaxanthin. The signals of H8/8′ ($^{1}J_{C8H8}$ =132 Hz), H10/10′ ($^{1}J_{C10H10}$ = 138 Hz) and H11/11′ ($^{1}J_{C11H11}$ = 143 Hz) show a splitting caused by the large $^{1}J_{CH}$-coupling. The aliphatic region of the spectrum is the same as for natural astaxanthin, except for the signal of H19/19′. This resonance is observed as a broad doublet ($^{1}J_{C19H19}$ = 126 Hz). The broad shape of the signals indicates that also $^{2}J_{CH}$-and $^{3}J_{CH}$-couplings occur. Also the signals of H7/7′ (J = 3 Hz) and H12/12′ (J =7 Hz) are split due to $^{2}J_{CH}$- or $^{3}J_{CH}$-couplings with nearby ^{13}C labels.

The observed J_{CH}-splittings in the ^{1}H NMR spectrum of [8,8′,9,9′,10,10′,11,11′,19,19′]-$^{13}C_{10}$ astaxanthin confirms the selective ^{13}C enrichment at the desired positions. The absence of a signal at the original position of H19/H19′ confirms that a high ^{13}C enrichment is achieved.

In order to establish that all the changes in the spectrum 3B are due to the presence of the ^{13}C isotopes a ^{13}C noise-decoupled ^{1}H NMR spectrum (600 MHz, $CDCl_3$) of [8,8′,9,9′,10,10′,11,11′,19,19′]-$^{13}C_{10}$ all-*E* astaxanthin (**1b**) was recorded.

In Figure 4 this spectrum is given (spectrum A), together with the ^{1}H NMR (600 MHz, $CDCl_3$) spectrum (spectrum B) of natural abundance all-*E* astaxanthin (**1**).

Comparison of these spectra reveals that the spectra of all-*E* astaxanthin (**1**) and [8,8′,9,9′,10,10′,11,11′,19,19′]-$^{13}C_{10}$ all-*E* astaxanthin (**1b**) are identical within experimental error, confirming that the additional splitting pattern in the spectrum of **1a** is caused by the introduction of the ^{13}C enrichment. The only significant difference between the two spectra is the signal of the 3,3′ OH group, which is broadened and shifted in the spectrum of natural abundance astaxanthin

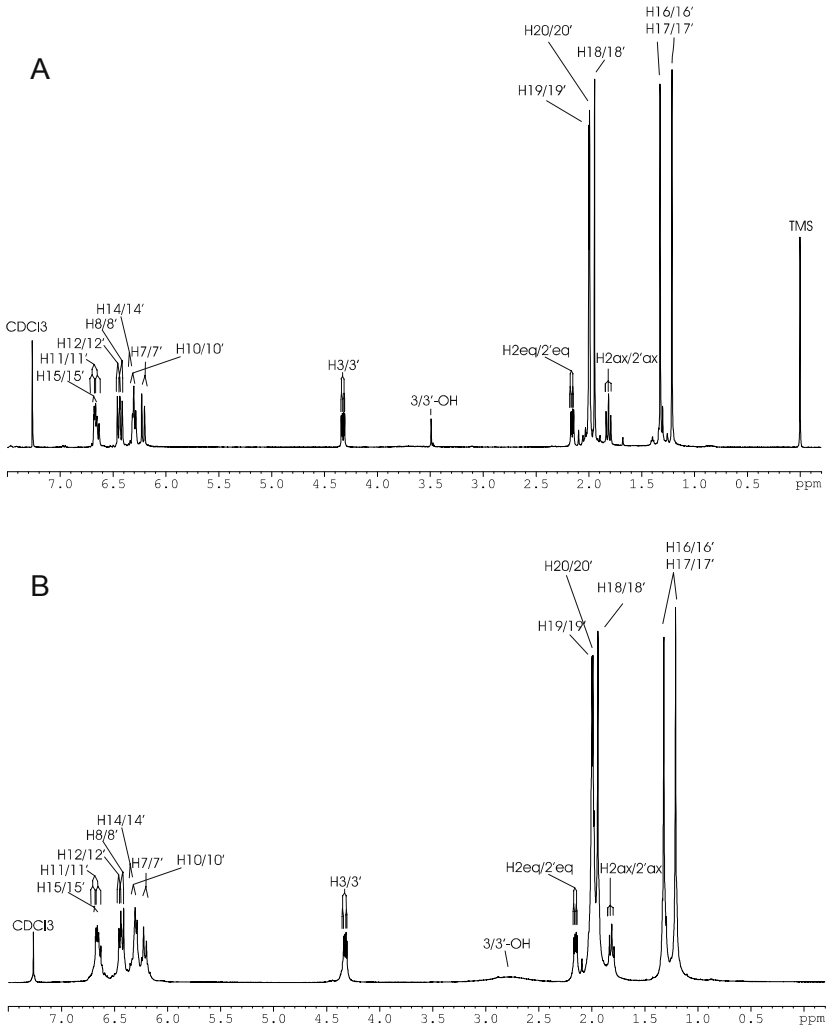

Figure 4. *^{13}C noise-decoupled ^{1}H (600 MHz, $CDCl_3$) NMR spectrum of [8,8′,9,9′,10,10′,11,11′,19,19′]-$^{13}C_{10}$ all-E astaxanthin (A) and ^{1}H NMR (600 MHz, $CDCl_3$) spectrum of natural abundance all-E astaxanthin (B).*

due to a higher humidity in the sample. The assigment of the signals and splitting pattern of [6,6′,7,7′]-$^{13}C_4$ astaxanthin (**1a**) can easily be determined from the ^{1}H NMR spectrum.

2.8 ^{13}C NMR SPECTROSCOPY

^{1}H noise-decoupled ^{13}C NMR spectroscopy can be used to confirm the position of the ^{13}C labels and to verify that no scrambling of the labels has taken place. Also the isomeric purity can easily be determined, since the signals of the *Z*-isomers resonate at a higher field. The 150 MHz ^{1}H noise-decoupled ^{13}C NMR spectra of [6,6′,7,7′]-$^{13}C_4$ all-*E* astaxanthin (**1a**), [8,8′,9,9′,10,10′,11,11′, 19,19′]-$^{13}C_{10}$ all-*E* astaxanthin (**1b**) and natural abundance all-*E* astaxanthin (**1**) and assignment of the signals are shown in Figure 5. In the spectrum (5C) of natural abundance astaxanthin, 20 signals can be observed. The chemical shift values are in agreement with the ^{13}C NMR data reported by Englert et al. for all-*E* astaxanthin, confirming the structure and purity of the synthesized compound.[19]

The ^{13}C NMR spectra of the ^{13}C-labeled astaxanthins are dominated by the ^{13}C-enriched positions. Since the level of ^{13}C is increased by a factor of 90, the intensity of the NMR peaks are enhanced 90-fold for these carbon atoms. The ^{13}C chemical shifts are the same as for natural abundance all-*E* astaxanthin, confirming the structure and purity of the ^{13}C-labeled astaxanthins.

The ^{13}C NMR spectrum of $^{13}C_4$ astaxanthin (**1a**, Figure 5B) shows two distinct doublets for the ^{13}C-enriched carbons C6/6′ ($^{1}J_{C6C7}$ = 55 Hz) and C7/7′ ($^{1}J_{C6C7}$ = 55 Hz). The signals of the unlabeled C atoms have a relatively low intensity, indicating that selective ^{13}C enrichment of positions 6/6′ and 7/7′ was achieved, and no scrambling of the ^{13}C labels has occurred. A closer look shows splitting of the signals of C1/1′ ($^{1}J_{C1C6}$ = 38 Hz), C5/5′ ($^{1}J_{C5C6}$ = 53 Hz) and C8/8′ ($^{1}J_{C7C8}$ = 73 Hz), which is in accordance with the ^{13}C labeling at positions 6/6′ and 7/7′. The absence of signals at the original position of C6/6′ and C7/7′ confirms that a high ^{13}C-enrichment (>99%) is achieved.

In the ^{13}C NMR spectrum of [8,8′,9,9′,10,10′,11,11′,19,19′]-$^{13}C_{10}$ astaxanthin (**1b**, Figure 5B) the signals of the ^{13}C-enriched positions are clearly recognized by their increased intensities. An enlargement of the significant regions in the spectrum is shown in Figure 6.

The increased intensity of the ^{13}C-labeled positions is clearly observed in the ^{13}C NMR spectrum of [8,8′,9,9′,10,10′,11,11′,19,19′]-$^{13}C_{10}$ astaxanthin (**1b**). The signals of the unlabeled C atoms have a relatively low intensity, indicating that selective >99% ^{13}C enrichment of positions 8/8′,9/9′,10/10′,11/11′ and 19/19′ was achieved, and no scrambling of the ^{13}C labels has occurred. Furthermore, the chemical shift values are in agreement with the data for all-*E* astaxanthin, confirming the structure and purity of the synthesized compound.

Due to the introduction of multiple ^{13}C labels, splitting of several signals is observed. The signal of C19/19′ shows a large splitting caused by the presence of the ^{13}C label at C9/9′, $^{1}J_{C9C19}$ = 39 Hz. Similar splitting of the signals of C8/8′ ($^{1}J_{C8C9}$ = 52 Hz) and C11/11′ ($^{1}J_{C10C11}$ = 50 Hz) is observed. The observed carbon-carbon couplings are in good agreement with selective ^{13}C labeling at positions 8,8′,9,9′,10,10′,11,11′ and 19,19′. The absence of signals at the original position of these C atoms confirms that a high ^{13}C-enrichment (>99%) is achieved.

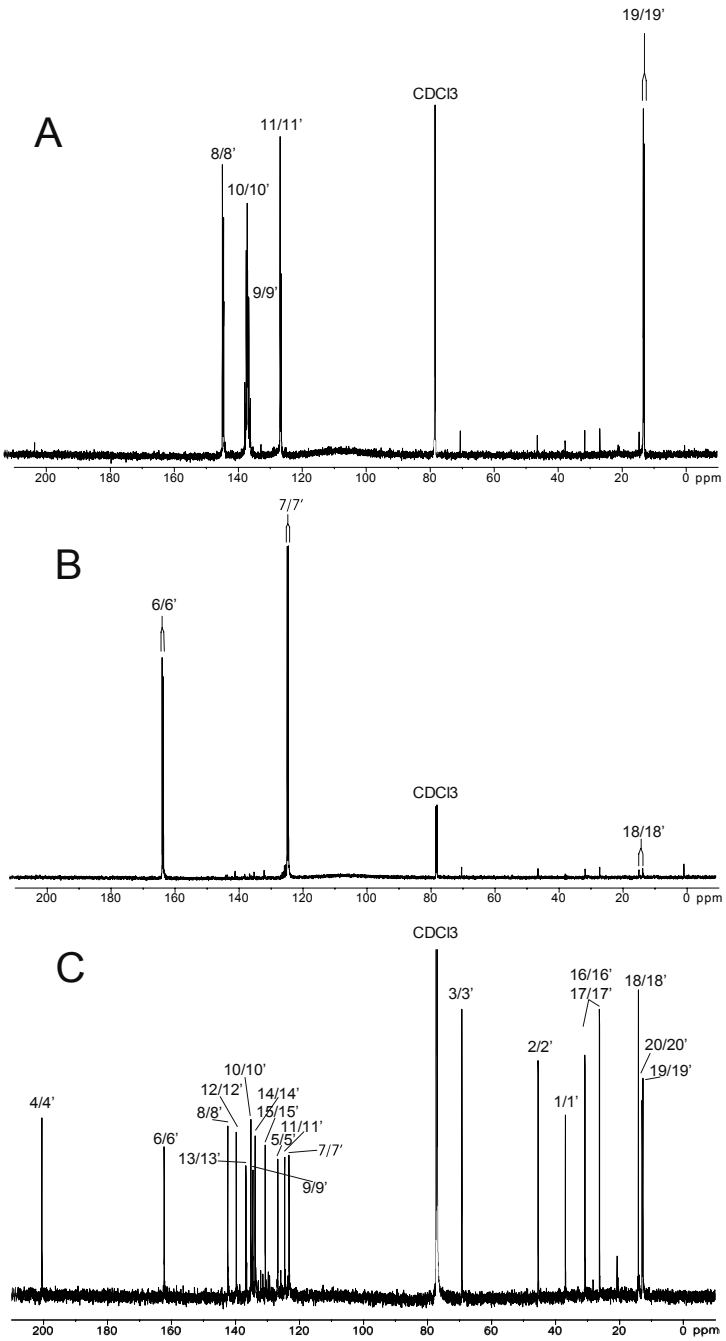

Figure 5. *150 MHz ^{13}C NMR spectrum of [6,6′,7,7′]-$^{13}C_4$ all-E astaxanthin (A), [8,8′,9,9′,10,10′,11,11′,19,19′]-$^{13}C_{10}$ all-E astaxanthin (B) and natural abundance all-E astaxanthin (C) in $CDCl_3$.*

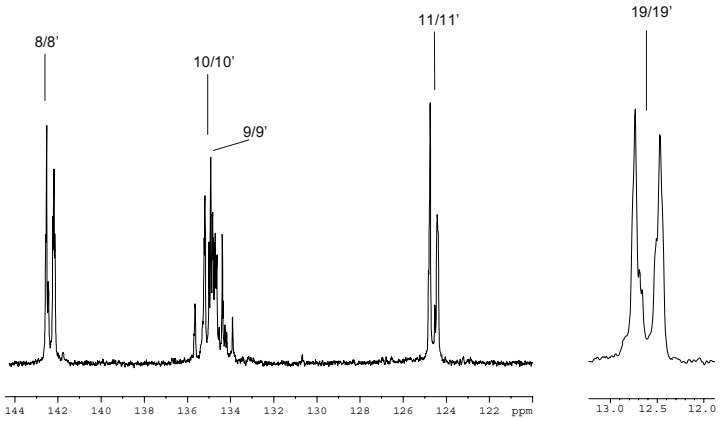

Figure 6. *Enlargement of the significant regions of the 150 MHz ^{13}C NMR spectrum ($CDCl_3$) of all-E [8,8',9,9',10,10',11,11',19,19']-$^{13}C_{10}$ astaxanthin (**1b**).*

The signals of C9/9' and C10/10' show a high order splitting pattern due to the presence of 3 and 2 neighbouring ^{13}C-enriched positions, from which the chemical shift values and J-couplings could not be determined accurately. Also splitting of the signals of C7/7' and C12/12' is observed.

The significant chemical shifts and coupling constants (J) for the ^{1}H NMR and ^{13}C NMR spectra of [6,6',7,7']-$^{13}C_4$ astaxanthin **1a** [8,8',9,9',10,10',11,11',19,19']-$^{13}C_{10}$ astaxanthin **1b** are given in tables 1-4.

Table 1. *^{1}H NMR data of [6,6',7,7']-$^{13}C_4$ astaxanthin (**1a**).*

δ(ppm)	H	Multiplicity	J(Hz)	Integral
1.32/1.21	H-16/H-17	d/d	$^{3}J_{C6H18}$ = 3.4/3.7	12
1.94	H-18	d	$^{3}J_{C6H18}$ = 4.8	6
2.16	H-2_{eq}	ddd	$^{3}J_{C6H2}$ = 6.0 $^{3}J_{H2H3}$ = 12.8/6.8	2
6.21	H-7	dd	$^{1}J_{C7H7}$ = 151.8 $^{3}J_{H7H8}$ = 15.8	2
6.43	H-8	dd	J_{CH} = 4.7 $^{3}J_{H7H8}$ = 15.8	2

Table 2. *^{1}H NMR data of [8,8′,9,9′,10,10′,11,11′,19,19′]-$^{13}C_{10}$ astaxanthin (**1b**).*

δ(ppm)	H	Multiplicity	J(Hz)	Integral
2.00	H-19	d	$^{1}J_{C19H19}$ = 126	6
6.21	H-7	dd	$^{3}J_{C9H7}$ = 4 $^{3}J_{H7H8}$ = 16.1	2
6.29	H-10	dddd	$^{1}J_{C10H10}$ = 138 $^{3}J_{H10H11}$ = 11.2 $^{3}J_{H10C8}$ = 11 $^{3}J_{H10C8}$ = 11	2
6.43	H-8	dd	$^{1}J_{C8H8}$ = 132 $^{3}J_{H7H8}$ = 16.1	2
6.45	H-12	dd	J_{CH} = 7 $^{3}J_{H11H12}$ = 14.7	2
6.66	H-11	ddd	$^{1}J_{C11H11}$ = 143 $^{3}J_{H11H12}$ = 14.7 $^{3}J_{H10H11}$ = 11.2	2

Table 3. *^{13}C NMR data of [6,6′,7,7′]-$^{13}C_{4}$ astaxanthin (**1a**).*

δ(ppm)	C	Multiplicity	J(Hz)
36.8	C-1	d	$^{1}J_{C1C6}$ = 38.2
123.3	C-7	d	$^{1}J_{C6C7}$ = 55
126.8	C-5	d	$^{1}J_{C5C6}$ = 52.5
142.3	C-8	d	$^{1}J_{C7C8}$ = 73.1
162.2	C-6	d	$^{1}J_{C6C7}$ = 55

Table 4. *^{13}C NMR data of [8,8′,9,9′,10,10′,11,11′,19,19′]-$^{13}C_{10}$ astaxanthin (**1b**).*

δ(ppm)	C	Multiplicity	J(Hz)
12.5	C-19	d	$^{1}J_{C9C19}$ = 39
123.2	C-7	d	$^{1}J_{C7C8}$ = 73
124.6	C-11	d	$^{1}J_{C10C11}$ = 50
134.6	C-9	ddd	$^{1}J_{C8C9}$ = 52 $^{1}J_{C9C10}$ = n.d [a] $^{1}J_{C9C19}$ = 39
135.2	C-10	dd	$^{1}J_{C9C10}$ = n.d.[a] $^{1}J_{C10C11}$ = 50
139.8	C-12	d	$^{1}J_{C11C12}$ = n.d.[a]
142.3	C-8	d	$^{1}J_{C8C9}$ = 52

[a] Not determined due to overlap of the signals.

2.9 CONCLUSION

In this chapter, the synthetic schemes that have been developed and optimized for the synthesis of $^{13}C_4$ astaxanthin and $^{13}C_{10}$ astaxanthin are described. The schemes are based on a modular strategy, which was developed to efficiently introduce ^{13}C labels at the desired positions in the carotenoids. The presented synthetic routes are based on known methods, with small modifications, and were successfully applied for the synthesis of [6,6′,7,7′]-$^{13}C_4$ all-*E* astaxanthin **1a** and [8,8′,9,9′,10,10′,11,11′,19,19′]-$^{13}C_{10}$ all-*E* astaxanthin **1b**.

The ^{1}H NMR and ^{13}C NMR characterization of the ^{13}C-labeled astaxanthins, and comparison of the spectra with the data of natural abundance all-*E* astaxanthin, shows that the desired compounds were obtained with good purity. The splitting pattern of the ^{1}H NMR and ^{13}C NMR spectra and increased intensity of the ^{13}C-labeled carbons in the ^{13}C NMR spectra confirmed selective ^{13}C enrichment at the desired postions, with a high isotope enrichment (>99%) was achieved. The ^{13}C NMR spectra of the ^{13}C-labeled compounds show that no scrambling of the ^{13}C labels had occurred.

EXPERIMENTAL

General Remarks: Unless stated otherwise, dry reactions were carried out in a dry nitrogen atmosphere, reaction vessels were flame-dried prior to use. Dry solvents were obtained by distillation (low-boiling petroleum ether 40-60°C with P_2O_5, toluene with CaH_2) and stored on sodium-wire. Dichloromethane (DCM) was dried with CaH_2, and stored on 4Å molecular sieves. THF was distilled from Na/benzophenone, or dried with molecular sieves (4Å). Solutions of NaCl and NH_4Cl refer to saturated solutions of the salts in water. SiO_2/H_2O is a homogeneous mixture of SiO_2 (400 g) and water (120 mL). Ether refers to diethyl ether. PE refers to distilled, low-boiling petroleum ether, bp. 40-60°C. Dibal-H refers to a 1.0 M solution of diisobutyl aluminium hydride in hexanes.

Reactions were monitored using thin-layer chromatography (TLC), on Merck F_{254} silica gel 60 aluminum sheets (0.2 mm). Spots were visualized with UV-light (254 nm) or treated with an oxidizing spray (2g $KMnO_4$ and 4g K_2CO_3 in 100 mL water). Column chromatography was performed using Merck silica gel 60 (0.040-0.063 nm, 230-400 mesh).

^{1}H NMR and ^{13}C NMR spectra were recorded in $CDCl_3$ or CD_3OD on a Bruker AM-600, Bruker AV-400 or a Bruker WM-300 apparatus with tetramethylsilane (TMS; $^{1H}\delta = 0.00$ ppm), $CDCl_3$ ($^{13C}\delta = 77.00$ ppm) or CD_3OD ($^{13C}\delta = 49.00$ ppm) as internal standard. Due to the presence of multiple ^{13}C labels, several ^{1}H and ^{13}C NMR spectra gave a complex splitting pattern, from which the chemical shift values and J-couplings could not be determined accurately. In those cases, the observed estimated values are given here.

All chemicals were purchased from Aldrich, Fluka or Acros Chimica.

3,7-Dimethyl-2,6-octadienenitrile (3)

At -20°C, *n*-BuLi (1.6 M, 60.9 mL, 97.4 mmol) was added to a solution of diisopropylamine (DIPA, 10.3 g, 101 mmol) in dry THF (100 mL). After 1 h the solution was cooled to -80°C, acetonitrile (2.0 g, 48.7 mmol) was added and the mixture was stirred for another hour at -80°C. A solution of diethylchlorophosphate (8.4 g, 48.7 mmol) in THF (20 mL) was slowly added, and after 30 min 6-methyl-5-heptene-2-one **2** (6.1 g, 40.6 mmol) in THF (10 mL) was added. The solution was allowed to warm to RT and stirred overnight. TLC analysis (20% diethyl ether/PE, $KMnO_4$-detection) showed complete conversion of the ketone. A solution of NH_4Cl(sat) was added, the mixture was extracted three times with ether and the organic layer was washed with NaCl(sat). The organic layers were dried with $MgSO_4$, filtered and the solvents evaporated in vacuo. The product was purified on a silica-gel column (20% diethyl ether/PE) to give a 2-*E*/*Z* mixture of 3,7-dimethyl-2,6-octadienenitrile **3** (5.06 g, 33.9 mmol, 84%).

^{1}H NMR ($CDCl_3$) δ (ppm) = 1.60 (s, 3 H, 7*Z*-CH_3), 1.69 (s, 3 H, 7*E*-CH_3), 2.05 (s, 3 H, 3-CH_3), 2.19 (br. s, 4 H, 4-H/5-H), 5.03 (m, 1 H, 6-H), 5.10 (s, 1 H, 2-H).

^{13}C NMR ($CDCl_3$) δ (ppm) = 17.5 (7*Z*-CH_3), 20.8 (3*E*-CH_3), 22.7 (3*Z*-CH_3), 25.7 (C-5), 25.7 (7*E*-CH_3), 36.1 (C-4*Z*), 38.4 (C-4*E*), 95.0 (C-2*Z*), 95.7 (C-2*E*), 116.8 (C-1*E*), 117.1 (C-1*E*), 122.0 (C-6), 133.0 (C-7), 164.9 (C-3).

[1,2]-$^{13}C_2$ 3,7-Dimethyl-2,6-octadienenitrile (3a)

Using a similar procedure as described above, $^{13}C_2$ acetonitril (2.0 g, 46.5 mmol) was deprotonated with

LDA [made from *n*-BuLi (58.1 mL, 92.9 mmol) and DIPA (9.8 g, 96.8 mmol) in dry THF (10 mL)] at -80°C. Subsequently, diethyl chlorophosphate (8.0 g, 46.5 mmol) and 6-methyl-5-heptene-2-one (4.9 g, 38.7 mmol) were added and the solution was allowed to warm to RT overnight. After workup and silica-gel purification, (20% diethyl ether/PE) an *E*/*Z*-mixture of [1,2]-$^{13}C_2$ 3,7-dimethyl-2,6-octadienenitrile **3a** (5.62 g, 37.2 mmol, 96%) was obtained.

^{1}H NMR ($CDCl_3$) δ (ppm) = 1.61 (s, 3 H, 7*Z*-CH_3), 1.69 (s, 3 H, 7*E*-CH_3), 2.05 (d, *J* = 6.0 Hz, 3 H, 3-CH_3), 2.18 (m, 4 H, 4-H/5-H), 5.04 (m, 1 H, 6-H), 5.10 (dd, *J* = 2.0 Hz/172 Hz, 1 H, 2-H).

^{13}C NMR ($CDCl_3$) δ (ppm) = 17.6 (7*Z*-CH_3), 20.9 (3*E*-CH_3), 25.5 (7*Z*-CH_3), 36.2 (C-4*Z*), 38.4 (C-4*E*), 95.1 (d, *J* = 78.9 Hz, C-2*Z*), 95.6 (d, *J* = 79.1 Hz, C-2*E*), 116.9 (d, *J* = 79.1 Hz, C-1*E*), 117.2 (d, *J* = 78.9 Hz, C-1*Z*), 122.1 (C-6), 133.1 (C-7), 164.9 (d, *J* = 74.4 Hz, C-3).

2,6,6-Trimethyl-2-cyclohexenecarbonitrile (4)

A solution of 3,7-dimethyl-2,6-octadienenitrile **3** (5.06 g, 33.9 mmol) in nitromethane (20 mL) was slowly added to sulfuric acid (5 mL) in nitromethane (50 mL) at 0°C. After stirring for 30 min at 0°C water (100 mL) was added and the mixture extracted three times with diethyl ether. The combined organic layers were washed twice with NaCl(sat) and neutralized with NaOAc(sat). After drying the organic layers with $MgSO_4$, the solution was concentrated in vacuo. Flash chromatography (silica gel, 10% diethyl ether/PE) gave a mixture of α-cyclonitrile (~95%; 4.24 g, 28.4 mmol, 84% yield) and β-cyclonitrile (~5%).

^{1}H NMR ($CDCl_3$) δ (ppm) = 1.04 (s, 3 H, 6-CH_3), 1.14 (s, 3 H, 6-CH_3), 1.5-1.6 (m, 3 H, 5-H), 1.83 (s, 3 H, 2-CH_3), 2.05 (m, 2 H, 4-H), 2.77 (br. s, 1 H, 1-H), 5.59 (br. s, 1 H, 3-H).

^{13}C NMR ($CDCl_3$) δ (ppm) = 22.4 (C-4), 22.4 (2-CH_3), 25.4 (6-CH_3), 26.7 (6-CH_3), 31.8 (C-6), 32.6 (C-5), 43.7 (C-1), 119.6 (CN), 124.5 (C-3), 126.3 (C-2).

[1]-^{13}C 2,6,6-Trimethyl-2-cyclohexene-^{13}C-carbonitrile (4a)

In a similar way to that described above, [1,2]-$^{13}C_2$ 3,7-dimethyl-2,6-octadienenitrile **3a** (5.62 g, 37.2 mmol) in nitromethane (20 mL) was added to a mixture of sulfuric acid in nitromethane at 0°C. After workup, [1]-^{13}C 2,6,6-trimethyl-2-cyclohexene-^{13}C-carbonitrile **4a** (4.67 g, 30.9 mmol, 83%) was obtained.

^{1}H NMR ($CDCl_3$) δ (ppm) = 1.04 (d, *J* = 5.3 Hz, 3 H, 6-CH_3), 1.14 (d, *J* = 4.7 Hz, 3 H, 6-CH_3), 1.3-1.8 (m, 2 H, 5-H), 1.83 (d, *J* = 4.7 Hz, 3 H, 2-CH_3), 2.05 (m, 2 H, 4-H), 2.77 (dd, *J* = 11.6 Hz/132.6 Hz, 1 H, 1-H), 5.59 (m, 1 H, 4-H).

^{13}C NMR ($CDCl_3$) δ (ppm) = 22.3 (C-4), 22.4 (2-CH_3), 25.3 (6-CH_3), 26.7 (6-CH_3), 31.7 (d, *J* = 32.7 Hz, C-6), 32.5 (d, *J* = 2.1 Hz, C-5), 43.6 (d, *J* = 55.3 Hz, C-1), 119.4 (d, *J* = 55.3 Hz, CN), 124.4 (d, *J* = 2.4 Hz, C-3), 126.3 (d, *J* = 35.2 Hz, C-2).

2,3-Epoxy-2,6,6-trimethylcyclohexanecarbonitrile (5)

A solution of **4** (4.24 g, 28.4 mmol) in ethyl acetate (40 mL) was added to *m*CPBA (70% in water, 9.1 g, 36.9 mmol) in ethyl acetate (40 mL) at 0°C and the solution was stirred overnight at RT. The solution was concentrated in vacuo, PE (150 mL) was added, and at 0°C TEA (4.6 g, 45.5 mmol) was added. After stirring for 10 min the suspension was filtered through silica gel and washed with 25% ether/3% TEA/PE and concentrated. When necessary, the resulting product was filtered a second time through silica gel to remove all

chlorobenzoic acid. This way, crude 2,3-epoxy-2,6,6-trimethylcyclohexanecarbonitrile **5** (4.04 g, 34.5 mmol, 86%) was obtained as a yellow liquid.

^{1}H NMR ($CDCl_3$) δ (ppm) = 1.05 (s, 3 H, 6-CH_3), 1.09 (s, 3 H, 6-CH_3), 1.20-1.35 (m, 2 H, 5-H), 1.55 (s, 3 H, 2-CH_3), 1.99 (m, 2 H, 4-H), 2.75 (s, 1 H, 1-H), 3.05 (s, 1 H, 3-H).

^{13}C NMR ($CDCl_3$) δ (ppm) = 20.7/21.5 (2-CH_3), 23.3 (C-4), 28.4 (C-6), 29.3/30.3 (6-CH_3), 31.3 (C-5), 44.7 (C-1), 55.3 (C-2), 58.6 (C-3), 118.5 (CN).

[1]-^{13}C 2,3-Epoxy-2,6,6-trimethylcyclohexane-^{13}C-carbonitrile (5)

By using the same procedure as described above, **4a** (4.67 g, 30.9 mmol) reacted with mCPBA (70%, 9.9 g, 40.2 mmol), to obtain crude 2,3-epoxy-2,6,6-trimethylcyclohexanecarbonitrile **5a** (4.67 g, 27.9 mmol, 90%).

^{1}H NMR ($CDCl_3$) δ (ppm) = 1.05 (s, 3 H, 6-CH_3), 1.09 (s, 3 H, 6-CH_3)**,** 1.2-1.4 (m, 2 H, 5-H), 1.55 (d, *J* = 3.1 Hz, 3 H, 2-CH_3), 1.8-2.1 (m, 2 H, 4-H), 2.74 (dd, *J* = 11.0 Hz/134.2 Hz, 1 H, 1-H), 3.05 (br. s, 1 H, 3-H).

^{13}C NMR ($CDCl_3$) δ (ppm) = 44.7 (d, *J* = 57 Hz, C-1), 118.5 (d, *J* = 57 Hz, CN).

3-Hydroxy-2,6,6-trimethyl-1-cyclohexenecarbonitrile (6)

Lithium diisopropylamide (LDA) was prepared at -20°C by adding *n*-BuLi (16.8 mL, 26.9 mmol) to a solution of DIPA (4.1 mL, 29.3 mmol) in dry THF. A solution of 2,3-epoxy-2,6,6-trimethylcyclohexanecarbonitrile **5** (4.04 g, 24.5 mmol) in dry THF (10 mL) was slowly added at -40°C, and the reaction mixture was allowed to warm to RT overnight. The mixture was neutralized by adding NH_4Cl(sat), and extracted three times with diethyl ether. The combined organic layers were washed with NaCl(sat) and dried with $MgSO_4$. After filtration and concentration in vacuo the crude product 3-hydroxy-2,6,6-trimethyl-1-cyclohexenecarbonitrile **6** (4.32 g, 24.5 mmol, 100%) was obtained.

^{1}H NMR ($CDCl_3$) δ **=** 1.14 (s, 3 H, 6-CH_3), 1.20 (s, 3 H, 6-CH_3), 1.4-2.0 (m, 4 H, 4-H/5-H), 2.10 (s, 3 H, 2-CH_3), 4.05 (t, *J* = 6.0 Hz, 3-H).

^{13}C NMR ($CDCl_3$) δ **=** 19.4 (2-CH_3), 27.6 (6-CH_3), 27.8 (C-4), 32.7 (C-5), 33.2 (C-6), 67.5 (C-3), 117.2 (CN), 119.4 (C-1), 152.5 (C-2).

[1]-^{13}C 3-Hydroxy-2,6,6-trimethyl-1-cyclohexene-^{13}C-carbonitrile (6a)

By using a similar procedure as described for the unlabeled product, **5a** (4.67 g, 27.9 mmol) was deprotonated with 1.1 equiv. LDA to give crude [1]-^{13}C 3-hydroxy-2,6,6-trimethyl-1-cyclohexene-^{13}C-carbonitrile **6a** (4.67 g, 27.9 mmol, 100%) as a dark yellow liquid.

^{1}H NMR ($CDCl_3$) δ = 1.14 (s, 3 H, 6-CH_3), 1.19 (s, 3 H, 6-CH_3), 1.3-2.0 (m, 4 H, 4-H/5-H), 2.09 (d, *J* = 5.5 Hz, 3 H, 2-CH_3), 4.05 (dt, *J* = 4 Hz, 1 H, 3-H).

^{13}C NMR ($CDCl_3$) δ **=** 116.9 (d, *J* = 75.3 Hz, CN), 119.9 (d, *J* = 75.3 Hz, C-1).

3-Oxo-2,6,6-trimethyl-1-cyclohexenecarbonitrile (7)

A solution of 3-hydroxy-2,6,6-trimethyl-1-cyclohexenecarbonitrile **6** (4.32 g, 24.5 mmol) in DCM (20 mL) was slowly added to a suspension of PCC/Al (20 wt%, 36.6 g, 34 mmol) in DCM (75 mL) at 0°C. The suspension

was stirred overnight at RT, filtered through silica gel, washed with diethyl ether and concentrated in vacuo. The brown-black suspension was filtered a second time through silica gel, until a clear yellow solution was obtained. The solvents were removed in vacuo and the resulting crude product was purified on a silica-gel column (20-40% diethyl ether/PE gradient elution) to give 3-oxo-2,6,6-trimethyl-1-cyclohexenecarbonitrile **7** (2.63 g,16.1 mmol, 62% over 3 steps).

^{1}H NMR ($CDCl_3$) δ = 1.34 (s, 6 H, 6-CH_3), 1.95 (t, *J* = 6.9 Hz, 2 H, 5-H), 2.06 (s, 3 H, 2-CH_3), 2.56 (t, *J* = 6.9 Hz, 2 H, 4-H).

^{13}C NMR ($CDCl_3$) δ **=** 15.2 (2-CH_3), 27.2 (6-CH_3), 33.8 (C-4), 34.4 (C-6), 35.7 (C-5), 115.6 (CN), 135.3 (C-1), 144.2 (C-2), 196.2 (C-3).

[1]-^{13}C 3-Oxo-2,6,6-trimethyl-1-cyclohexene-^{13}C-carbonitrile (7a)

By using the procedure described above, crude [1]-^{13}C 3-hydroxy-2,6,6-trimethyl-1-cyclohexene-^{13}C-carbonitrile **6a** (4.67 g, 27.9 mmol) was oxidized with PCC/Al (20 wt%, 39.1 g, 36.3 mmol). After workup and purification, [1]-^{13}C 3-oxo-2,6,6-trimethyl-1-cyclohexene-^{13}C-carbonitrile **7a** (3.35 g, 20.3 mmol, 73%) was obtained as a pale yellow liquid.

^{1}**H NMR** ($CDCl_3$) δ = 1.34 (d, *J* = 4.8 Hz, 6 H, 6-CH_3), 1.96 (dt, *J* = 5.9 Hz/6.9 Hz, 2 H, 2-H), 2.05 (d, *J* = 6.2 Hz, 3 H, 2-CH_3), 2.56 (t, *J* = 6.9 Hz, 2 H, 3-H).

^{13}**C NMR** ($CDCl_3$) δ **=** 15.1 (2-CH_3), 27.1 (6-CH_3), 33.8 (C-4), 34.3 (d, *J* = 41.5 Hz, C-6), 35.6 (C-5), 115.5 (d, *J* = 74.4 Hz, CN), 134.9 (d, *J* = 74.4 Hz, C-1), 144.1 (d, *J* = 70.2 Hz, C-2), 196.2 (C-4).

2,10,10-Trimethyl-4,7-dioxaspiro[4,5]dec-1-enecarbonitrile (8)

A catalytic amount of *p*-toluenesulfonic acid was added to a mixture of 3-oxo-2,6,6-trimethyl-1-cyclohexenecarbonitrile **7** (2.63 g, 16.1 mmol), trimethyl orthoformate (3.5 mL) and ethylene glycol (2.7 mL). After stirring for 2 h, TLC (25% diethyl ether/PE) showed complete conversion of the starting material and the reaction was quenched by adding $NaHCO_3$(sat). The mixture was extracted three times with diethyl ether, the combined organic layers were washed with NaCl(sat) and dried with $MgSO_4$. After removal of the solids by filtration and concentration in vacuo, the crude product was dissolved in acetone (75 mL) and 10 drops HCl (1 M) were added. The mixture was stirred for 5 min and K_2CO_3 and $MgSO_4$ were added. The solids were removed by filtration and the solvents were removed in vacuo. After flash-column chromatography (silica gel, 25% diethyl ether/2% TEA/PE) 2,10,10-trimethyl-4,7-dioxaspiro[4,5]dec-1-enecarbonitrile **8** (3.27 g, 15.8 mmol, 98%) was obtained.

^{1}**H NMR** ($CDCl_3$) δ = 1.18 (s, 6 H, 10-CH_3), 1.60-1.85 (m, 4 H, 8-H/9-H), 1.97 (s, 3 H, 2-CH_3), 4.02 (s, 4 H, 5-H/6-H).

^{13}**C NMR** ($CDCl_3$) δ **=** 15.6 (2-CH_3), 27.3 (10-CH_3), 29.3 (C-8), 33.3 (C-10), 33.8 (C-9), 65.2 (C-5/C-6), 105.0 (C-4), 116.4 (CN), 122.5 (C-1), 149.7 (C-2).

[1]-^{13}C 2,10,10-Trimethyl-4,7-dioxaspiro[4,5]dec-1-ene-^{13}C-carbonitrile (8a)

By using a similar procedure as described for the unlabeled compound, [1]-^{13}C 3-oxo-2,6,6-trimethyl-1-cyclohexene-^{13}C-carbonitrile **7a** (3.35 g, 20.3 mmol) was converted into the corresponding acetal **8a** (4.16 g, 19.9 mmol, 98%).

^{1}**H NMR** ($CDCl_3$) δ = 1.18 (d, *J* = 4.4 Hz, 6 H, 10-CH_3), 1.66-1.80 (m, 4 H, 8-H/9-H), 1.96 (d, *J* = 5.0 Hz, 3 H, 2-CH_3), 4.02 (br. s, 4 H, 5-H/6-H).

^{13}**C NMR** ($CDCl_3$) δ = 15.7 (2-CH_3), 27.4 (10-CH_3), 29.4 (C-8), 33.4 (d, *J* = 46.3 Hz, C-10), 34.0 (C-9), 65.3 (C-5/C-6), 105.2 (C-4), 116.5 (d, *J* = 74.6 Hz, CN), 122.7 (d, *J* = 74.6, C-1), 149.7 (d, *J* = 73.8 Hz, C-2).

2,10,10-Trimethyl-4,7-dioxaspiro[4,5]dec-1-enecarbaldehyde (9)

At -60°C, Dibal-H (20.5 mL, 20.5 mmol) was added to a solution of 2,10,10-trimethyl-4,7-dioxaspiro[4,5]dec-1-enecarbonitrile **8** (3.27 g, 15.8 mmol) in dry PE. The solution was allowed to warm to RT during 1 h and stirred for another hour at RT. Subsequently, the solution was cooled to -20°C and SiO_2/H_2O (36 g) was added. The suspension was stirred for 1 h at 0°C, K_2CO_3 and $MgSO_4$ were added, and the solids were removed by filtration. The crude product was concentrated in vacuo, and purified on a flash-column (silica gel, 50% diethyl ether/1% TEA/PE) to give 2,10,10-trimethyl-4,7-dioxaspiro[4,5]dec-1-enecarbaldehyde **9** (2.97 g, 14.1 mmol, 89%).

^{1}**H NMR** ($CDCl_3$) δ = 1.21 (s, 6 H, 10-CH_3), 1.58 (m, 2 H, 9-H), 1.79 (m, 2 H, 8-H), 2.01 (s, 3 H, 2-CH_3), 4.07 (s, 4 H, 5-H/6-H), 10.16 (s, 1 H, *H*C=O).

^{13}**C NMR** ($CDCl_3$) δ = 10.9 (2-CH_3), 26.9 (10-CH_3), 29.3 (C-8), 33.3 (C-10), 36.5 (C-9), 65.4 (C-5/C-6), 107.1 (C-4), 143.7 (C-1), 149.5 (C-2), 193.8 (*C*=O).

[1]-^{13}C 2,10,10-Trimethyl-4,7-dioxaspiro[4,5]dec-1-ene-^{13}C-carbaldehyde (9a)

Reduction of [1]-^{13}C 2,10,10-trimethyl-4,7-dioxaspiro[4,5]dec-1-ene-^{13}C-carbonitrile **8a** (4.16 g, 19.9 mmol) with Dibal-H (25.9 mL, 25.9 mmol) to the corresponding aldehyde was carried out using the same procedure as described above, to obtain [1]-^{13}C-2,10,10-trimethyl-4,7-dioxaspiro[4,5]dec-1-ene-^{13}C-carbaldehyde **9a** (3.64 g,17.1 mmol, 86%).

^{1}**H NMR** ($CDCl_3$) δ = 1.20 (d, *J* = 3.8 Hz, 6 H, 10-CH_3), 1.53-1.59 (m, 2 H, 9-H), 1.76-1.80 (m, 2 H, 8-H), 2.01 (d, *J* = 4.3 Hz, 3 H, 2-CH_3), 4.06 (br. s, 4 H, 5-H/6-H), 10.16 (dd, *J* = 11.0 Hz/173.4 Hz, 1 H, *H*C=O).

^{13}**C NMR** ($CDCl_3$) δ = 10.9 (2-CH_3), 26.8 (10-CH_3), 29.2 (C-8), 33.2 (d, *J* = 39.4, C-10), 36.5 (C-9), 65.3 (C-5/C-6), 106.9 (C-4), 144.7 (d, *J* = 50.9 Hz, C-1), 149.4 (d, *J* = 68.9 Hz, C-2), 193.4 (d, *J* = 50.9 Hz, *C*=O).

Bromoacetic acid

Trifluoroacetic acid anhydride (TFAA; 21 mL, 147 mmol) was slowly added to acetic acid **10** (3.0 g, 50 mmol) at 0°C. Bromine (8.0 g, 2.6 mL, 50 mmol) was added and the brown mixture was stirred at RT for 22 h, in the course of which the mixture became colorless. Water (2.7 mL, 150 mmol) was added at 0°C and the mixture stirred for 30 min. Trifluoroacetic acid (TFA) was removed by destillation, and the resulting bromoacetic acid was collected as a white solid. The distillate was found to contain a small additional amount of bromoacetic acid, which was collected by removing TFA under a nitrogen flow, to obtain white, solid bromoacetic acid (6.71 g, 48.3 mmol, 97%).

^{1}**H NMR** ($CDCl_3$) δ (ppm) = 3.92 (s, 2 H, 2-H).

^{13}**C NMR** ($CDCl_3$) δ (ppm) = 173.1 (C-1), 25.2 (C-2).

$^{13}C_2$ Bromoacetic acid

By using the same procedure as described above, $^{13}C_2$ acetic acid **10b** (3.0 g, 48.3 mmol) was converted to $^{13}C_2$ bromoacetic acid (6.80 g, 48.2 mmol, 99%).

^{1}H NMR ($CDCl_3$) δ (ppm) = 3.92 (dd, *J* = 4.7 Hz/153 Hz, 2 H, 2-H), 10.37 (s, 1 H, OH).

^{13}C NMR ($CDCl_3$) δ (ppm) = 25.2 (d, *J* = 52.6 Hz, C-2), 173.1 (d, *J* = 52.6 Hz, C-1).

Ethyl bromoacetate (11)

Oxalyl chloride (4.6 mL, 6.7 g, 53 mmol) was added to bromoacetic acid (6.71 g, 48.3 mmol) and the mixture was stirred for 30 h. After cooling to 0°C ethanol (3.4 mL, 58 mmol) was slowly added. The reaction was quenched after 30 min by adding brine. The mixture was extracted three times with diethyl ether, washed with $NaHCO_3$- and NaCl-solutions, dried with Na_2SO_4, filtered and the solvent was evaporated in vacuo, to yield ethyl bromoacetate **11** (7.41 g, 44.4 mmol, 92%).

^{1}H NMR ($CDCl_3$) δ (ppm) = 1.30 (t, *J* = 7.2 Hz, 3 H, OCH_2CH_3), 3.87 (s, 2 H, 2-H), 4.23 (q, *J* = 7.2 Hz, 2 H, OCH_2CH_3).

^{13}C NMR ($CDCl_3$) δ (ppm) = 13.7 (OCH_2CH_3), 40.7 (C-2), 62.0 (OCH_2CH_3), 166.9 (C-1).

[1,2]-$^{13}C_2$ Ethyl bromoacetate (11b)

By using the same procedure as described before, $^{13}C_2$ bromoacetic acid (6.8 g, 48.2 mmol) reacted with ethanol to give [1,2]-$^{13}C_2$ ethyl bromoacetate **11b** (7.50 g, 44.4 mmol, 92%)

^{1}H NMR ($CDCl_3$) δ (ppm) = 1.30 (t, *J* = 7.2 Hz, 3 H, OCH_2CH_3), 3.87 (dd, *J* = 4.3 Hz/153.4 Hz, 2 H, 2-H), 4.23 (dq, *J* = 3.2 Hz/7.2 Hz, 2 H, OCH_2CH_3).

^{13}C NMR ($CDCl_3$) δ (ppm) = 13.7 (OCH_2CH_3), 25.8 (d, *J* = 65.1 Hz, C-2), 62.0 (OCH_2CH_3), 166.9 (d, *J* = 65.1 Hz, C-1).

Triethyl phosphonoacetate (12)

Triethyl phosphite (8.4 mL, 8.1 g, 48.8 mmol) was added to ethyl bromoacetate **11** (7.51 g, 44.4 mmol) and the mixture was refluxed at 180°C for 5 h, while ethyl bromide was removed occasionally by suction. After distillation at reduced pressure triethyl phosphonoacetate **12** (9.67 g, 42.8 mmol, 96%) was obtained as a colorless oil.

^{1}H NMR ($CDCl_3$) δ (ppm) = 1.35 (m, 9 H, OCH_2CH_3), 2.97 (d, *J* = 21.6 Hz, 2 H, 2-H), 4.18 (m, 6 H, OCH_2CH_3).

^{13}C NMR ($CDCl_3$) δ (ppm) = 13.8 (OCH_2CH_3), 16.0 ($POCH_2CH_3$), 34.0 (d, *J* = 134.0 Hz, C-2), 61.2 (OCH_2CH_3), 62.3 ($POCH_2CH_3$), 165.5 (C-1).

[1,2]-$^{13}C_2$ Triethyl phosphonoacetate (12a)

In a similar way to that described above, [1,2]-$^{13}C_2$ ethyl bromoacetate **11b** (7.5 g, 44.4 mmol) reacted with triethyl phosphite to give [1,2]-$^{13}C_2$ triethyl phosphonoacetate **12b** (9.03 g, 40 mmol, 90%).

^{1}H NMR ($CDCl_3$) δ (ppm) = 1.35 (m, 9 H, OCH_2CH_3), 2.97 (ddd, *J* = 7.4 Hz/21.6 Hz/129.9 Hz, 2 H, 2-H), 4.18 (m, 6 H, OCH_2CH_3).

^{13}C NMR ($CDCl_3$) δ (ppm) = 13.8 (OCH_2CH_3), 16.0 ($POCH_2CH_3$), 34.0 (dd, *J* = 58.8 Hz/134.0 Hz, C-2), 61.2 (OCH_2CH_3), 62.3 ($POCH_2CH_3$), 165.5 (d, *J* = 58.8 Hz, C-1).

Ethyl 2-chloro acetoacetate (14)

Sulfuryl chloride (SO_2Cl_2; 3.7 mL, 6.2 g, 46.0 mmol) was added to ethyl acetoacetate **13** (5.9 mL, 6.0 g, 46.0 mmol) at 0°C and the mixture was stirred overnight at RT. Traces of sulfuryl chloride were removed in vacuo, to give 2-chloro ethyl acetoacetate **14** (7.5 g, 45.6 mmol, 99%).

^{1}H NMR ($CDCl_3$) δ (ppm) = 1.32 (t, *J* = 7.1 Hz, 3 H, OCH_2CH_3), 2.39 (s, 3 H, 1-H), 4.30 (q, *J* = 7.1 Hz, 2 H, OCH_2CH_3), 4.78 (s, 1 H, 2-H).

^{13}C NMR ($CDCl_3$) δ (ppm) = 13.8 (OCH_2CH_3), 26.1 (C-4), 61.2 (C-2), 63.0 (OCH_2CH_3), 164.7 (C-1), 196.3 (C-3).

[1,2,3,4]-$^{13}C_4$ Ethyl 2-chloro acetoacetate (14b)

[1,2,3,4]-$^{13}C_4$ Ethyl acetoacetate **13b** (6.0 g, 44.8 mmol) reacted with sulfuryl chloride (6.2 g, 23.0 mmol), using the same procedure as described above, to give [1,2,3,4]-$^{13}C_4$ 2-chloro ethyl acetoacetate **14b** (7.55 g, 44.8 mmol, 100%).

^{1}H NMR ($CDCl_3$) δ (ppm) = 1.32 (t, *J* = 7.1 Hz, 3 H, OCH_2CH_3), 2.39 (ddd, *J* = 1.3 Hz/6.3 Hz/130.8 Hz, 3 H, 1-H), 4.30 (dq, *J* = 3.3 Hz/7.1 Hz, 2 H, OCH_2CH_3), 4.78 (ddd, *J* = 5.6 Hz/5.6 Hz/154.4 Hz, 1 H, 2-H).

^{13}C NMR ($CDCl_3$) δ (ppm) = 13.8 (OCH_2CH_3), 26.1 (dd, *J* = 15.5 Hz/44.9 Hz, C-4), 61.2 (ddd, *J* = 15.5 Hz/38.4 Hz/62.4 Hz, C-2), 63.0 (OCH_2CH_3), 164.7 (d, *J* = 62.4 Hz, C-1), 196.3 (dd, *J* = 38.4 Hz/44.9 Hz, C-3).

Chloroacetone (15)

Ethyl 2-chloro acetoacetate **14** (3.6 g, 21.9 mmol) was dissolved in THF (75 mL) and H_2O (2 mL) and H_2SO_4 (2.3 mL) were added. The solution was refluxed for 2 days and the reaction was quenched with brine. The mixture was extracted three times with diethyl ether, the combined organic phases were washed with a saturated NaCl solution and dried with $MgSO_4$. The solid was removed by filtration and the diethyl ether was removed using a rotary evaporater. Chloroacetone **15** was stored in THF and mol. sieves were added to keep the mixture dry. The product was used for the next reaction without further purification.

[1,2,3]-$^{13}C_3$ Chloroacetone (15b)

[1,2,3,4]-$^{13}C_4$ Ethyl 2-chloro acetoacetate **14b** (3.7 g, 22.0 mmol) was converted into [1,2,3]-$^{13}C_3$ chloroacetone **15b** using the same procedure as described above. The product was stored in THF with mol. sieves and used in the next reaction without further purification.

Ethyl 3-methyl-4-chlorocrotonate (16)

Triethyl phosphonacetate **12** (8 g, 35.8 mmol) was dissolved in dry THF in a 500 mL three-necked round-bottomed flask under a nitrogen atmosphere. The solution was cooled to -80 °C and *n*-BuLi (19.2 mL, 30.7 mmol) was added using a syringe. The anion was formed while the mixture was stirred for 30 min at -80 °C, after which chloroacetone **15** in THF was added using a dropping funnel. The mixture was allowed to warm to RT and stirred at for 2 h. A saturated NH_4Cl solution was added and the mixture was extracted

three times with diethyl ether. The combined organic layers were washed with brine and dried with $MgSO_4$. This was removed by filtration and the solution was concentrated in vacuo. The resulting brown oil was purified by flash chromatography (10% diethyl ether/PE) to obtain ethyl 3-methyl-4-chlorocrotonate **16** (2.56 g, 15.3 mmol, 72% over 2 steps) as a mixture of *E*/*Z* isomers.

^{1}H NMR ($CDCl_3$) δ (ppm) = 1.29 (t, *J* = 7.2 Hz, 3 H, OCH_2CH_3), 2.03 (s, 3 H, 3-CH_3*Z*), 2.24 (s, 3 H, 3-CH_3*E*), 4.05 (s, 2 H, 4*E*-H), 4.18 (q, *J* = 7.2 Hz, 2 H, OCH_2CH_3), 4.68 (s, 2 H, 4*Z*-H), 5.79 (s, 1 H, 2*Z*-H), 5.96 (s, 1 H, 2*E*-H).

^{13}C NMR ($CDCl_3$) δ (ppm) = 14.1 (OCH_2CH_3), 16.6 (3-CH_3*Z*), 22.6 (3-CH_3*E*), 42.0 (C-4*Z*), 49.8 (C-4*E*), 59.9 (OCH_2CH_3), 118.8 (C-2*E*), 119.5 (C-2*Z*), 151.8 (C-3*E*), 152.1 (C-3*Z*), 165.8 (C-1).

[1,2,3,4,3-methyl]-$^{13}C_5$ Ethyl 3-methyl-4-chlorocrotonate (16b)

By using the same procedure as described above, [1,2]-$^{13}C_2$ triethyl phosphonoacetate **12b** (9.7 g, 42.8 mmol) reacted with [1,2,3]-$^{13}C_3$ chloroacetone **15b** to give [1,2,3,4,3-methyl]-$^{13}C_5$ ethyl 3-methyl-4-chlorocrotonate **16b** (3.23 g, 19.3 mmol, 88% over 2 steps). Excess triethyl phosphonoacetate was collected by washing the flash-column with diethyl ether and subsequent distillation under reduced pressure, to recover pure [1,2]-$^{13}C_2$ triethyl phosphonoacetate **12b** (2.71 g, 12.0 mmol).

^{1}H NMR ($CDCl_3$) δ (ppm) = 1.29 (t, *J* = 7.2 Hz, 3 H, OCH_2CH_3), 2.03 (dddd, *J* = 4.3 Hz/4.3 Hz/4.9 Hz/128.0 Hz, 3 H, 3-CH_3*Z*), 2.24 (dddd, *J* = 4.1 Hz/4.1 Hz/4.7 Hz/128.9 Hz, 3 H, 3-CH_3*E*), 4.05 (dddd, *J* = 3.6 Hz/3.6 Hz/4.3 Hz/150.2 Hz, 2 H, 4*E*-H), 4.18 (dq, *J* = 2.0 Hz/7.2 Hz, 2 H, OCH_2CH_3), 4.68 (dddd, *J* = 4.0 Hz/4.0 Hz/4.2 Hz/153.4 Hz, 2 H, 4*Z*-H), 5.79 (ddd, *J* = 7.4 Hz/7.4 Hz/161.5 Hz, 1 H, 2*Z*-H), 5.96 (ddd, *J* = 7.5 Hz/7.5 Hz/161.4 Hz, 1 H, 2*E*-H).

^{13}C NMR ($CDCl_3$) δ (ppm) = 14.1 (OCH_2CH_3), 16.6 (d, *J* = 41.7 Hz, 3-CH_3*Z*), 22.6 (d, *J* = 43.1 Hz, 3-CH_3*E*), 42.0 (d, *J* = 42.9 Hz, C-4*Z*), 49.8 (d, *J* = 43.4 Hz, C-4*E*), 59.9 (m, OCH_2CH_3), 118.8 (m, C-2*E*), 119.5 (m, C-2*Z*), 151.8 (m, C-3*E*), 152.1 (m, C-3*Z*), 165.8 (dd, *J* = 3.5 Hz/8.8 Hz, C-1).

Triethyl 3-methyl-4-phosphonocrotonate (17)

Triethyl phosphite (2.9 mL, 2.8 g, 16.8 mmol) was added to ethyl 3-methyl-4-chlorocrotonate **16** (2.56 g, 15.3 mmol) and the mixture was refluxed for 5 h at 180°C, while the formed chloroethane was occasionally removed by applying suction. Distillation under reduced pressure gave triethyl 3-methyl-4-phosphonocrotonate **17** (mixture of *E*/*Z* isomers; 3.70 g, 14.0 mmol, 92%) as a colorless oil.

^{1}H NMR ($CDCl_3$) δ (ppm) = 1.31 (m, 9 H, OCH_2CH_3), 2.06 (m, 3 H, 3-CH_3*Z*), 2.31 (m, 3 H, 3-CH_3*E*), 2.70 (d, *J* = 23.3 Hz, 2 H, 4*E*-H), 3.48 (d, *J* = 24.7 Hz, 2 H, 4*Z*-H), 4.14 (m, 6 H, OCH_2CH_3), 5.80 (s, 1 H, 2-H).

^{13}C NMR ($CDCl_3$) δ (ppm) = 14.0 (OCH_2CH_3), 16.0 ($POCH_2CH_3$), 19.6 (3-CH_3*Z*), 25.7 (3-CH_3*E*), 31.2 (d, *J* = 33.6 Hz, C-4*Z*), 38.2 (d, *J* = 37.7 Hz, C-4*E*), 59.4 (OCH_2CH_3), 61.8 (m, $POCH_2CH_3$), 118.5 (d, *J* = 11.7 Hz, C-2*Z*), 119.6 (d, *J* = 11.7 Hz, C-2*E*), 149.2 (d, *J* = 11.7 Hz, C-3), 165.6 (C-1*E*), 165.6 (C-1*Z*).

[1,2,3,4,3-methyl]-$^{13}C_5$ Triethyl 3-methyl-4-phosphonocrotonate (17b)

The $^{13}C_5$ phosphonate ester **17b** was prepared by refluxing [1,2,3,4,3-methyl]-$^{13}C_5$ ethyl 3-methyl-4-chlorocrotonate **16b** (3.23 g, 19.3 mmol) and triethyl phosphite (3.7 mL, 3.5 g, 21.2 mmol) for 5 h. After distillation the desired product **17b** (4.61 g, 17.1 mmol, 89%) was obtained.

^{1}H NMR ($CDCl_3$) δ (ppm) = 1.31 (m, 9 H, OCH_2CH_3), 2.06 (dm, *J* = 127.9 Hz, 3 H, 3-CH_3*Z*), 2.31 (dm, *J* = 129.9 Hz, 3 H, 3-CH_3*E*), 2.70 (dddd, *J* = 4.9 Hz/4.9 Hz/23.3 Hz/128.0 Hz, 2 H, 4*E*-H), 3.48 (dddd, *J* = 5.4 Hz/5.4 Hz/24.7 Hz/134.3 Hz, 2 H, 4*Z*-H), 4.14 (m, 6 H, OCH_2CH_3), 5.80 (ddd, *J* = 5.6 Hz/5.6 Hz/158.9 Hz, 1 H, 2-H).

^{13}C NMR ($CDCl_3$) δ (ppm) = 14.1 (OCH_2CH_3), 16.2 ($POCH_2CH_3$), 19.8 (d, *J* = 41.8 Hz, 3-CH_3*Z*), 25.9 (d, *J* = 41.7 Hz, 3-CH_3*E*), 31.3 (dd, *J* = 39.1 Hz/133.6 Hz, C-4*Z*), 38.3 (dd, *J* = 39.7 Hz/135.4 Hz, C-4*E*), 59.5 (OCH_2CH_3), 61.9 (m, $POCH_2CH_3$), 118.5 (m, C-2*Z*), 119.6 (m, C-2*E*), 149.2 (m, C-3), 165.8 (d, *J* = 76.1 Hz, C-1*Z*), 165.8 (d, *J* = 76.1 Hz, C-1*E*).

Ethyl 2*E*,4*E*-3-methyl-5-(2,10,10-trimethyl-4,7-dioxaspiro[4,5]dec-1-en-1-yl)-2,4-pentadienoate (24)

In a 250 mL three-necked round-bottomed flask diisopropylamine (2.11 mL, 1.53 g, 15.1 mmol) was dissolved in dry THF (100 mL). The solution was cooled to -20°C and *n*-BuLi (8.75 mL, 14 mmol) was added. After 30 min at -20°C triethyl 3-methyl-4-phosphonocrotonate **17** (3.4 mL, 3.7 g, 14.0 mmol) in THF (10 mL) was slowly added using a dropping funnel. After 30 min the mixture was allowed to warm to 0°C and 2,10,10-trimethyl-4,7-dioxaspiro[4,5]dec-1-enecarbaldehyde **9** in THF (20 mL) was added. The reaction was stirred overnight at RT and followed on TLC (50% diethyl ether/PE).

When TLC showed complete conversion of the aldehyde, the mixture was poured in a saturated NaCl-solution and extracted three times with diethyl ether. The combined organic layers were washed with saturated NaCl and dried with $MgSO_4$. After filtration and evaporation of the solvent the mixture was purified on a flash column (2% triethylamine/10% diethyl ether/PE). This resulted in a yellow oil of product **18** (2.97 g, 9.3 mmol, 86%), which became solid during storage at -20°C.

^{1}H NMR ($CDCl_3$) δ (ppm) = 1.03 (s, 6 H, 1-CH_3), 1.29 (t, *J* = 7.1 Hz, 3 H, OCH_2CH_3), 1.57-1.83 (m, 4 H, 2-H/3-H), 1.66 (s, 3 H, 5-CH_3), 2.32 (s, 3 H, 9-CH_3), 4.02 (s, 4 H, OCH_2CH_2O), 4.18 (q, *J* = 7.1 Hz, 2 H, OCH_2CH_3), 5.75 (s, 1 H, 10-H), 6.12 (d, *J* = 16.1 Hz, 8-H), 6.48 (d, *J* = 16.1 Hz, 7-H).

^{13}C NMR ($CDCl_3$) δ (ppm) = 13.5 (5-CH_3), 13.5 (OCH_2CH_3), 14.2 (9-CH_3), 27.7 (1-CH_3), 30.0 (C-3), 34.7 (C-1), 35.6 (C-2), 59.6 (OCH_2CH_3), 65.1 (OCH_2CH_2O), 107.7 (C-4), 119.1 (C-10), 129.5 (C-5), 132.4 (C-7), 137.5 (C-8), 144.5 (C-6), 151.8 (C-9), 166.9 (C-11).

Ethyl 2*E*,4*E*-3-methyl-5-([1,2]-$^{13}C_2$ 2,10,10-trimethyl-4,7-dioxaspiro[4,5]dec-1-en-1-yl)-2,4-pentadienoate (18a)

Using the same procedure as described before, $^{13}C_2$ aldehyde **9a** (3.64 g, 17.1 mmol) reacted with phosphonate **17** (5.4 mL, 5.9 g, 22.2 mmol) to give ethyl 2*E*,4*E*-3-methyl-5-([1,2]-$^{13}C_2$ 2,10,10-trimethyl-4,7-dioxaspiro[4,5]dec-1-en-1-yl)-2,4-pentadienoate **18a** (4.60 g, 14.3 mmol, 83%).

^{1}H NMR ($CDCl_3$) δ (ppm) = 1.03 (d, *J* = 3.7 Hz, 6 H, 1-CH_3), 1.29 (t, *J* = 7.1 Hz, 3 H, OCH_2CH_3), 1.57-1.83 (m, 4 H, 2-H/3-H), 1.66 (d, *J* = 5.2 Hz, 3 H, 5-CH_3), 2.32 (s, 3 H, 9-CH_3), 4.02 (s, 4 H, OCH_2CH_2O), 4.18 (q, *J* = 7.1 Hz, 2 H, OCH_2CH_3), 5.75 (s, 1 H, 10-H), 6.11 (dd, *J* = 4.6 Hz/16.1 Hz, 1 H, 8-H), 6.48 (dd, *J* = 16.1 Hz/150.3 Hz, 1 H, 7-H).

^{13}C NMR ($CDCl_3$) δ (ppm) = 13.5 (5-CH_3), 13.5 (OCH_2CH_3), 14.2 (9-CH_3), 27.7 (1-CH_3), 30.0 (C-3), 34.7 (C-1), 35.6 (C-2), 59.6 (OCH_2CH_3), 65.1 (OCH_2CH_2O), 107.7 (C-4), 119.1 (C-10), 129.5 (d, *J* = 73.9 Hz, C-5), 132.4 (d, *J* = 55.0 Hz, C-7), 137.5 (d, *J* = 71.3 Hz, C-8), 144.5 (d, *J* = 55.0 Hz, C-6), 151.8 (C-9), 166.9 (C-11).

[1,2,3,4,3-methyl]-$^{13}C_5$ Ethyl 2*E*,4*E*-3-methyl-5-(2,10,10-trimethyl-4,7-dioxaspiro[4,5]dec-1-en-1-yl)-2,4-pentadienoate (18b)

A similar procedure as described before was used to react 2,10,10-trimethyl-4,7-dioxaspiro[4,5]dec-1-ene-carbaldehyde **9** (2.54 g, 12.1 mmol) with [1,2,3,4,3-methyl]-$^{13}C_5$ triethyl 3-methyl-4-phosphonocrotonate **17b** (4.24 g, 15.7 mmol) to give [1,2,3,4,3-methyl]-$^{13}C_5$ ethyl 2*E*,4*E*-3-methyl-5-(2,10,10-trimethyl-4,7-dioxaspiro[4,5]dec-1-en-1-yl)-2,4-pentadienoate **18b** (3.48 g, 10.7 mmol, 88%).

^{1}H NMR ($CDCl_3$) δ (ppm) = 1.03 (s, 6 H, 1-CH_3), 1.29 (t, *J* = 7.1 Hz, 3 H, OCH_2CH_3), 1.57-1.83 (m, 4 H, 2-H/3-H), 1.66 (s, 3 H, 5-CH_3), 2.34 (ddd, *J* = 4.7 Hz/4.7 Hz/128.8 Hz, 3 H, 9-CH_3), 4.02 (s, 4 H, OCH_2CH_2O), 4.17 (dq, *J* = 3.1 Hz/7.1 Hz, 2 H, OCH_2CH_3), 5.75 (dt, *J* = 7.6 Hz/159.7 Hz, 1 H, 10-H), 6.12 (dddd, *J* = 3.6 Hz/3.6 Hz/16.1 Hz/155 Hz, 1 H, 8-H), 6.48 (dd, *J* = 5.7 Hz/16.1 Hz, 1 H, 7-H).

^{13}C NMR ($CDCl_3$) δ (ppm) = 13.5 (d, *J* = 41.0 Hz, 5-CH_3), 13.5 (OCH_2CH_3), 14.2 (9-CH_3), 27.7 (1-CH_3), 30.0 (C-3), 34.7 (C-1), 35.6 (C-2), 59.6 (OCH_2CH_3), 65.1 (OCH_2CH_2O), 107.7 (C-4), 119.1 (dd, *J* = 74.7 Hz/77.6 Hz, C-10), 129.5 (C-5), 132.4 (d, *J* = 51.4 Hz, C-7), 137.5 (dd, *J* = 7 Hz/52.7 Hz, C-8), 144.5 (C-6), 151.8 (ddd, *J* = 41.0 Hz/52.7 Hz/74.7 Hz, C-9), 166.9 (dd, *J* = 8 Hz/77.6 Hz, C-11).

2*E*,4*E*-3-Methyl-5-(2,10,10-trimethyl-4,7-dioxaspiro[4,5]dec-1-en-yl)-2,4-pentadienol (19)

A 250 mL three-necked round-bottomed flask was equipped with a septum inlet, outlet and a pentane-thermometer. Under a nitrogen flow, the ester **18** (2.97 g, 9.3 mmol) was dissolved in dry PE and the solution was cooled to -80°C, after which Dibal-H (20.5 mL, 20.5 mmol) was slowly added using a syringe. The reaction was allowed to warm to -40°C in 1 h. When TLC (50% diethyl ether/PE) showed complete conversion of the starting material a mixture of silica gel and water (36 g) was added. The mixture was stirred for 1 h at 0°C, K_2CO_3 and $MgSO_4$ were added and the solids were removed by filtration and washed with diethyl ether. After concentration the product was purified by column chromatography (silica gel, gradient 50-98% diethyl ether/PE + 2% TEA), resulting in the alcohol **19** (1.37 g, 4.92 mmol, 53%).

^{1}H NMR ($CDCl_3$) δ (ppm) = 1.03 (s, 6 H, 1-CH_3), 1.61 (m, 2 H, 2-H), 1.67 (s, 3 H, 5-CH_3), 1.80 (m, 2 H, 3-H), 1.83 (s, 3 H, 9-CH_3), 4.01 (s, 4 H, OCH_2CH_2O), 4.28 (d, *J* = 6.5 Hz, 1 H, 11-H), 5.64 (t, *J* = 6.5 Hz, 1 H, 10-H), 6.07 (s, 2 H, 7-H/8-H).

^{13}C NMR ($CDCl_3$) δ (ppm) = 12.2 (9-CH_3), 13.4 (5-CH_3), 27.7 (1-CH_3), 30.1 (C-3), 34.5 (C-1), 35.9 (C-2), 58.6 (C-11), 64.9 (OCH_2CH_2O), 107.9 (C-4), 125.5 (C-7), 128.0 (C-5), 130.6 (C-10), 135.1 (C-9), 138.4 (C-8), 145.2 (C-6).

[5]-^{13}C 2*E*,4*E*-3-Methyl-5-([1]-^{13}C 2,10,10-trimethyl-4,7-dioxaspiro[4,5]dec-1-en-yl)-2,4-pentadienol (19a)

Ethyl 2*E*,4*E*-3-methyl-5-([1,2]-$^{13}C_2$ 2,10,10-trimethyl-4,7-dioxaspiro[4,5]dec-1-en-1-yl)-2,4-pentadienoate **18a** (4.6 g, 14.3 mmol) was reduced with Dibal-H (31.5 mL, 31.5 mmol) to give 2*E*,4*E*-3-methyl-5-([1,2]-$^{13}C_2$ 2,10,10-trimethyl-4,7-dioxaspiro[4,5]dec-1-en-yl)-2,4-pentadienol **19a** (2.12 g, 7.56 mmol, 53%).

^{1}H NMR ($CDCl_3$) δ (ppm) = 1.03 (s, 6 H, 1-CH_3), 1.55-1.90 (m, 4 H, 2-H/3-H), 1.66 (d, *J* = 5.1 Hz, 3 H, 5-CH_3), 1.83 (s, 3 H, 9-CH_3), 4.01 (s, 4 H, OCH_2CH_2O), 4.29 (d, *J* = 6.9 Hz, 2 H, 11-H), 5.63 (t, *J* = 6.9 Hz, 1 H, 10-H), 6.06 (dd, *J* = 16.2 Hz/153.0 Hz, 1 H, 7-H), 6.07 (ddd, *J* = 3.0 Hz/4.5 Hz/16.2 Hz, 1 H, 8-H).

^{13}C NMR ($CDCl_3$) δ (ppm) = 11.4 (9-CH_3), 13.0 (d, *J* = 88.9 Hz), 27.8 (1-CH_3), 30.2 (C-3), 34.6 (d, *J* = 50.6 Hz), 36.0 (C-2), 58.8 (C-11), 65.1 (OCH_2CH_2O), 108.1 (C-4), 125.8 (d, *J* = 54.3 Hz, C-7), 128.0 (d, *J* = n.d., C-5), 130.0 (C-10), 135.0 (C-9), 138.3 (d, *J* = 71.7 Hz, C-8), 145.3 (d, *J* = 54.3 Hz, C-6).

[1,2,3,4,3-methyl]-$^{13}C_5$2*E*,4*E*-3-Methyl-5-(2,10,10-trimethyl-4,7-dioxaspiro[4,5]dec-1-en-yl)-2,4-pentadienol (19b)

By using the same procedure as described before, [1,2,3,4,3-methyl]-$^{13}C_5$ ethyl 2*E*,4*E*-3-methyl-5-(2,10,10-trimethyl-4,7-dioxaspiro[4,5]dec-1-en-1-yl)-2,4-pentadienoate **18b** (3.48 g, 10.7 mmol) was reduced with Dibal-H (23.5 mL, 23.5 mmol) to obtain the corresponding $^{13}C_5$ alcohol **19b** (1.17 g, 4.13 mmol, 39%).

^{1}H NMR ($CDCl_3$) δ (ppm) = 1.02 (s, 6 H, 1-CH_3), 1.61 (m, 2 H, 2-H), 1.66 (s, 3 H, 5-CH_3), 1.80 (m, 2 H, 3-H), 1.84 (ddd, *J* = 4.7 Hz/4.7 Hz/126.4 Hz, 3 H, 9-CH_3), 4.01 (s, 4 H, OCH_2CH_2O), 4.29 (ddd, *J* = 6.0 Hz/6.5 Hz/142.6 Hz, 1 H, 11-H), 5.63 (ddd, *J* = 7.6 Hz/7.6 Hz/154.5 Hz, 1 H, 10-H), 6.07 (dddd, *J* = 4.7 Hz/4.7 Hz/15.0 Hz/153.5 Hz, 1 H, 8-H), 6.07 (ddd, *J* = 4.7 Hz/4.7 Hz/15.0 Hz, 1 H, 7-H).

^{13}C NMR ($CDCl_3$) δ (ppm) = 12.4 (d, *J* = 42.2 Hz, 9-CH_3), 13.6 (5-CH_3), 27.7 (1-CH_3), 30.1 (C-3), 34.7 (C-1), 36.1 (C-2), 59.4 (d, *J* = 47.7 Hz, C-11), 65.1 (OCH_2CH_2O), 108.1 (C-4), 126.0 (d, *J* = 71.0 Hz, C-7), 128.0 (C-5), 129.6 (dd, *J* = 47.7 Hz/71.0 Hz, C-10), 135.1 (ddd, *J* = 42.2 Hz/56.2 Hz/71.0 Hz, C-9), 138.3 (d, *J* = 56.2 Hz, C-8), 145.2 (C-6).

2*E*,4*E*-3-Methyl-5-(-2,6,6-trimethyl-3-oxo-1-cyclohexen-1-yl)-2,4-pentadienol (20)

A few drops of HCl (1 M) were added to a solution of 2*E*,4*E*-3-methyl-5-(2,10,10-trimethyl-4,7-dioxaspiro[4,5]dec-1-en-yl)-2,4-pentadienol **19** (1.37 g, 4.92 mmol) in acetone (125 mL), until the solution was acidic. After a few minutes, solid K_2CO_3 and $MgSO_4$ were added. The mixture was stirred for 10 minutes, and the solids were removed by filtration and washed with diethyl ether. The solvents were removed in vacuo, and the product was purified by flash-chromatography (50% diethyl ether/PE). The solution was concentrated in vacuo to obtain the desired product **20** (1.04 g, 44 mmol, 90%).

^{1}H NMR ($CDCl_3$) δ (ppm) = 1.17 (s, 6 H, 1-CH_3), 1.82 (s, 3 H, 5-CH_3), 1.86 (t, *J* = 6.9 Hz, 2 H, 2-H), 1.87 (s, 3 H, 9-CH_3), 2.51 (t, *J* = 6.9 Hz, 2 H, 3-H), 4.33 (d, *J* = 6.9 Hz, 2 H, 11-H), 5.76 (t, *J* = 6.9 Hz, 1 H, 10-H), 6.21 (s, 2 H, 7-H/8-H).

^{13}C NMR ($CDCl_3$) δ (ppm) = 12.0 (9-CH_3), 13.3 (5-CH_3), 27.1 (1-CH_3), 33.8 (C-3), 35.3 (C-1), 36.8 (C-2), 58.6 (C-11), 123.6 (C-7), 129.2 (C-9), 133.0 (C-5), 134.2 (C-10), 140.0 (C-8), 161.5 (C-6), 199.4 (C-4).

[5]-^{13}C 2*E*,4*E*-3-Methyl-5-([1]-^{13}C-2,6,6-trimethyl-3-oxo-1-cyclohexen-1-yl)-2,4-pentadienol (20a)

Hydrolysis of the $^{13}C_2$acetal **19a** (2.12 g, 7.6 mmol) gave the corresponding $^{13}C_2$ketone **20a** (1.70 g, 7.2 mmol, 95%).

^{1}H NMR ($CDCl_3$) δ (ppm) = 1.17 (d, *J* = 3.8 Hz, 6 H, 1-CH_3), 1.83 (d, *J* = 4.9 Hz, 3 H, 5-CH_3), 1.86 (t, *J* = 6.7 Hz, 2 H, 2-H), 1.87 (s, 3 H, 9-CH_3), 2.50 (t, *J* = 6.7 Hz, 2 H, 3-H), 4.34 (d, *J* = 6.7 Hz, 2 H, 11-H), 5.75 (t, *J* = 6.7 Hz, 1 H, 10-H), 6.19 (dd, *J* = 16.3 Hz/154.4 Hz, 1 H, 7-H), 6.21 (dd, *J* = 4.8 Hz/16.3 Hz, 1 H, 8-H).

^{13}C NMR ($CDCl_3$) δ (ppm) = 12.2 (9-CH_3), 13.5 (5-CH_3), 27.4 (1-CH_3), 34.1 (C-3), 35.6 (d, *J* = 39.3 Hz, C-1), 37.2 (C-2), 59.1 (C-11), 124.3 (d, *J* = 53.7 Hz, C-7), 129.6 (d, *J* = 67.3 Hz, C-5), 132.6 (C-10), 135.1 (C-9), 140.0 (d, *J* = 70.7 Hz, C-8), 161.4 (d, *J* = 53.7 Hz, C-6), 199.4 (C-4).

[1,2,3,4,3-methyl]-$^{13}C_5$ 2*E*,4*E*-3-Methyl-5-(2,6,6-trimethyl-3-oxo-1-cyclohexen-1-yl)-2,4-pentadienol (20b)

By using the same procedure as described before, [1,2,3,4,3-methyl]-$^{13}C_5$ 2*E*,4*E*-3-methyl-5-(2,10,10-trimethyl-4,7-dioxaspiro[4,5]dec-1-en-yl)-2,4-pentadienol **19b** (1.17 g, 4.1 mmol) was hydrolyzed to give [1,2,3,4,3-methyl]-$^{13}C_5$ 2*E*,4*E*-3-methyl-5-(2,6,6-trimethyl-3-oxo-1-cyclohexen-1-yl)-2,4-pentadienol **20b** (0.92 g, 3.8 mmol, 93%).

^{1}H NMR ($CDCl_3$) δ (ppm) = 1.17 (s, 6 H, 1-CH_3), 1.82 (s, 3 H, 5-CH_3), 1.85 (t, *J* = 6.9 Hz, 2 H, 2-H), 1.87 (dq, *J* = 4.6 Hz/126.6 Hz, 3 H, 9-CH_3), 2.50 (t, *J* = 6.9 Hz, 2 H, 3-H), 4.34 (dd, *J* = 6.7 Hz/142.0 Hz, 2 H, 11-H), 5.76 (dt, *J* = 6.7 Hz/152.5 Hz, 1 H, 10-H), 6.19 (dd, *J* = 5.0 Hz/16.3 Hz, 1 H, 7-H), 6.22 (ddq, *J* = 4.6 Hz/16.3 Hz/138.8 Hz, 1 H, 8-H).

^{13}C NMR ($CDCl_3$) δ (ppm) = 12.2 (d, *J* = 42.2 Hz, 9-CH_3), 13.5 (5-CH_3), 27.3 (1-CH_3), 34.1 (C-3), 35.5 (C-1), 37.1 (C-2), 59.0 (C-11), 124.3 (d, *J* = 45.1 Hz, C-7), 132.7 (dd, *J* = 47.4 Hz/71.5 Hz, C-10), 133.0 (C-5), 135.0 (ddd, *J* = 42.2 Hz/52.7 Hz/71.5 Hz, C-9), 140.0 (d, *J* = 52.7 Hz, C-8), 161.5 (C-6), 199.5 (C-4).

2*E*,4*E*-3-Methyl-5-(4-hydroxy-2,6,6-trimethyl-3-oxo-1-cyclohexen-1-yl)-2,4-pentadienol (21)

Diisopropylamine (1.98 g, 19.5 mmol, 2.75 mL) was dissolved in dry, freshly distilled THF. The solution was cooled to -20°C and *n*-BuLi (11.1 mL, 17.8 mmol) was added via a syringe. After 10 min the LDA-solution was cooled to -80°C and 2*E*,4*E*-3-methyl-5-(2,6,6-trimethyl-3-oxo-1-cyclohexen-1-yl)-2,4-pentadienol **20** (1.04 g, 4.4 mmol) in 20 mL dry THF was added. After 30 min a solution of (+)-(8,8-dichlorocamphoryl-sulfonyl)oxaziridine (5.3 g, 17.8 mmol) in THF was slowly added. The reaction was allowed to warm up to RT and followed by TLC (diethyl ether). When all starting material had reacted, the reaction was quenched by adding saturated NH_4Cl and Na_2SO_3 solutions. The mixture was extracted three times with diethyl ether and the combined organic layers were washed with saturated NaCl and dried with $MgSO_4$. The solids were removed by filtration. Concentration in vacuo gave a mixture of (+)-(8,8-dichlorocamphorylsulfonyl)imine and 2*E*,4*E*-3-methyl-5-(4-hydroxy-2,6,6-trimethyl-3-oxo-1-cyclohexen-1-yl)-2,4-pentadienol. After silica-gel column chromatography (50-100% diethyl ether/PE) the diol **21** (0.56 g, 2.2 mmol, 50%) was obtained.

^{1}H NMR ($CDCl_3$) δ (ppm) = 1.18 (s, 3 H, 1-CH_3), 1.30 (s, 3 H, 1-CH_3), 1.81 (t, *J* = 13.8 Hz, 1 H, 2-H_{ax}), 1.87 (s, 3 H, 9-CH_3), 1.89 (s, 3 H, 5-CH_3), 2.16 (dd, *J* = 5.5 Hz/12.6 Hz, 1 H, 2-H_{eq}), 3.71 (s, 1 H, OH), 4.33 (dd, *J* = 5.5 Hz/13.8 Hz, 1 H, 3-H), 4.35 (d, *J* = 6.6 Hz, 2 H, 11-H), 5.78 (t, *J* = 6.6 Hz, 1 H, 10-H), 6.16 (d, *J* = 16.3 Hz, 1 H, 7-H), 6.28 (d, *J* = 16.3 Hz, 1 H, 8-H).

^{13}C NMR ($CDCl_3$) δ (ppm) = 12.2 (9-CH_3), 13.7 (5-CH_3), 25.8 (1-CH_3), 36.4 (C-1), 45.3 (C-2), 59.1 (C-11), 69.2 (C-3), 123.4 (C-7), 126.7 (C-5), 133.6 (C-10), 134.6 (C-9), 141.0 (C-8), 162.2 (C-6), 200.4 (C-4).

[5]-^{13}C 2*E*,4*E*-3-Methyl-5-([1]-^{13}C 4-hydroxy-2,6,6-trimethyl-3-oxo-1-cyclohexen-1-yl)-2,4-pentadienol (21a)

The same procedure as described above was used to synthesize [5]-^{13}C 2*E*,4*E*-3-methyl-5-([1]-^{13}C 4-hydroxy-2,6,6-trimethyl-3-oxo-1-cyclohexen-1-yl)-2,4-pentadienol **21a** (0.90 g, 3.6 mmol, 53%) from the corresponding $^{13}C_2$ alcohol **20a** (1.7 g, 7.2 mmol).

^{1}H NMR ($CDCl_3$) δ (ppm) = 1.18 (d, *J* = 3.9 Hz, 3 H, 1-CH_3), 1.30 (d, *J* = 3.6 Hz, 3 H, 1-CH_3), 1.81 (t, *J* = 13.2 Hz, 1 H, 2-H_{ax}), 1.86 (s, 3 H, 9-CH_3), 1.88 (d, *J* = 4.9 Hz, 3 H, 5-CH_3), 2.16 (dd, *J* = 5.6 Hz/12.0 Hz, 1 H, 2-H_{eq}), 3.87 (s, 1 H, OH), 4.32 (dd, *J* = 5.7 Hz/13.8 Hz, 1 H, 3-H), 4.34 (d, *J* = 6.6 Hz, 2 H, 11-H), 5.78 (t, *J* = 6.6 Hz, 1 H, 10-H), 6.17 (dd, *J* = 16.3 Hz/155.2 Hz, 1 H, 7-H), 6.28 (ddd, *J* = 3.0 Hz/4.9 Hz/16.3 Hz, 1 H, 8-H).

^{13}C NMR ($CDCl_3$) δ (ppm) = 12.1 (9-CH_3), 13.6 (5-CH_3), 25.7 (1-CH_3), 36.5 (d, *J* = 39.0 Hz, C-1), 45.0 (C-2), 58.9 (C-11), 69.2 (C-3), 123.4 (d, *J* = 54.0 Hz, C-7), 131.6 (d, *J* = 53.1 Hz, C-5), 133.5 (d, *J* = 8.0 Hz, C-10), 134.6 (d, *J* = 5.7 Hz, C-9), 141.0 (d, *J* = 71.3 Hz, C-8), 162.2 (d, *J* = 54.0 Hz, C-6), 200.4 (C-4).

[1,2,3,4,3-methyl]-$^{13}C_5$ 2*E*,4*E*-3-Methyl-5-(4-hydroxy-2,6,6-trimethyl-3-oxo-1-cyclohexen-1-yl)-2,4-pentadienol (21b)

Using the same procedure as described above, [1,2,3,4,3-methyl]-$^{13}C_5$ 2*E*,4*E*-3-methyl-5-(2,6,6-trimethyl-3-oxo-1-cyclohexen-1-yl)-2,4-pentadienol **20b** (0.9 g, 3.8 mmol) was converted into [1,2,3,4,3-methyl]-$^{13}C_5$ 2*E*,4*E*-3-methyl-5-(4-hydroxy-2,6,6-trimethyl-3-oxo-1-cyclohexen-1-yl)-2,4-pentadienol **21b** (0.52 g, 2.0 mmol, 54%).

^{1}H NMR ($CDCl_3$) δ (ppm) = 1.18 (s, 3 H, 1-CH_3), 1.30 (s, 3 H, 1-CH_3), 1.81 (t, *J* = 13.2 Hz, 1 H, 2-H_{ax}), 1.87 (dd, *J* = 4.5 Hz/126.6 Hz, 3 H, 9-CH_3), 1.89 (s, 3 H, 5-CH_3), 2.16 (dd, *J* = 5.5 Hz/12.6 Hz, 1 H, 2-H_{eq}), 3.71 (s, 1 H, OH), 4.32 (dd, *J* = 5.5 Hz/13.9 Hz, 1 H, 3-H), 4.35 (dd, *J* = 7.5 Hz/142.3 Hz, 2 H, 11-H), 5.77 (dt, *J* = 7.5 Hz/152.4 Hz, 1 H, 10-H), 6.17 (dd, *J* = 4.9 Hz/16.5 Hz, 1 H, 7-H), 6.27 (dd, *J* = 16.5 Hz/155.4 Hz, 1 H, 8-H).

^{13}C NMR ($CDCl_3$) δ (ppm) = 12.3 (d, *J* = 42.2 Hz, 9-CH_3), 13.7 (5-CH_3), 25.8 (1-CH_3), 36.7 (C-1), 45.3 (C-2), 59.3 (d, *J* = 47.3 Hz, C-11), 69.2 (C-3), 123.8 (d, *J* = 71.3 Hz, C-7), 131.4 (C-5), 133.1 (dd, *J* = 47.3 Hz/71.5 Hz, C-10), 135.2 (ddd, *J* = 42.2 Hz/53.1 Hz/71.5 Hz, C-9), 141.0 (dddd, *J* = 2.8 Hz/2.8 Hz/2.8 Hz/53.1 Hz, C-8), 162.2 (C-6), 200.5 (C-4).

(2*E*,4*E*-3-Methyl-5-(4-hydroxy-2,6,6-trimethyl-3-oxo-1-cyclohexen-1-yl)-2,4-pentadien-1-yl)-phosphonium bromide (22)

A solution of diol **21** (0.56 g, 2.2 mmol) in DCM (50 mL) was cooled to 0°C and HBr (47%, 0.53 mL, 4.5 mmol) was slowly added. The mixture was stirred for 30 min and followed by TLC (diethyl ether). If necessary, two more equivalents of HBr were added until TLC showed complete conversion of the starting material. A saturated NaCl solution was added and the mixture was extracted three times with ethyl acetate. The combined organic layers were dried with $MgSO_4$ and the solids were removed by filtration. 1,2-Epoxybutane was added until the solution was at pH 7. The solution was concentrated to a volume of circa 20 mL and ethyl acetate (30 mL) and 1,2-epoxybutane (0.5 mL) were added. Subsequently, the solution was concentrated again to a volume of 20 mL. This solution was slowly added to a solution of triphenylphosphine (0.59 g, 2.2 mmol) in ethyl acetate/1,2-epoxybutane (20 mL/0.2 mL) and the mixture was stirred at room temperature for at least

24 h, during which a white preciptate was formed. TLC analysis (diethyl ether) showed complete conversion of the starting material. The white solid product was collected by filtration, washed with diethyl ether, and dried in vacuo to give the phosphonium salt **22** (0.65 g, 1.13 mmol, 50%).

^{1}H NMR ($CDCl_3$) δ (ppm) = 1.12/1.26 (2s, 6 H, 1-CH_3), 1.47 (d, *J* = 3.7 Hz, 3 H, 9-CH_3), 1.77 (t, *J* = 12.9 Hz, 1 H, 2-H_{ax}), 1.81 (s, 3 H, 5-CH_3), 2.24 (dd, *J* = 5.6 Hz/7.1 Hz, 1 H, 2-H_{eq}), 3.67 (s, 1 H, OH), 4.29 (dd, *J* = 5.6 Hz/13.9 Hz, 1 H, 3-H), 4.90 (m, 2 H, 11-H), 5.58 (dd, *J* = 7.5 Hz/7.5 Hz, 1 H, 10-H), 6.06 (d, *J* = 16.2 Hz, 1 H, 7-H), 6.17 (d, *J* = 16.2 Hz, 1 H, 8-H), 7.64-7.92 (m, 15 H, phenyl).

^{13}C NMR ($CDCl_3$) δ (ppm) = 12.5 (C-19), 13.4 (C-18), 24.8 (d, *J* = 45.5 Hz, C-11), 25.5/30.1 (C-16/17), 36.3 (C-1), 44.9 (C-2), 68.8 (C-3), 117.3 (d, *J* = 85.6 Hz, C-10), 125.1 (C-7), 126.9 (C-5), 130.1/133.4/134.9 (C-phenyl), 138.8 (C-8), 142.3 (C-9), 161.0 (C-6), 200.0 (C-1).

[5]-^{13}C (2*E*,4*E*-3-Methyl-5-([1]-^{13}C (4-hydroxy-2,6,6-trimethyl-3-oxo-1-cyclohexen-1-yl)-2,4-pentadien-1-yl)-phosphonium bromide (22a)

[5]-^{13}C 2*E*,4*E*-3-Methyl-5-([1]-^{13}C 4-hydroxy-2,6,6-trimethyl-3-oxo-1-cyclohexen-1-yl)-2,4-pentadienol **21a** (0.90 g, 3.6 mmol) reacted with HBr and triphenylphosphine using the same procedure as described above, to yield pure [5]-^{13}C (2*E*,4*E*-3-methyl-5-([1]-^{13}C (4-hydroxy-2,6,6-trimethyl-3-oxo-1-cyclohexen-1-yl)-2,4-pentadien-1-yl)-phosphonium bromide **22a** (0.88 g, 1.5 mmol, 43%).

^{1}H NMR ($CDCl_3$) δ (ppm) = 1.13/1.27 (2d, *J* = 3.8 Hz, 6 H, 1-CH_3), 1.48 (d, *J* = 3.7 Hz, 3 H, 9-CH_3), 1.77 (t, *J* = 13.3 Hz, 1 H, 2-H_{ax}), 1.81 (d, *J* = 4.9 Hz, 3 H, 5-CH_3), 2.14 (dd, *J* = 5.9 Hz/12.9 Hz, 1 H, 2-H_{eq}), 3.75 (s, 1 H, OH), 4.31 (dd, *J* = 5.6 Hz/13.9 Hz, 1 H, 3-H), 4.88/4.94 (dd, *J* = 7.0 Hz/7.3 Hz, 2 H, 11-H), 5.61 (dt, *J* = 7.0 Hz/7.3 Hz, 1 H, 10-H), 6.09 (dd, *J* = 16.3 Hz/139.2 Hz, 1 H, 7-H), 6.19 (d, *J* = 16.3 Hz, 1 H, 8-H), 7.70-7.94 (m, 15 H, phenyl).

^{13}C NMR ($CDCl_3$) δ (ppm) = 12.1 (9-CH_3), 13.0 (d, *J* = 5.2 Hz, 5-CH_3), 24.4 (d, *J* = 50.2 Hz, C-11), 25.2 (1-CH_3), 35.8 (d, *J* = 39.4 Hz, C-1), 44.5 (C-2), 68.4 (C-3), 117.1 (d, *J* = 85.5 Hz, C-10), 124.8 (dd, *J* = 53.7 Hz, *J* = 4.7 Hz, C-7), 128.1 (d, *J* = 53.6 Hz, C-5), 129.7 (d, *J* = 12.5 Hz, C-phenyl), 133.1 (d, *J* = 9.8 Hz, C-phenyl), 134.5 (d, *J* = 2.9 Hz, C-phenyl), 138.4 (dd, *J* = 6.1 Hz/71.8 Hz, C-8), 141.8 (dd, *J* = 5.5 Hz/13.6 Hz, C-9), 160.5 (dd, *J* = 1.9 Hz/55.5 Hz, C-6), 199.6 (C-4).

[1,2,3,4,3-methyl]-$^{13}C_5$ (2*E*,4*E*-3-Methyl-5-(4-hydroxy-2,6,6-trimethyl-3-oxo-1-cyclohexen-1-yl)-2,4-pentadien-1-yl)-phosphonium bromide (22b)

By using the same procedure as described before, $^{13}C_5$ Wittig salt **22b** (0.63 g, 1.1 mmol, 53%) was synthesized, starting from the corresponding $^{13}C_5$ diol **21b** (0.52 g, (2.04 mmol).

^{1}H NMR ($CDCl_3$) δ (ppm) = 1.11/1.26 (2s, 6 H, 1-CH_3), 1.48 (dd, *J* = 3.7 Hz/127.3 Hz, 3 H, 9-CH_3), 1.77 (t, *J* = 13.3 Hz, 1 H, 2-H_{ax}), 1.81 (s, 3 H, 5-CH_3), 2.13 (dd, *J* = 5.6 Hz/12.7 Hz, 1 H, 2-H_{eq}), 4.29 (dd, *J* = 5.6 Hz/13.8 Hz, 2 H, 3-H), 3.65 (s, 1 H, OH), 4.91/4.99 (ddd, *J* = 7.0 Hz/7.0 Hz/134.8 Hz, 2 H, 11-H), 5.56 (ddt, *J* = 7.0 Hz/7.0 Hz/151.0 Hz, 1 H, 10-H), 6.06 (d, *J* = 16.2 Hz, 1 H, 7-H), 6.16 (dd, *J* = 16.2 Hz/142.3 Hz, 1 H, 8-H), 7.70-7.94 (m, 15 H, phenyl).

^{13}C NMR ($CDCl_3$) δ (ppm) = 12.7 (d, *J* = 43.5 Hz, 9-CH_3), 13.4 (5-CH_3), 25.1 (dd, *J* = 46.6 Hz/46.6 Hz, C-11), 25.6 (1-CH_3), 36.4 (C-1), 45.1 (C-2), 69.0 (C-3), 117.5 (ddd, *J* = 46.6 Hz/73.4 Hz/84.3 Hz, C-10), 126.8 (C-5), 130.2 (d, *J*

= 12.7 Hz, C-phenyl), 133.7 (d, *J* = 9.5 Hz, C-phenyl), 135.0 (d, *J* = 3.2 Hz, C-phenyl), 139.0 (d, *J* = 53.0 Hz, C-8), 142.3 (dddd, *J* = 11.8 Hz/43.5 Hz/53.0 Hz/73.4 Hz, C-9), 161.2 (C-6), 200.1 (C-4).

Astaxanthin (1)

In dim red light, 2,7-dimethylocta-2,4,6-triene-1,8-dial **23** (78 mg, 0.48 mmol) and (2*E*,4*E*-3-methyl-5-(2,6,6-trimethyl-3-oxo-1-cyclohexen-1-yl)-2,4-pentadien-1-yl)-phosphonium bromide **22** (0.65 g, 1.1 mmol) were dissolved in 1,2-epoxybutane (15 mL) and refluxed overnight in a nitrogen atmosphere. When TLC (50% diethyl ether/PE) showed complete conversion of the starting material, the mixture was allowed to cool to RT and absolute ethanol (30 mL) was added. Via distillation 1,2-epoxybutane was removed, and after cooling the solution back to RT, astaxanthin precipitated as small, dark crystals. The precipitate was collected by filtration, washed with cold ethanol and removed from the filter with dichloromethane. *n*-Heptane (30 mL) was added, and dichloromethane was removed via distillation. The solution in *n*-heptane was refluxed overnight in a nitrogen atmosphere, and then cooled to 0ºC. The formed crystals of all-*trans* astaxanthin were collected by filtration, and recrystallized with dichloromethane/methanol and dichloromethane/*n*-hexane, to yield pure all-*trans* astaxanthin **1** (80 mg, 0.13 mmol, 28%).

^{1}H NMR ($CDCl_3$) δ (ppm) = 1.21/1.32 (s, 12 H, 16-H/17-H), 1.81 (t, *J* = 13.3 Hz, 2 H, 2-H_{ax}), 1.94 (s, 6 H, 18-H), 1.99 (s, 6 H, 20-H), 2.00 (s, 6 H, 19-H), 2.16 (dd, *J* = 5.6 Hz/12.6 Hz, 2 H, 2-H_{eq}), 3.68 (br. s, 2 H, OH), 4.32 (dd, *J* = 5.6 Hz/13.8 Hz, 2 H, 3-H), 6.21 (d, *J* = 16.1 Hz, 2 H, 7-H), 6.29 (d, *J* = 11.3 Hz, 2 H, 10-H), 6.31 (d, *J* = 7.4 Hz, 2 H, 14-H), 6.43 (d, *J* = 16.1 Hz, 2 H, 8-H), 6.47 (d, *J* = 14.8 Hz, 2 H, 12-H), 6.66 (dd, *J* = 11.3 Hz/14.8 Hz, 2 H, 11-H), 6.67 (d, *J* = 7.4 Hz, 2 H, 15-H).

^{13}C NMR ($CDCl_3$) δ (ppm) = 12.5 (C-19), 12.8 (C-20), 14.0 (C-18), 26.2/30.7 (C-16/C-17), 36.8 (C-1), 45.4 (C-2), 69.2 (C-3), 123.2 (C-7), 124.6 (C-11), 126.8 (C-5), 130.6 (C-15), 133.8 (C-14), 134.6 (C-9), 135.2 (C-10), 136.8 (C-13), 139.8 (C-12), 142.3 (C-8), 162.2 (C-6), 200.4 (C-4).

[6,6′,7,7′]-$^{13}C_4$ Astaxanthin (1a)

The same procedure as used for the synthesis of natural abundance astaxanthin was carried out for the synthesis of $^{13}C_4$ astaxanthin **1a**; $^{13}C_2$Wittig salt **22a** (0.88 g, 1.5 mmol) and C_{10}dialdehyde **23** (0.11 g, 0.68 mmol) gave, after isomerization and purification, pure all-*trans* $^{13}C_4$ astaxanthin **1a (**0.14 g, 0.23 mmol, 34%).

^{1}H NMR ($CDCl_3$) δ (ppm) = 1.21/1.32 (2d, *J* = 3.4 Hz/3.7 Hz, 12 H, 16-H/17-H), 1.81 (t, *J* = 13.2 Hz, 2 H, 2-H_{ax}), 1.94 (d, *J* = 4.8 Hz, 6 H, 18-H), 1.99 (s, 6 H, 20-H), 2.00 (s, 6 H, 19-H), 2.16 (ddd, *J* = 6.0 Hz/6.8 Hz/12.8 Hz, 2 H, 2-H_{eq}), 3.68 (s, 2 H, OH), 4.32 (dd, *J* = 5.6 Hz/13.8 Hz, 2 H, 3-H), 6.21 (dd, *J* = 15.8 Hz/152 Hz, 2 H, 7-H), 6.29 (d, *J* = 11.5 Hz, 2 H, 10-H), 6.31 (d, *J* = 7.9 Hz, 2 H, 14-H), 6.43 (dd, *J* = 4.7 Hz/15.8 Hz, 2 H, 8-H), 6.45 (d, *J* = 14.4 Hz, 2 H, 12-H), 6.64 (dd, *J* = 11.5 Hz/14.4 Hz, 2 H, 11-H), 6.67 (d, *J* = 7.9 Hz, 2 H, 15-H).

^{13}C NMR ($CDCl_3$) δ (ppm) = 12.6 (C-19), 12.8 (C-20), 14.0 (C-18), 26.1/30.7 (C-16/C-17), 36.8 (d, *J* = 38.2 Hz, C-1), 45.4 (C-2), 69.2 (C-3), 123.3 (d, *J* = 55 Hz, C-7), 124.6 (C-11), 126.8 (d, *J* = 52.5 Hz, C-5), 130.7 (C-15), 133.8 (C-14), 134.6 (C-9), 135.2 (C-10), 136.7 (C-13), 139.7 (C-12), 142.3 (d, *J* = 73.1 Hz, C-8), 162.2 (d, *J* = 55 Hz, C-6), 200.4 (C-4).

[8,8′,9,9′,10,10′,11,11′,19,19′]- $^{13}C_{10}$ Astaxanthin (1b)

The same procedure as described above for the synthesis of natural abundance astaxanthin was used for the synthesis of $^{13}C_{10}$ astaxanthin; $^{13}C_5$ Wittig salt **22b** (0.60 g, 1.0 mmol) and C_{10} dialdehyde **23** (74 mg, 0.45 mmol) were dissolved in 1,2-epoxybutane (15 mL) and refluxed overnight. After crystallization, isomerization in *n*-heptane, and subsequent recrystallization in DCM/methanol and DCM/*n*-hexane, purple crystals of pure all-*trans* $^{13}C_{10}$ astaxanthin **1b** (50 mg, 0.08 mmol, 18%) were obtained.

^{1}H NMR ($CDCl_3$) δ (ppm) = 1.21/1.32 (s, 12 H, 16-H/17-H), 1.81 (t, *J* = 13.3 Hz, 2 H, 2-H_{ax}), 1.94 (s, 6 H, 18-H), 1.99 (s, 6 H, 20-H), 2.00 (d, *J* = 126 Hz, 6 H, 19-H), 2.16 (dd, *J* = 5.6 Hz/12.6 Hz, 2 H, 2-H_{eq}), 3.68 (br. s, 2 H, OH), 4.32 (dd, *J* = 5.6 Hz/13.8 Hz, 2 H, 3-H), 6.21 (dd, *J* = 4.0 Hz/16.1 Hz, 2 H, 7-H), 6.29 (ddd, *J* = 11.0 Hz/11.2 Hz/138 Hz, 2 H, 10-H), 6.31 (d, *J* = 7.5 Hz, 2 H, 14-H), 6.43 (dd, *J* = 16.1 Hz/132 Hz, 2 H, 8-H), 6.45 (dd, *J* = 7.0 Hz/14.7 Hz, 2 H, 12-H), 6.66 (ddd, *J* = 11.2 Hz/14.7 Hz/143 Hz, 2 H, 11-H), 6.67 (d, *J* = 7.5 Hz, 2 H, 15-H).

^{13}C NMR ($CDCl_3$) δ (ppm) = 12.5 (d, *J* = 39 Hz, C-19), 12.8 (C-20), 14.0 (C-18), 26.2/30.7 (C-16/C-17), 36.8 (C-1), 45.4 (C-2), 69.2 (C-3), 123.0 (d, *J* = 73 Hz, C-7), 124.6 (d, *J* = 50 Hz, C-11), 126.8 (C-5), 130.6 (C-15), 133.8 (C-14), 134.6 (ddd, *J* = 39 Hz/52 Hz/n.d.,C-9), 135.2 (dd, *J* = 50 Hz/n.d., C-10), 136.7 (C-13), 139.8 (d, *J* = n.d., C-12), 142.3 (d, *J* = 52 Hz, C-8), 162.2 (C-6), 200.4 (C-4).

REFERENCES

[1] Jansen FJHM, Lugtenburg J, *Eur. J. Org. Chem.* **2000**, 829-836.
[2] Jansen FJHM, Kwestro M, Schmitt D, Lugtenburg J, *Recl. Trav. Chim. Pays-Bas* **1994**, *113*, 552-562.
[3] Jansen FJHM, Lugtenburg J, *Pure Appl. Chem.* **1994**, *66*(5), 963-972.
[4] Jansen FJHM, Lugtenburg J in *Carotenoids, Volume 2: Synthesis*; Britton G, Liaaen-Jensen S, Pfander H; Eds. Birkhäuser Verlag: Basel, 1996, 233-258.
[5] Weesie RJ, Jansen FJHM, Merlin JC, Lugtenburg J, De Groot HJM, *Biochemistry* **1997**, *36*, 2085-2090.
[6] (a) Weesie RJ, Merlin JC, Lugtenburg J, Britton G, Jansen FJHM, Cornard JP, *Biospectroscopy* **1999**, *5*, 19-33. (b) Weesie RJ, Merlin JC, De Groot HJM, Lugtenburg J, Jansen FJHM, Cornard JP, *Biospectroscopy* **1999**, *5*, 358-370.
[7] Creemers AFL, Lugtenburg J, *J. Am. Chem. Soc.* **2002**, *124*, 6324-6334.
[8] Ouwerkerk N, Van Boom JH, Lugtenburg J, Raap J, *Eur. J. Org. Chem.* **2000**, 861-866.
[9] Jansen FJHM, *PhD. Thesis*, 1996, 48-55.
[10] Davis FA, Sheppard AC, Chen B-C, Haque MS, *J. Am. Chem. Soc.* **1990**, *112*, 6679-6690.
[11] Davies FA, Vishwakarma LC, Billmers JM, Finn J, *J. Org. Chem.* **1984**, *49*, 3241-3243.
[12] Davies FA, Chattopadhyay S, Towson JC, Reddy T, *J. Org. Chem.* **1988**, *53*, 2087-2089.
[13] Ernst H in *Carotenoids, Volume 2: Synthesis*; Britton G, Liaaen-Jensen S, Pfander H; Eds. Birkhäuser Verlag: Basel, 1996, 79-102.
[14] Widmer E, Zell R, Broger EA, Crameri Y, Wagner HP, Dinkel J, Schlageter M, Lukáč T, *Helv. Chim. Acta* **1981**, *64*, 2436.
[15] Widmer E, Zell R, Lukáč T, Casadei M, Schönholzer P, Broger EA, *Helv. Chim. Acta* **1981**, *64*, 2405.
[16] Widmer E, Soukop M, Zell R, Broger EA, Wagner HP, Infeld M, *Helv. Chim. Acta* **1990**, *73*, 861.
[17] Englert G, *Helv. Chim. Acta* **1975**, *58*, 2367.
[18] Courtin JMJ, 't Lam GK, Peters AJM, Lugtenburg J, *Recl. Trav. Chim. Pays-Bas* **1985** *104*(11), 281-288.
[19] Englert G, Kienzle F, Noack K, *Helv. Chim Acta* **1977**, *60*, 1209.

CHAPTER 3

SPECTROSCOPY AND QUANTUM CHEMICAL MODELING REVEAL A PREDOMINANT CONTRIBUTION OF EXCITONIC INTERACTIONS TO THE BATHOCHROMIC SHIFT IN α-CRUSTACYANIN, THE BLUE CAROTENOPROTEIN IN THE CARAPACE OF THE LOBSTER *HOMARUS GAMMARUS*

Published in *J. Am. Chem. Soc.* 127, 2005, 1438-1445.

To resolve the molecular basis of the coloration mechanism of α-crustacyanin, ^{13}C-labeled astaxanthins were used as chromophores for solid-state ^{13}C NMR and resonance Raman spectroscopy of [6,6′,7,7′]-$^{13}C_4$ α-crustacyanin and [8,8′,9,9′,10,10′,11,11′,19,19′]-$^{13}C_{10}$ α-crustacyanin. The experimental data were complemented with time-dependent density functional theory calculations on several models based on the structural information available for β-crustacyanin. The data rule out major changes and strong polarization effects in the ground-state electron density of astaxanthin upon binding to the protein. Conformational changes in the chromophore and hydrogen-bond interactions between the astaxanthin and the protein can account for only about one-third of the total bathochromic shift in α-crustacyanin. The exciton coupling due to the proximity of two astaxanthin chromophores is found to be large, suggesting that aggregation effects in the protein represent the primary source of the color change.

3.1 INTRODUCTION

Carotenoids are the most widespread class of pigments in both plants and animals. They are responsible for many natural yellow, orange, or red colors. In addition, when carotenoids are associated with proteins, these colors can be modified to green, purple, or blue by the formation of carotenoid-protein complexes. A well-known example of this phenomenon is provided by the lobster *Homarus gammarus*, which is deep blue (λ_{max} = 632 nm, aq PO_4 buffer). Heat causes the lobster to change color from blue to red. The high temperature denatures the protein under liberation of the "red" astaxanthin (λ_{max} = 472 nm in *n*-hexane, λ_{max} = 478 nm in acetone). The bathochromic shift of the astaxanthin chromophore in α-crustacyanin has intrigued scientists for many years.

In a seminal paper, Buchwald and Jencks reported that α-crustacyanin can be irreversibly dissociated in eight β-crustacyanin units.[1] β-Crustacyanin consists of two apoprotein units and two bound astaxanthin units. They also reported the visible, optical rotary dispersion and circular dichroism (CD) spectra of α- and β-crustacyanin. In both systems, the main CD band exhibits a change of sign at the absorption maximum with a negative and a positive peak at wavelengths above and below the absorption maximum, respectively. Renström et al. found that the CD spectra are not influenced by the intrinsic chirality of the astaxanthin in α-crustacyanin.[2] The negative chirality demonstrated by the CD spectra indicates an exciton coupling of the astaxanthins similar to that predicted by exciton theory.[3] Among the possible mechanisms for the perturbed optical properties of astaxanthin in α-crustacyanin, it was also suggested that distortion, such as twisted double bonds induced by the protein, may play a role.[1]

The subsequent resonance Raman (RR) spectroscopy of α-crustacyanin by Carey et al. indicated that the astaxanthin chromophore shows no distortion due to twists in the double bonds of the conjugated system and is in agreement with free relaxed carotenes.[4] On the basis of this resonance Raman study, the hypothesis of the exciton mechanism was discarded and it was concluded that the bathochromic shift is caused by a charge polarization mechanism possibly induced by charged groups and/or by hydrogen bonds in the binding site.[4]

More recently, to obtain structural information with atomic resolution, a solid-state ^{13}C NMR and resonance Raman spectroscopic study was performed on α-crustacyanin regenerated with astaxanthins that are symmetrically $^{13}C_2$-enriched in the central part.[5-7] The ^{13}C NMR data show substantial downfield shifts of 4.2 and 7.1 ppm for the 14,14′ position and 5.4 and 7.5 ppm for the 12,12′ carbon positions in α-crustacyanin.[5,6] Under the assumption that there is no exciton coupling and together with semiempirical theoretical calculations that fitted the electronic absorption properties, this work led to the hypothesis that there is a strong electrostatic polarization originating from the keto groups, most likely a double protonation.[7] The resonance Raman spectra from the same ^{13}C isotopomers of α-crustacyanin showed that the pattern of the changes in the double bond frequency region differs from that in free astaxanthin itself and all-*E* spheroidene.[7,8]

Recently, the X-ray structure of β-crustacyanin at 3.2 Å resolution has been published.[9] The X-ray study shows that in β-crustacyanin two astaxanthins are present in parallel planes that cross at a distance of 7 Å just a little outside the centers of the chromophores, as shown in Figure 1. The vectors of the central axis are oriented at 120°. The conformation around the 6-7 and 6'-7' bonds is planar s-trans, in contrast to free astaxanthin, which has a s-cis conformation. The oxygen at the 4'-keto group is close to His-90 and His-92 for astaxanthin 1 and 2, respectively. The two other keto groups have interactions with Asp, two Tyr residues, a Ser, and a bound water molecule. Although the increased conjugation due to the end ring's coplanarization should lead to a bathochromic shift with respect to free astaxanthin, it has been stated that this effect is not sufficient to explain the color of β-crustacyanin.[9]

Despite considerable progress made in structural and spectroscopic studies, a clear converging picture on the dominant mechanism for the bathochromic shift in crustacyanin is still missing. There are two main hypotheses that are still debated: (i) the "on-site" (intramolecular) mechanism involving protein-induced conformational changes and/or charge-polarization effects modifying the electronic ground state of the chromophore; and (ii) the aggregation (intermolecular) mechanism due to the interaction of the chromophores in the subunits of crustacyanin inducing an exciton coupling of the transition dipole moments in the excited state.

To resolve the precise molecular basis of the coloration mechanism of α-crustacyanin ^{13}C-labeled astaxanthins were used as chromophores for solid-state ^{13}C NMR and resonance Raman spectroscopy of [6,6′,7,7′]-$^{13}C_4$ α-crustacyanin (**1a**) and [8,8′,9,9′,10,10′,11,11′,19,19′]-$^{13}C_{10}$

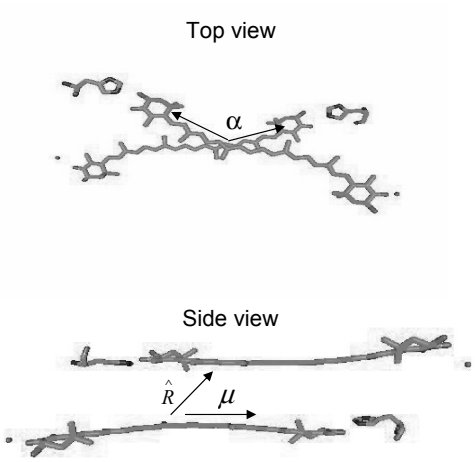

Figure 1. *Top view and side view of two astaxanthin molecules in β-crustacyanin. α is the angle between the long axes of the astaxanthin molecules; $\hat{R}$ is the unit vector connecting the center of mass of the two molecules, and μ shows the orientation of the transition dipole moment along the axis. The atomic coordinates have been extracted from the Protein Data Bank file (PDB code 1GKA).*

α-crustacyanin (**1b**), establishing the electronic charge distribution and vibrational contribution of the remaining sp^2 carbon atoms. Figure 2 shows the structure and numbering of the all-*E* astaxanthin (3,3′-didehydro-β,β-carotene-4,4′-dione) chromophore. The position of the ^{13}C enrichment is marked with (A) for [6,6′,7,7′]-$^{13}C_4$ astaxanthin (**2a**) and with (B) for [8,8′,9,9′,10,10′, 11,11′,19,19′]-$^{13}C_{10}$ astaxanthin (**2b**).

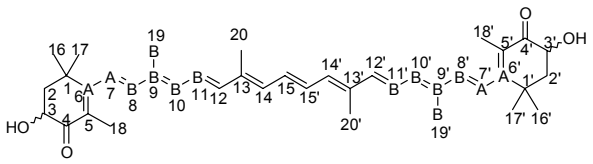

Figure 2. *Molecular structure and IUPAC numbering of synthetic all-E astaxanthin (3,3′-didehydro-β,β-carotene-4,4′-dione) as a mixture of 25% (3R,3′R), 25% (3S,3′S) and 50% (3R,3′S).*
*A is the ^{13}C for [6,6′,7,7′]-$^{13}C_4$-all-E astaxanthin (**2a**)*
*B is the ^{13}C for [8,8′,9,9′,10,10′,11,11′,19,19′]-$^{13}C_{10}$-all-E astaxanthin (**2b**)*

The spectroscopic data were complemented with quantum mechanical calculations of the electronic ground state and excitation energies of various astaxanthin models based on the structural information available for β-crustacyanin. The theoretical investigation is crucial to identifying the relative importance of different mechanisms that may contribute to the total bathochromic shift.

3.2 MATERIALS AND METHODS

3.2.1 Synthesis of ^{13}C-Labeled Astaxanthins

The synthetic strategy for preparing astaxanthin with 99% ^{13}C enrichment at any position or combination of positions is described in Chapter 2. For ^{13}C enrichment of the 6,6′,7,7′-position, the commercially available $^{13}C_2$-acetonitrile was used. The ^{13}C incorporation at the 8,8′,9,9′, 10,10′,11,11′,19,19′ positions was effected by $^{13}C_5$-triethyl-3-methyl-4-phosphonocrotonate, which was prepared analogous to the corresponding nitrile derivative which was used earlier for the synthesis of uniformly ^{13}C-enriched retinal.[10,11]

A quantity of 140 mg (0.23 mmol) of all-*E* [6,6′,7,7′]-$^{13}C_4$ astaxanthin (**2a**) (25% (3*R*,3′*R*), 25% (3*S*,3′*S*) and 50% (3*R*,3′*S*)) was obtained in 10 steps starting from 1.3 g (30.7 mmol) $^{13}C_2$-acetonitrile. Similarly, 50 mg (0.08 mmol) of all-*E* [8,8′,9,9′,10,10′,11,11′,19,19′]-$^{13}C_{10}$ astaxanthin (**2b**) (25% (3*R*,3′*R*), 25% (3*S*,3′*S*) and 50% (3*R*,3′*S*)) was obtained. Solution ^1H and ^{13}C NMR spectra were recorded of **2a** and **2b** and compared with the spectra of unlabeled astaxanthin, to observe the effect of the specific ^{13}C enrichment on the NMR spectra, and to verify the position and level of the ^{13}C enrichment. NMR spectroscopy confirmed the purity of the all-*E* [6,6′,7,7′]-$^{13}C_4$

astaxanthin **2a** and [8,8′,9,9′,10,10′,11,11′,19,19′]-$^{13}C_{10}$ astaxanthin **2b** and >99% ^{13}C enrichment at the desired positions. The NMR characterization is discussed in Chapter 2.

3.2.2 Isolation and Reconstitution of α-Crustacyanin

The blue protein α-crustacyanin was extracted from lobster carapace and subsequently purified by anion-exchange and gel-filtration chromatography according to the procedure described by Zagalsky.[12] The purity of α-crustacyanin was determined by the ratio of absorbance at 632 nm and 280 nm, and fractions with A_{632}:A_{280} > 3.5 were used for reconstitution. The total amount of α-crustacyanin was determined from the absorbance at 632 nm. A molar extinction coefficient, $\varepsilon = 1.25 \times 10^5\ M^{-1}\ cm^{-1}$, was used.

The reconstitution procedure was based on the method described by Zagalsky.[12] Briefly, astaxanthin was removed from the carotenoprotein with acetone/ether extraction. To the resulting colorless apoprotein was quickly added the labeled carotenoid (**2a** or **2b**) in acetone, the mixture was stirred, and phosphate-buffer was added. The color of the complex quickly turned blue-purple. The mixture was dialyzed overnight against 5 L phosphate buffer, pH 7.0, and the reconstituted complex was purified on a short gel-filtration column; the purity was determined by the A_{632}:A_{280} ratio with UV-vis spectroscopy. This method yielded [6,6′,7,7′]-$^{13}C_4$ α-crustacyanin (**1a**) and [8,8′,9,9′,10,10′,11,11′,19,19′]-$^{13}C_{10}$ α-crustacyanin (**1b**).

3.2.3 Solution NMR Spectroscopy

^1H NMR spectra, ^1H-^{13}C-decoupled NMR spectra, and ^{13}C NMR spectra of astaxanthin in $CDCl_3$ were recorded on a Bruker AM-600 spectrometer using tetramethylsilane (^1H δ = 0 ppm) or $CDCl_3$ (^{13}C δ = 77.00 pm) as internal standard.

3.2.4 Solid-State NMR Spectroscopy

Approximately 10 mg of α-crustacyanin reconstituted with ^{13}C-labeled astaxanthin was used for each SSNMR sample. The solutions were first concentrated with a 100 kDa Macrosep centrifugal concentrator to a volume of 2 mL. Subsequently, 10 kDa Eppendorf centrifugal concentrators were used to reduce the volume to 200 µL. The resulting very dense blue solutions were transferred to a 4 mm MAS rotor with a homemade centrifugal swing-out device. NMR spectra were recorded at 188 MHz ^{13}C frequency using a Bruker DSX-750 spectrometer equipped with a double-resonance MAS probe. The samples were cooled to 223 K, and the MAS spin rate was 12 kHz for all experiments. The CP/MAS spectra were recorded using 2.0 ms ramped cross-polarization and two-pulse phase modulation decoupling during acquisition.[13,14] Radio frequency-driven (RFDR) dipolar recoupling correlation spectra were acquired using a pathway-selective phase-cycling method.[15] The 2D heteronuclear correlation (HETCOR) spectra were recorded with phase-modulated Lee-Goldburg decoupling during the t_1-period.[16,17]

3.2.5 Resonance Raman Spectroscopy

A home-built confocal Raman microspectrometer was used to measure Raman spectra of the carotenoids (dissolved in $CHCl_3$) and carotenoproteins (dissolved in aqueous phosphate buffer). A Kr ion laser (Coherent Innova 90-K) with an emission wavelength of 647.1 nm was used to excite the Raman scattering. The laser power on the sample was 5 mW. A dichroic beam splitter (660 DCLP, Chroma Technology Corp.) was used in order to separate the Raman scattered light from the laser light, which was further suppressed by a holographic notch filter (Kaiser Optical Systems Inc.) with an optical density of 4.0 at the excitation wavelength.

The measurement time per spectrum was 50 s. The spectrograph stage (Jobin-Yvon HR460) was equipped with a blazed holographic grating with 1200 l/mm. This resulted in a dispersion of 0.8 cm/pixel on a CCD camera (Roper Scientific, Inc.). This camera contains a liquid-nitrogen-cooled, back-illuminated chip with 1100 × 330 pixels and a pixel size of 24 × 24 μm^2. The setup is connected to a computer that controls the instrument settings, the data read-out, and the data storage.

3.2.6 Computational Methods and Details

The geometry optimization of astaxanthin and of the various models considered here was performed with the semiempirical AM1 method. The calculation of excitation energies and transition dipole moments to the optically allowed ^1B_u excited state was performed using time-dependent density functional theory (TDDFT).[18] The BLYP generalized gradient approximations was used for the exchange and correlation functional.[19] The calculations were done with a triple-ζ Slater-type orbital (STO) basis set with a single set of polarization functions using the Amsterdam Density Functional (ADF) package.[20]

TDDFT allows calculating properties, such as excitation energies, through the linear density response of the system to the external time-dependent field. It is known that TDDFT shows a systematic underestimation of the excitation to the optically allowed ^1B_u state in linear polyenes by about 0.5-0.7 eV.[21] However, the general trend of decreasing excitation energy with chain length is correctly reproduced. Since here the bathochromic shift of the absorption energy is of interest rather than the absolute values, TDDFT represents a good compromise between accuracy and computational efficiency for our models. Indeed, the use of more accurate multi-configuration self-consistent field (MCSCF) calculations would be computationally prohibitive for the large molecules studied here.

The aggregation effects are estimated using a simple dipole-dipole approximation of the interaction between the two astaxanthins in the geometry of the β-crustacyanin dimer. Within this approximation, the interaction that gives an estimate of the exciton splitting can be written as

$$V_{12} = \frac{1}{4\pi\varepsilon_0} \frac{\mu_1 \ \mu_2 \ \ 3(\mu_1 \ \hat{R})(\mu_2 \ \hat{R})}{R^3}$$

Here, μ is the transition dipole moment; $\hat{R}$ is the unit vector connecting the two molecules, and R is the distance between the two molecules. The transition dipole moment is obtained from the TDDFT calculation, and the orientation factor is estimated using the β-crustacyanin structure. The dielectric constant in the vacuum was used, though inside the protein it may generally be larger.

3.3 RESULTS

3.3.1 Solid-State NMR Spectroscopy of α-Crustacyanin

^{13}C CP/MAS NMR data were collected from natural abundance α-crustacyanin, [6,6′,7,7′]-$^{13}C_4$ α-crustacyanin (**1a**) and [8,8′,9,9′,10,10′,11,11′,19,19′]-$^{13}C_{10}$ α-crustacyanin (**1b**) (Figure 3). The natural abundance spectrum of α-crustacyanin shows the characteristic features of a protein spectrum. Between 0 and 40 ppm, the signals of the aliphatic side chains of the amino acids are observed. Around 50 ppm, the resonances from C_α atoms are found, while around 120 ppm, the responses of the aromatic amino acid residues are recognized. The sharp signal at 170 ppm is assigned to the carbonyl-carbon of the peptide bonds.

In the spectra of Figure 3, the signals marked with (*) are not detected for the natural abundance sample and arise from the ^{13}C labels of the chromophore. The signal at 120 ppm in Figure 3A is assigned to the ^{13}C label at C7/C7′ of the chromophore since the shift is comparable with δ(C7) = 123.3 ppm observed for astaxanthin in $CDCl_3$.[22] The signal from the ^{13}C label at C6/C6′ of the chromophore at 162 ppm is also close to δ(C6) = 162.4 ppm for the C6 of free astaxanthin in $CDCl_3$. The NMR response appears symmetric as no difference between C6 and C6′ and between C7 and C7′ was observed within the resolution of the NMR spectra.

In the spectrum of **1b**, the strongest signal is at 11 ppm, which is assigned to C19/C19′ (Figure 3B). This shift is close to the shift of C19/C19′ in solution (δ(C19) = 12.6 ppm in $CDCl_3$).[22] The signals between 120 and 150 ppm from C8 – C11 can be assigned using 2D homonuclear (^{13}C-^{13}C) and 2D heteronuclear (^{1}H-^{13}C) dipolar correlation techniques. Figure 4 shows the contour region of the 2D RFDR and 2D HETCOR NMR spectra of [8,8′,9,9′,10,10′,11,11′,19,19′]-$^{13}C_{10}$ α-crustacyanin. Starting from the signal of C19/C19′, we assigned the label clusters. The signal of C11/C11′ was found at 123 ppm, similar to the value in solution (δ(C11) = 124.1 ppm in $CDCl_3$).[22] A correlation between C11 and C10 was found, and the C10/C10′chemical shift was determined at 144 ppm. This value is about 9 ppm higher compared to the value in solution (δ(C10) = 135.1 ppm in $CDCl_3$).[22] From C10, correlations to C8 and C9 were found at 142, 134, and 131 ppm. The signals at 134 and 131 ppm show no correlation in the HETCOR spectrum and are assigned to C9 and C9′. These values are comparable to the chemical shift of C9 for astaxanthin in solution (δ(C9) = 134.7 ppm in $CDCl_3$).[22] Finally, the signal at 142 ppm was assigned to C8/C8′. Again, this signal is comparable to the value for astaxanthin in solution (δ(C8) = 142.2 ppm in $CDCl_3$).[22] Table 1 gives

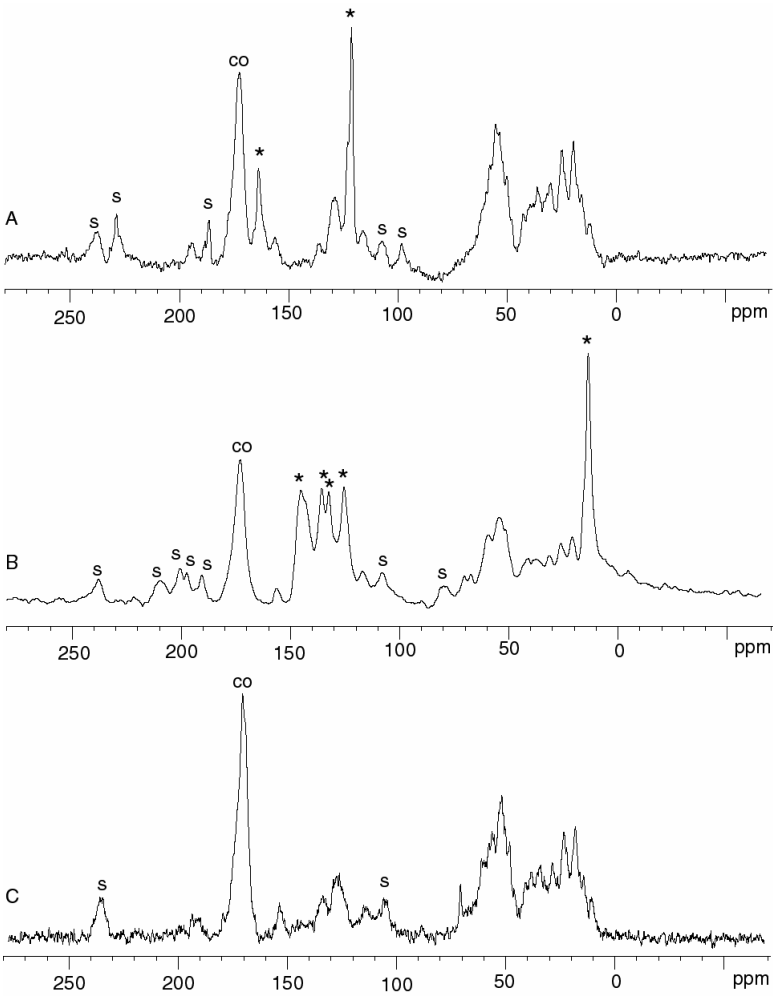

Figure 3. *^{13}C CP/MAS NMR spectra of α-crustacyanin: A, reconstituted with [6,6′,7,7′]-$^{13}C_4$ astaxanthin (**1a**); B, reconstituted with [8,8′,9,9′,10,10′,11,11′,19,19′]-$^{13}C_{10}$ astaxanthin (**1b**), and the natural abundance spectrum (C). The signals arising from the ^{13}C enrichment are indicated with (*). The spinning sidebands are marked with (s). The signal arising from the carbonyl carbons of the protein is marked with (CO). The spectra are recorded at 188 MHz ^{13}C frequency and 223 K with a MAS spin rate of 12 kHz.*

the ^{13}C NMR data of astaxanthin in α-crustacyanin, and the comparison with the free carotenoid in $CDCl_3$.

From the NMR data, C8/C8′, C10/C10′, C11/C11′, and C19/C19′ could not be discriminated, which shows that for these carbon sites, the interactions of the chromophore with the protein on

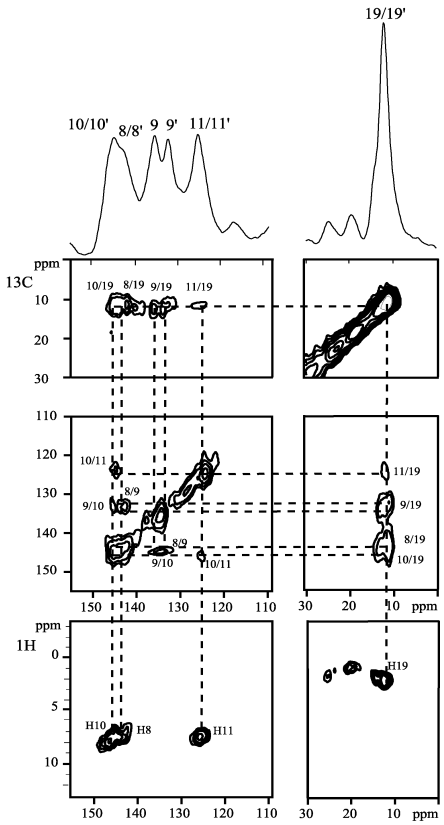

Figure 4. *Contour region of the 2D homonuclear (^{13}C-^{13}C) and 2D heteronuclear (^{1}H-^{13}C) dipolar correlation spectra of [8,8',9,9',10,10',11,11',19,19']-$^{13}C_{10}$ α-crustacyanin (**1b**). The ^{13}C-^{13}C correlations and ^{13}C-^{1}H correlations are shown.*

both halves of the astaxanthin are similar. Only for C9/C9', C12/C12', and C14/14' are slightly different chemical shifts observed, confirming that the binding of the chromophore is not fully symmetrical.[6] The slight asymmetry is probably caused by a difference in protein environment, although it is not clear why these specific signals can be resolved as distinct signals, whereas the signals of other pairs overlap.

It was found that only minor changes in the ground-state electron density of the C atoms 8-11 of astaxanthin occur upon binding. In particular, small shifts to higher field are found for C7/C7' (-3 ppm) and C9/C9'(-1/-4 ppm), and a relatively large downfield shift is detected for C10/C10' (+9 ppm). The small effect for the C8 effectively rules out the hypothesis of a polarization originating from the keto groups of the chromophore. NMR studies on protonated canthaxanthin show that a strong electrostatic effect, like a single or double protonation, should give increasingly larger changes in the chemical shift values of the even-numbered atoms closer to the ring,[23] in contrast with the observed data for astaxanthin in α-crustacyanin.

Table 1. *^{13}C NMR Data of Astaxanthin in Solution and Astaxanthin bound in α-Crustacyanin.*

C atom	$\delta_{solution}$ [a]	$\delta_{\alpha\text{-crustacyanin}}$ [b]		$\Delta_{binding}$	
4/4′	200.4	203.4		3.0	
6/6′	162.4	162		0	
7/7′	123.3	120		-3	
8/8′	142.2	142		0	
9/9′	134.7	133.8	130.5	-0.9	-4.2
10/10′	135.1	144		9	
11/11′	124.1	123		-1	
12/12′	139.7	145.1	147.2	5.4	7.5
13/13′	136.7	135.2		-1.5	
14/14′	133.8	138.0	140.9	4.2	7.1
15/15′	130.7	129.5		-1.2	
19/19′	12.6	11.1		-1.5	
20/20′	12.8	11.1		-1.7	

[a]Data from Englert et al.[22]

[b]Data of C4/4′, C12/12′, C13/13′, C14/14′, C15/15′, and C20/20′ from Britton et al.[6]

3.3.2 Resonance Raman Characterization of ^{13}C-Labeled Astaxanthin

The resonance Raman spectra of astaxanthin, [6,6′,7,7′]-$^{13}C_4$ astaxanthin (**2a**), and [8,8′,9,9′,10,10′,11,11′,19,19′]-$^{13}C_{10}$ astaxanthin (**2b**) are shown in Figure 5. The spectra of β,β-carotene and [12,12′,13,13′,14,14′,15,15′,20,20′]-$^{13}C_{10}$ β,β-carotene are added for comparison.

The RR spectrum of unlabeled astaxanthin (Figure 5C) is characterized by three main lines at 1520 (ν_1), 1158 (ν_2), and 1005 cm^{-1} (ν_3), in agreement with data for all-*E* astaxanthin published before by other groups.[24,25] The intense line around 1520 cm^{-1} has been assigned to the C=C stretch vibrations of the central part of the polyene chain. The line of astaxanthin at 1158 cm^{-1} has been assigned previously to a combination of the unmethylated C-C stretch and the C-H in-plane bending vibrations. The ν_3-line at 1005 cm^{-1} is relatively weak compared to the ν_1 and ν_2 signals and is assigned to the CH_3 in-plane rocking vibrations.

The Raman spectra of $^{13}C_4$ astaxanthin (**2a**, see Figure 5A) and $^{13}C_{10}$ astaxanthin (**2b**, see Figure 5B) were compared with the spectrum of natural abundance astaxanthin (Figure 5C) to study the effect of the ^{13}C labeling. The spectrum of [6,6′,7,7′]-$^{13}C_4$ astaxanthin (**2a**) is almost identical to the spectrum of unlabeled astaxanthin, with the main lines at 1516, 1156, and 1005 cm^{-1}. The ^{13}C labels are at the end of the central polyene chain and have little or no effect on the RR spectrum.

The bands of [8,8′,9,9′,10,10′,11,11′,19,19′]-$^{13}C_{10}$ astaxanthin (**2b**, see Figure 5B) are shifted compared to those of unlabeled astaxanthin. Although the shape and relative intensities of the lines are similar, a significant shift to lower frequencies is observed for the main lines. The ν_1-line is shifted to 1509 cm^{-1} (-11 cm^{-1}), the ν_2-line is shifted to 1147 cm^{-1} (-11 cm^{-1}), and the ν_3-line is

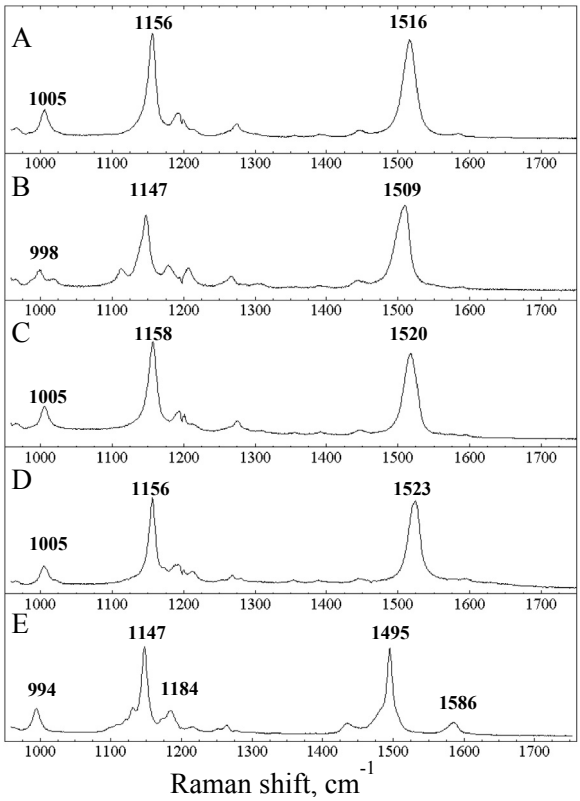

Figure 5. *Resonance Raman spectra: (A) [6,6',7,7']-$^{13}C_4$ astaxanthin (**2a**); (B) [8,8',9,9',10,10',11,11',19,19']-$^{13}C_{10}$ astaxanthin (**2b**); (C) natural abundance astaxanthine; (D) β,β-carotene; and (E) [12,12',13,13',14,14',15,15',20,20']-$^{13}C_{10}$ β,β-carotene.*

shifted by -7 cm^{-1} from 1005 to 998 cm^{-1}. Moreover, the ^{13}C isotope substitution leads to a more complex band pattern near the ν_2-line, where a band is observed at 1115 cm^{-1}, and the weak band of astaxanthin around 1200 cm^{-1} is split into bands at 1185 and 1205 cm^{-1}.

The RR spectrum of β,β-carotene (see Figure 5D) is very similar to the spectrum of astaxanthin, though the end-groups are different.[8] The spectrum of $^{13}C_{10}$ β,β-carotene (Figure 5E), with ^{13}C labels in the central part of the polyene chain, is clearly different from the spectrum of unlabeled β,β-carotene, with shifts of the ν_1-line (-28 cm^{-1}), ν_2-line (-9 cm^{-1}), and ν_3-line (-11 cm^{-1}). The ^{13}C isotope substitution in β,β-carotene also leads to more complex spectral features around the ν_2-band, and a Raman band at 1125 cm^{-1} can be observed as a shoulder. In addition, the intensity of the broad line at 1586 cm^{-1} is increased, and small changes in the fingerprint region are observed. This confirms that ^{13}C labeling in the central parts of carotenoids significantly changes the RR spectra.

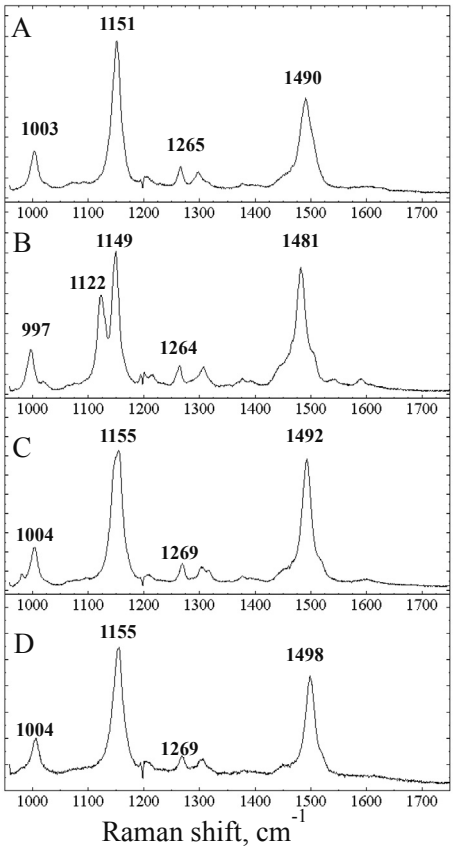

Figure 6. *Resonance Raman spectra: (A) α-crustacyanin reconstituted with [6,6′,7,7′]-$^{13}C_4$ astaxanthin (**1a**); (B) α-crustacyanin reconstituted with [8,8′,9,9′,10,10′,11,11′,19,19′]-$^{13}C_{10}$ astaxanthin (**1b**); (C) natural abundance α-crustacyanin; and (D) natural abundance β-crustacyanin.*

3.3.3 Resonance Raman Characterization of α-Crustacyanin

The resonance Raman spectra of α-crustacyanin, $^{13}C_4$ α-crustacyanin (**1a**), and $^{13}C_{10}$ α-crustacyanin (**1b**) are shown in Figure 6. The spectrum of α-crustacyanin (see Figure 6C) is distinctly different from the spectra of astaxanthin. The ν_1-line is shifted from 1520 to 1492 cm^{-1}, a shift which is correlated with the change in absorption maximum from 472 to 632 nm, qualitatively following the empirical relationship between ν_1 and $1/\lambda_{max}$.[26,27] In the fingerprint region between 1250 and 1400 cm^{-1}, new Raman bands appear that are absent in free astaxanthin. The vibrations of the ν_2- and ν_3-line do not shift upon binding, although small shoulders appear on these bands.

The spectrum of $^{13}C_4$ α-crustacyanin (Figure 6A) is similar to the spectrum of natural abundance α-crustacyanin. Only minor shifts of the ν_1-line (1490 cm^{-1}), the ν_2-line (1151 cm^{-1}), and the ν_3-line (1003 cm^{-1}) are observed, compared to those of the natural abundance α-crustacyanin.

However, the spectrum of $^{13}C_{10}$ α-crustacyanin (see Figure 6B) shows distinct differences compared to that of natural abundance α-crustacyanin. The ν_1-line shows a downshift of 11 cm^{-1}, from 1492 cm^{-1} in natural abundance astaxanthin to 1481 cm^{-1} in **1b**. The ν_2-line in α-crustacyanin is shifted –6 cm^{-1} to 1149 cm^{-1} and is broadened. The broadening is related to a protein-induced splitting in otherwise degenerate vibrational modes. The ^{13}C isotope labeling in α-crustacyanin demonstrates a complete lifting of the degeneracy as an intense band arises next to the ν_2 band at 1122 cm^{-1}. The ν_3-line shifts from 1005 to 997 cm^{-1} due to ^{13}C labels in **1b**.

For comparison, the spectrum of β-crustacyanin was also recorded, as shown in Figure 6D. The band positions of the ν_2- and ν_3-line are the same as those for α-crustacyanin, although the broadening of the ν_2-line is smaller for β-crustacyanin than for α-crustacyanin. The ν_1-line is shifted to 1498 cm^{-1}, which is in line with the λ_{max} (586 nm) of β-crustacyanin being smaller than for α-crustacyanin (632 nm).[26] This indicates that the interactions of the chromophore with the protein are similar in α- and β-crustacyanin.

3.3.4 Models and Quantum Chemical Calculations

To analyze the relative importance of the possible mechanisms contributing to the total bathochromic shift, the following models were considered: (I) free astaxanthin, (II) 6-s-*trans* astaxanthin with the end rings coplanar to the polyene chain, and (III) 6-s-*trans* astaxanthin, including a hydrogen-bonded histidine analogue (methylimidazole) and a water molecule according to the X-ray data on β-crustacyanin.[9] Comparison of model I and model II gives a measure of the shift induced by the increased conjugation due to the ring coplanarization. Model III shows the importance of the polarization effects due to the hydrogen bonding with the keto oxygens.

Table 2 reports the first excitation energy with a considerable oscillator strength obtained with TDDFT for the three carotenoid models described above. This excitation corresponds to the allowed ^1B_u-like excited state and can be described to a large extent as a HOMO to LUMO transition (contributing to more than 80% of the excitation) in all cases. To compare the shift in nanometers with the experimental values, the values in the second column are shifted by 0.7 eV. With this offset, the excitation energy of the free astaxanthin model corresponds closely to the experimental value for astaxanthin. As discussed above, the underestimation of the excitation energy within TDDFT is in line with previous theoretical investigations for long polyenes. Nevertheless, the shift due to a change in conformation or to the presence of hydrogen bonds is reliable.

In the free s-*cis* astaxanthin model optimized within the semiempirical AM1 approach, the end rings form a dihedral angle of ~ 46˚ with the polyene chain. This is in close agreement with the

Table 2. *Excitation Energies for Carotenoid Models I, II, and III Obtained with TDDFT*[a]

model	Δ*E* (eV)	Δ*E* (eV) + 0.7 eV shift
I (s-*cis* astaxanthin)	1.89	2.59 (478 nm)
II (s-*trans* astaxanthin)	1.77	2.47 (502 nm)
III (s-*trans* astaxanthin + water + His)	1.70	2.40 (517 nm)
III + exciton splitting		1.91 (650 nm)

[a] In the second column, the TDDFT results are shifted for a comparison with the experimental data (see text). In parentheses, the corresponding λ_{max} in nanometers is given. The excitation energy in the last row is obtained by adding the estimated exciton splitting to the TDDFT result of model III.

43° angle observed in X-ray studies of canthaxanthin.[28] According to the X-ray structure of β-crustacyanin,[9] the astaxanthin chromophores bound to the protein are in an all-*E* conformation with the end rings essentially coplanar to the polyene chain. Thus, the main conformational change from free astaxanthin to the chromophore in β-crustacyanin consists of the coplanarization of the end rings, inducing a more extended conjugated chain. Comparing models I and II, it is found that this protein-induced conformational change produces a shift of 0.12 eV ($\Delta\lambda_{max}$ = 24 nm). The next step is the inclusion of polarization effects induced by hydrogen-bonding interaction. The X-ray structure of β-crustacyanin[9] has revealed an asymmetric environment of the chromophore with a histidine and a water molecule hydrogen bonded to the keto oxygens. In model III, these interactions are included explicitly and a further shift in the excitation energy is obtained, though relatively small, giving a total shift of 0.19 eV ($\Delta\lambda_{max}$ = 39 nm) compared to the s-*cis*-astaxanthin model.

The Mulliken partial atomic charge differences between models I and III have also been calculated. It was found that the hydrogen bonds induce a small positive charge on the chromophore, which is consistent with the small positive charge difference estimated on the basis of ^{13}C chemical shift data for α-crustacyanin, thus further supporting the conclusion that keto groups are not protonated and no strong polarization occurs upon binding.

An analysis of the HOMO and LUMO orbitals for models I and III shows that a charge displacement from the center of the chromophore toward the rings occurs upon excitation in the model including the hydrogen bonding with the protein environment, while little charge displacement is observed for the free chromophore. Subsequently, the importance of aggregation effects for the bathochromic shift mechanism was considered. A first-order estimate of the exciton splitting induced by the proximity of the chromophores in the protein can be obtained using the dipole-dipole approximation. The X-ray structural information available for β-crustacyanin was used to evaluate the geometrical factor, and the transition dipole moment within the TDDFT for model III was computed. The two bound astaxanthins in β-crustacyanin approach each other within 7 Å at a position close to the C11-C12 bond. As can be seen in Figure

1, the long axes of the molecules form an angle of about 120˚. The computed transition dipole moment is very intense (~ 19 D) and oriented parallel to the long axis of the molecule pointing toward the ring hydrogen bonded to the His residue. By using this information together with the orientation factor in the dipole-dipole approximation, an exciton splitting of 0.49 eV was obtained. By adding the exciton splitting to the previously computed on-site shift for model III, a λ_{max}= 650 nm is obtained (see Table 2). Even considering the limitation of the simple dipole-dipole approximation used here, it can be conclude that the aggregation effects appear to give the largest contribution in determining the total bathochromic shift.

3.4 DISCUSSION

In principle, two hypotheses could serve as a basis for understanding the bathochromic shift. The first hypothesis is exciton coupling of the transition dipole moments in the excited state, and the second hypothesis is interactions of the protein with the astaxanthin chromophore in the ground state via a polarization mechanism. The exciton coupling hypothesis was first suggested on the basis of the observed circular dichroism spectra of α- and β-crustacyanin.[1,29,30] However, the importance of this effect has been underestimated since it was expected that a strong coupling should give rise also to large changes in the shape of the absorption bands which were not observed.[1] The resonance Raman spectra of Salares et al.[4] showed a lowering in the $\nu_{C=C}$ frequency indicative of electron delocalization in the electronic ground state. On the basis of these Raman spectra, the polarization hypothesis was strongly supported and it has since become favored as the primary basis of the bathochromic shift. Moreover, it was pointed out that the argument that a large red shift in the absorption maximum should be accompanied by a change in absorption profile was not necessarily true.[4]

In view of the results from the SSNMR, Raman spectroscopy and quantum chemical calculations, these two hypotheses for the bathochromic shift can now be evaluated in more detail. First, it should be noted that the SSNMR and Raman spectroscopy analyses are performed on α-crustacyanin, whereas the computational analysis is carried out on models based on the known structure of β-crustacyanin. It is assumed that the effects that are responsible for the bathochromic shift in both carotenoproteins are qualitatively comparable and that the chromophore-protein interactions are similar in α- and β-crustacyanin. This is based on the knowledge that α-crustacyanin is an aggregate of eight β-crustacyanin units and supported by the similar shape of the UV-vis, optical rotary dispersion, Raman spectra, and same sign pattern in CD spectra of α- and β-crustacyanin.[1,30]

The SSNMR experiments show that no strong polarization effect in the ground state takes place upon binding of astaxanthin in the protein. Now the earlier hypothesis that a large charge effect, such as protonation, near the keto groups of the chromophore is responsible for the bathochromic shift can definitely be discarded. Indeed, a strong electrostatic effect, such as

the one induced by protonation, should give much larger changes in the chemical shifts of the atoms close to the ring.[23] The rather small NMR chemical shift differences (see Table 1) are indicative of small changes in the ground-state electronic distribution due to the rotation of the end rings and to polarization effects due possibly to hydrogen bonding with the protein. These conclusions are consistent with the X-ray analysis of the binding site of β-crustacyanin. Although the resolution of the X-ray data is not sufficient to determine protonation states, no charged amino acids were observed in the proximity of the astaxanthin ring.[9] The SSNMR data show that the absence of strong polarization effects due to charged residues is true also in α-crustacyanin.

A comparison of the resonance Raman spectra of astaxanthin and α-crustacyanin, show that the ν_1-line, which is assigned to the C=C stretch vibration, is shifted to a lower wavenumber, consistent with previous Raman studies. The observed downshift of the ν_1-line can be correlated to the rotation around the C6-C7 bond of the chromophore from 6-s-cis to 6-s-trans. This conformational change extends the conjugated polyene, leading to a larger delocalization of the π-electron system. However, the observed shift does not quantitatively fit the empirical relationship found for carotenoids between the ν_1-vibration and $1/\lambda_{max}$.[26] This indicates that in addition to the extension of the conjugated system, other factors must contribute to the bathochromic shift.

Also a striking change was observed in the spectral region near the ν_2-line of the carotenoprotein with ^{13}C labels in the chromophore at the [8,8′,9,9′,10,10′,11,11′,19,19′] (**1b**) positions where an intense band is present at 1122 cm^{-1}, while in free ^{13}C-labeled carotenoids, a weak band appears. The enhanced intensity of this band is a direct indication that the electronic excited state delocalizes upon binding to the protein, adding Raman oscillator strength to this mode.

Quantum chemical calculations on molecular models obtained from the X-ray data of β-crustacyanin show that the transition from 6-s-*cis*-astaxanthin to 6-s-*trans*- is accompanied by a considerable change in λ_{max} to 502 nm. This is by far not sufficient to account for the full bathochromic shift that occurs upon binding.[31] Also, the effect of hydrogen bonding due to the presence of a water molecule and a histidine close to the astaxanthin carbonyl gives rise to a small bathochromic shift, the combined effects shifting λ_{max} to 517 nm. Therefore, on the basis of the TDDFT calculations, it can be concluded that the total protein-induced on-site effects on the bathochromic shift are not very large and can account for only about 30% of the total observed bathochromic shift in α-crustacyanin and 40% of the bathochromic shift in β-crustacyanin.

The charge displacement from the center of the chromophore toward the end rings upon excitation shown by the analysis of the HOMO and LUMO orbitals is in line with the large effect observed on the Raman ν_2-line. This charge displacement is also consistent with Stark experiments showing an enhancement in the excited-state dipole moment for α-crustacyanin compared to that of isolated astaxanthin.[32]

The study described in this chapter strongly supports the hypothesis of exciton coupling as the main source of the bathochromic shift. Indeed, when the dipole-dipole interactions between the astaxanthin molecules in β-crustacyanin are taken into account, a large exciton splitting is found. The exciton splitting and the angle of about 120˚ between the dipole moments are consistent with the negative chirality observed in CD spectra of α- and β-crustacyanin.[1-3,29] When the exciton coupling is added to the on-site effects due to the more extended conjugation and hydrogen-bonding polarization, a $\lambda_{max} \approx 650$ nm is obtained. The calculated total shift is even larger than the observed bathochromic shift. In fact, the estimate of the exciton splitting is based on the structural information on the dimer in β-crustacyanin, where $\lambda_{max} = 586$ nm. It is very likely that the simple approximation of the dipole-dipole interaction in the excited state used here overestimates the exciton splitting. Further refinement in the modeling is needed to obtain a more quantitative estimate of the exciton splitting. Nevertheless, it can clearly be concluded that aggregation effects give the largest contribution to the observed color shift.

The bathochromic shift of α-crustacyanin is larger than that of β-crustacyanin ($\lambda_{max} = 632$ nm and 586 nm, respectively). The X-ray analysis of β-crustacyanin suggests that subunit-subunit interaction can take place in the aggregation of eight dimers in α-crustacyanin.[9] This interaction could induce a larger exciton splitting in α-crustacyanin, though a proper description of this effect needs further investigation.

3.5 CONCLUSION

The coloration mechanism of astaxanthin in α-crustacyanin was explored by using solid-state NMR and resonance Raman spectroscopy complemented by quantum chemical calculations based on time-dependent DFT. Solid-state NMR spectra of the ^{13}C-enriched α-crustacyanin show that only minor changes in the ground-state electron density of astaxanthin occur upon binding, thus ruling out the hypothesis of a strong polarization. From the comparison of Raman spectra for ^{13}C-labeled astaxanthin and α-crustacyanin, can be concluded that delocalization of the electronic excited state of the polyene chain close to the ring occurs upon binding. Time-dependent DFT calculations show that the protein-induced conformational changes and polarization effects contribute to about 30% of the total bathochromic shift in α-crustacyanin. The exciton coupling due to the proximity of the astaxanthin chromophores, estimated using the β-crustacyanin dimer structure, is found to be large and can account for the additional absorption shift.

REFERENCES

[1] Buchwald M, Jencks WP, *Biochemistry* **1968**, *7*, 844-859.
[2] Renström B, Rönneberg H, Borch G, Liaaen-Jensen S, *Comp. Biochem. Physiol. B* **1982**, *71*, 249-252.
[3] Nakanishi K, Berova N in *Circular Dichroism Principles and Applications;* Nakanishi K, Berova N, Woody R; Eds. VCH Publishers: New York, 1994, pp. 361-398.
[4] Salares VR, Young NM, Beukers HJ, Carey PR, *Biochim. Biophys. Acta* **1979**, *576*, 176-191.
[5] Weesie RJ, Askin D, Jansen FJHM, De Groot HJM, Lugtenburg J, Britton G, *FEBS Lett.* **1995**, *362*, 34-38.
[6] Weesie RJ, Jansen FJHM, Merlin JC, Lugtenburg J, Britton G, De Groot HJM, *Biochemistry* **1997**, *36*, 7288-7296.
[7] Weesie RJ, Merlin JC, De Groot HJM, Britton G, Lugtenburg J, Jansen FJHM, Cornard JP, *Biospectroscopy* **1999**, *5*, 358-370.
[8] Dokter AM, Van Hemert MC, In 't Velt CM, Van der Hoef K, Lugtenburg J, Frank HA, Groenen EJJ, *J. Phys. Chem. A* **2002**, *106*, 9463-9469.
[9] Cianci M, Rizkallah PJ, Olczak A, Raferty J, Chayen NE, Zagalsky PF, Helliwel JR, *Proc. Natl. Acad. Sci. U.S.A.* **2002**, *99*, 9795-9811.
[10] Jansen FJHM, Lugtenburg J, *Eur. J. Org. Chem.* **2000**, 829-836.
[11] Creemers AFL, Lugtenburg J, *J. Am. Chem. Soc.* **2002**, *124*, 6324-6334.
[12] Zagalsky PF, *Methods Enzymol.* **1985**, *111B*, 216-247.
[13] Pines A, Gibby MG, Waugh JS, *J. Chem. Phys.* **1973**, *59*, 569-573.
[14] Balaban TS, Holzwarth AR, Schaffner K, Boender GJ, De Groot HJM, *Biochemistry* **1995**, *34*, 15259-15266.
[15] Boender GJ, Raap J, Prytulla S, Oschkinat H, De Groot HJM, *Chem. Phys. Lett.* **1995**, *237*, 502-508.
[16] Van Rossum BJ, Boender GJ, De Groot HJM, *J. Magn. Reson. A* **1996**, *120*, 274-277.
[17] Vinogradov E, Madhu PK, Vega S, *Chem. Phys. Lett.* **1999**, *314*, 443-450.
[18] (a) Gross EKU, Kohn W, *Adv. Quantum Chem.* **1990**, *21*, 255. (b) Casida ME in *Recent Developments and Applications of Modern Density Functional Theory;* Seminario JM, Ed.; Elsevier: Amsterdam, 1996.
[19] (a) Becke AD, *J. Chem. Phys.* **1986**, *84*, 4524. (b) Lee C, Yang W, Parr R, *Phys. Rev. B* **1998**, *37*, 785.
[20] (a) Fonseca Guerra C, Snijders JG, Te Velde G, Baerends EJ, *Theor. Chem. Acc.* **1998**, *99*, 391. (b) Van Gisbergen SJA, Snijders JG, Baerends EJ, *J. Comput. Phys. Commun.* **1999**, *118*, 119.
[21] Hsu C, Hirata S, Head-Gordon M, *J. Phys. Chem. A* **2001**, *105*, 451-458.
[22] Englert G, Kienzle F, Noack K, *Helv. Chim. Acta* **1977**, *60*, 1209
[23] Kjeldahl-Andersen G, Lutnaes BF, Liaaen-Jensen S, *Org. Biomol. Chem.* **2004**, *2*(4), 489-498.
[24] Weesie RJ, Merlin JC, Lugtenburg J, Britton G, Jansen FJHM, Cornard JP, *Biospectroscopy* **1999**, *5*, 19-33.
[25] Merlin JC, *Pure Appl. Chem.* **1985**, *57*(5), 785-792.
[26] Merlin JC, *Raman Spectrosc.* **1987**, *18*, 519-523.
[27] Rimai L, Heyde ME, Gill D, *J. Am. Chem. Soc.* **1971**, *93*, 6776-6780.
[28] Bart JCJ, Macgillavry CH, *Acta Cryst. B.* **1968**, *24*, 1587.
[29] Pawlikowski M, *Acta Phys. Pol.* **1988**, *A74*, 145-149.
[30] Britton G, Weesie RJ, Askin D, Warburton JD, Gallardo-Guerrero L, Jansen FJHM, De Groot HJM, Lugtenburg J, Cornard JP, Merlin JC, *Pure Appl. Chem.* **1997**, *69*, 2075-2084.
[31] Durjeeb B, Eriksson LA, *Chem. Phys Lett.* **2003**, *375*, 30-38.
[32] Krawczyk S, Britton G, *Biochim. Biophys. Acta* **2001**, *1544*, 301-310.

CHAPTER 4

SYNTHETIC SCHEME FOR THE PREPARATION OF ^{13}C-LABELED 2,7-DIMETHYLOCTA-2,4,6-TRIENE-1,8-DIAL, THE CENTRAL PART OF CAROTENOIDS

Published in *Eur. J. Org. Chem.* 2002, 4217-4221.

Starting from acetic acid and methyl iodide an efficient modular synthetic scheme has been developed for the synthesis of ^{13}C-labeled 2,7-dimethylocta-2,4,6-triene-1,8-dial, which is a suitable building block in the synthesis of carotenoids with tenfold ^{13}C-enrichment in the central part.

4.1 INTRODUCTION

For a better understanding of the relation between diet and health knowledge of the metabolic pathways of nutrients is required.[1] Such studies in the field of metabolomics are rapidly getting more scientific attention in the past few years. Essential tools in metabolomics are mass spectrometry and NMR spectroscopy, which are suitable techniques for the analysis of metabolites.[2-4] ^{13}C and ^{2}H labeled isotopomers of nutrients are very useful as internal standards for the quantification of metabolites using mass spectrometry.[5] The combination of NMR analysis with stable ^{13}C and ^{15}N isotope labeling is a powerful tool for metabolomic analysis, enhancing the NMR sensitivity for the nutrients of interest via isotope labeling.[6]

Fundamental information about the concentration level of various carotenoids in the human body and its organs down to the cellular level is essential to study the health effects of carotenoids.[7-20] Recently a method was published to quantify, without perturbation, the nutritional status of β-carotene at the physiological level in individuals, by addition of ^{13}C-labeled β-carotene to their food.[21,22] Using mass spectrometry the levels of the isotopically ^{13}C-labeled β-carotene and its metabolites were monitored. Also resonance Raman spectroscopy can be used to obtain information on the presence and quantity of carotenoids in living human tissue, like skin and retina.[23-26] When ^{13}C-labeled carotenoids are added to the food of individuals, resonance Raman spectroscopy can be used to distinguish between different carotenoids and determine their presence and amount in humans in vivo in a non-invasive way.[27,28]

Extending the use of mass spectrometry, NMR spectroscopy and resonance Raman spectroscopy methods to other carotenoids that are present in our diet is now of utmost importance to study the presence, quantity, bioconversion and bioavailability of carotenoids in individuals. To perform such analyses, labeled carotenoids will be indispensable, which requires development of efficient synthetic strategies applicable to a range of carotenoids. It is well known that almost all carotenoids can be prepared using 2,7-dimethylocta-2,4,6-triene-1,8-dial (C_{10}-dialdehyde) and the appropriate end groups.[29-35] The synthesis of ^{13}C-labeled C_{10}-dialdehyde described in the literature has the severe drawback that it is inconvenient for multifold ^{13}C labeling, and multiple schemes are necessary to introduce ^{13}C labels at different positions.[36-39]

This chapter describes an efficient synthetic scheme for ^{13}C-enriched C_{10}-dialdehyde up to the $^{13}C_{10}$ level. Using a modular total organic synthetic strategy we can now specifically introduce ^{13}C labels at any position or combination of positions. By varying the end groups, we can conveniently obtain a library of multifold ^{13}C-labeled carotenoids.

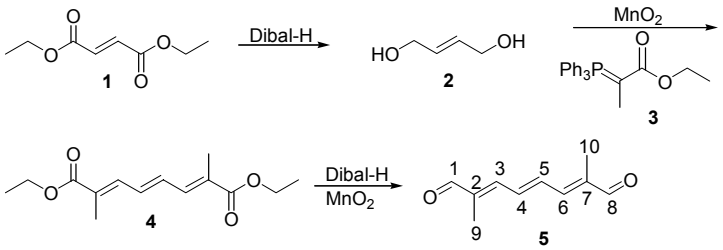

Scheme 1. *Synthesis of 2,7-dimethyl-octa-2,4,6-triene-1,8-dial (**5**).*

4.2 RESULTS

A scheme was developed in which the sp^2-atoms of C_{10}-dialdehyde are derived from acetic acid and the methyl groups from methyl iodide. Both starting materials are commercially available in 99% ^{13}C-enriched form at a reasonable price. Earlier we have described the high-yield conversion of $^{13}C_2$ acetic acid into $^{13}C_4$ diethyl fumarate (**1**)[40] and $^{13}C_2$ acetic acid and ^{13}C methyl iodide into [1-(ethoxycarbonyl)ethyl]triphenylphosphonium iodide (**3**).[37-43] Scheme 1 indicates that (**1**) can be reduced with Dibal-H into but-2-ene-1,4-diol (**2**). This diol can be converted in a double MnO_2 oxidation and double Wittig coupling, in a one-pot reaction, to diethyl 2,7-dimethylocta-2,4,6-trien-1,8-oate (**4**) in excellent yield.

Treatment with Dibal-H followed by oxidation with MnO_2 gives the required all-*trans* 2,7-dimethylocta-2,4,6-triene-1,8-dial (**5**).[37,38] The final product (**5**) proved to be identical in all analytical aspects to the authentic material.

The Wittig reaction was first tried with two equivalents of phosphorane **3**, which gave 61% of the desired product (**4**) and 19% of the ethyl 2-methyl-6-oxo-2,4-hexadienoate (**8**; see Scheme 2). After optimization, best results for this reaction were obtained with 2.4 equivalents of the phosphorane. This is a drawback when labeled materials are used, but the good yield [91% based on (**2**)], short route and easy workup and purification make this reaction very useful.

The overall yield for the synthesis, based on methyl iodide and acetic acid, is 61% for ^{13}C labels at positions 1-2 and 7-10, and 45% for central positions 3-6.

4.3 DISCUSSION

Scheme 1 involves the double oxidation and double Wittig coupling of but-2-ene-1,4-diol (**2**), to give C_{10}-diester **4** in a one-pot reaction. But-2-ene-1,4-diol (**2**) is oxidized with MnO_2, in the presence of phosphorane **3**. Following the reaction closely by TLC, it was found that ethyl 2-methyl-6-oxo-2,4-hexadienoate (**8**) is formed as an intermediate, which reacts with the phosphorane **3** in a Wittig coupling to give diester **4**.

Probably the reaction proceeds by oxidation of one hydroxyl group of **2** to an aldehyde, which reacts with the phosphorane **3** to give ethyl 6-hydroxy-2-methyl-2,4-hexadienoate. Subsequently, the second hydroxyl group is oxidized to an aldehyde, which reacts in a second Wittig coupling with **3** to give the desired product **4**

Before we developed the method described above, a protection and deprotection scheme was developed to synthesize the C_{10}-diester **4**, as shown in Scheme 2.

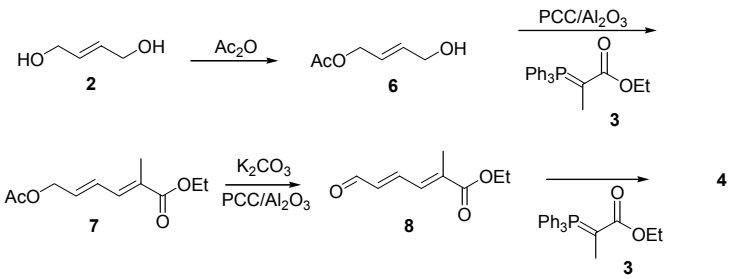

Scheme 2. *Alternative synthesis of diethyl 2,7-dimethylocta-2,4,6-trien-1,8-oate (**4**).*

The diol (**2**) reacts with one equivalent acetic anhydride to give a mixture consisting of 50% monoacetate, 25% unchanged diol and 25% diacetate.[44] These product can easily be separated by washing the organic solution containing the mixture with water, which removes the diol. The diester can be separated by silica-gel column chromatography. The diester is reconverted to the diol with KOH, and, together with the unchanged diol from the acetylation reaction, acetylated again as described above. The monoacetate **6** is oxidized with pyridinium chlorochromate on basic alumina (PCC/Al) to give 4-acetoxy crotonaldehyde, which is allowed to react under Wittig conditions with **3** to give ethyl 6-acetoxy-2-methylhexa-2,4-dienoate (**7**).

Selective conversion of the 6-acetoxy function in **7** to the alcohol without saponification of the ethyl ester is effected by hydrolysis with K_2CO_3 in ethanol to give ethyl 6-hydroxy-2-methyl-2,4-hexadienoate. Subsequent oxidation of the alcohol gives ethyl 2-methyl-6-oxo-2,4-hexadienoate (**8**), which is coupled via another Wittig reaction with (**3**) to give diethyl 2,7-dimethylocta-2,4,6-trien-1,8-oate (**4**). This compound is converted into the C_{10}-dialdehyde **5** as described above.

In this scheme both Wittig couplings are carried out with one equivalent of the phosphorane **3**, which makes this scheme useful for efficient introduction of ^{13}C labels at positions 1,2 and 9 of the final C_{10}-dialdehyde **5**.

As alternative for the base-labile acetate group for protection of but-2-ene-1,4-diol, the acid sensitive tetrahydropyran(THP)-ether can be used, giving a statistical mixture of unchanged diol, mono- and di-ether (1:2:1).[45] After oxidation and subsequent Wittig reaction with the C_3-phosphorane **3** the THP-ether can be removed with a trace of acid (*p*-toluenesulfonic acid) to obtain ethyl 2-methyl-6-oxo-2,4-hexadienoate (**8**) after oxidation, similar to the route in

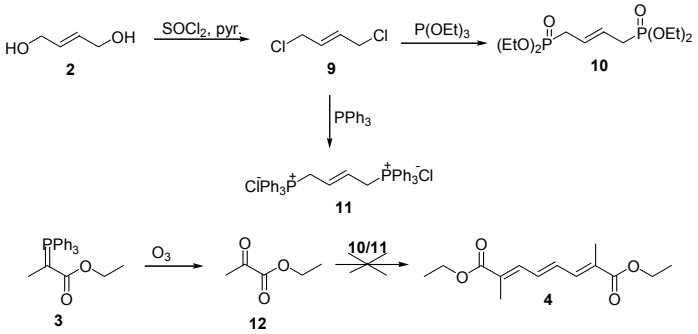

Scheme 3. *Scheme for the synthesis of C_{10}-diester **4** via a double Wittig coupling.*

Scheme 2. This alternative route can be preferred when basic conditions in one of the synthetic steps are undesired.

Another scheme to reduce the number of steps is converting **3** into ethyl pyruvate according to literature,[40,46] and couple this to either 1,4-bis(diethoxyphosphoryl)-2-butene **10** or 1,4-bis(triphenylphosphonium)-2-butene dibromide **11**, which are both made in two steps from but-2-ene-1,4-diol (**2**). Both the Wittig coupling and the phosphonate coupling of ethyl pyruvate **12** only gave degradation products and starting material, even though several different conditions were tried. This is shown in Scheme 3.

4.4 CONCLUSION

The synthetic scheme described in this chapter allows the quick and easy preparation of isotopically ^{13}C-labeled 2,7-dimethylocta-2,4,6-triene-1,8-dial. The key step in this synthesis is the double MnO_2-oxidation of but-2-ene-1,4-diol (**2**) in the presence of C_3-phosphorane **3**, to give the C_{10}-diester **4** in a one-pot reaction. All carotenoids can now be prepared with selective or uniform ^{13}C enrichment in the central part via this synthetic scheme for the preparation of 2,7-dimethylocta-2,4,6-triene-1,8-dial

EXPERIMENTAL

But-2-ene-1,4-diol (2)

Under a nitrogen atmosphere, a solution of diethyl fumarate (**1**; 2.0 g, 11.6 mmol) in dry PE was cooled to -60°C, and di-isobutyl aluminium hydride (Dibal-H; 4.4 equiv., 51 mL 1 M-solution in hexanes, 51 mmol) was added with a syringe. The solution was allowed to warm up to -20°C in 1 hour, after which TLC (diethyl ether) showed complete conversion of the starting material. At -20°C, SiO_2/H_2O (83.9 g) was added, and the mixture was stirred for 1 hour at 0°C. K_2CO_3 and $MgSO_4$ were added, and the solids were removed by filtration and washed thoroughly with diethyl ether. The solution was concentrated in vacuo, to give but-2-ene-1,4-diol (**2**; 0.82 g, 9.3 mmol, 80%).

^{1}H NMR (300 MHz, CD_3OD) δ (ppm) = 4.11 (d, *J* = 3.8 Hz, 4 H, 1-H/4-H), 4.91 (s, 2 H, OH), 5.87 (t, *J* = 3.8 Hz, 2 H, 2-H/3-H).

^{13}C NMR (75 MHz, CD_3OD) δ (ppm) = 63.0 (C-1/C-4), 131.1 (C-2/C-3).

4-Acetoxy-2-buten-1-ol (6)

Acetic anhydride (2.55 g, 25 mmol) was slowly added to a solution of but-2-ene-1,4-diol (**2**; 2.20 g, 25 mmol) and pyridine (2.37 g, 30 mmol) in dry toluene. The mixture was stirred at room temperature (RT) for 1 hour after which TLC analysis (diethyl ether) showed a mixture of starting compound, monoacetate and diacetate. H_2O was added, and the mixture was extracted three times with diethyl ether. The combined organic layers were dried with $MgSO_4$ and concentrated in vacuo. After purification on a silica column (50% diethyl ether/PE) the monoacetate (**6**; 1.36 g, 10.5 mmol, 42%) was collected. Unchanged diol was collected by extracting the water layer thoroughly with dichloromethane; the organic layers were combined, dried with $MgSO_4$ and solvents were removed in vacuo. Diacetate, collected after column chromatography, was treated with KOH to obtain another batch of diol.

^{1}H NMR (300 MHz, $CDCl_3$) δ (ppm) = 2.06 (s, 3 H, CH_3 acetoxy), 4.24 (d, *J* = 6.2 Hz, 2 H, 4-H), 4.57 (br. s, 1 H, OH), 4.66 (d, *J* = 6.5 Hz, 2 H, 1-H), 5.62 (dt, *J* = 6.2 Hz/12.3 Hz, 1 H, 3-H), 5.80 (dt, *J* = 6.5 Hz/12.3 Hz, 1 H, 2-H).

^{13}C NMR (75 MHz, $CDCl_3$) δ (ppm) = 20.7 (CH_3 acetoxy), 57.9 (C-4), 59.9 (C-1), 125.0 (C-2), 133.1 (C-3), 171.1 (C=O acetoxy).

Ethyl 6-acetoxy-2-methylhexa-2,4-dienoate (7)

At 0°C, 4-acetoxy-2-buten-1-ol (**6**; 1.36 g, 10.5 mmol) was added to a suspension of pyridinium chlorochromate on basic alumina (PCC/Al 20 wt%; 14.8 g, 13.7 mmol) in DCM. The mixture was stirred at RT until TLC analysis (diethyl ether) showed complete conversion of the starting compound. PCC/Al was removed by flash chromatography, the solids were washed with diethyl ether, and the organic solvents were removed in vacuo, to give 4-acetoxy-crotonaldehyde (1.0 g, 7.8 mmol, 74%).

^{1}H NMR (300 MHz, $CDCl_3$) δ (ppm) = 2.14 (s, 3 H, CH_3 acetoxy), 4.87 (d, *J* = 4.4 Hz, 2 H, 4-H), 6.28 (dd, *J* =7.9 Hz/15.9 Hz, 1 H, 2-H), 6.88 (dt, *J* = 4.3 Hz/15.9 Hz, 1 H, 3-H), 9.59 (d, *J* = 7.9 Hz, 1 H, 1-H).

^{13}C NMR (75 MHz, $CDCl_3$) δ (ppm) = 20.2 (CH_3 acetoxy), 62.0 (C-4), 131.6 (C-2), 149.5 (C-3), 169.8 (C=O acetoxy), 192.5 (C-1).

4-Acetoxy-crotonaldehyde (1.0 g, 7.8 mmol) was dissolved in 5 mL DCM and C_3-phosphorane **3** (2.83 g, 7.8 mmol) in DCM was added. The solution was stirred for 30 min at RT and followed by TLC-analysis (15% diethyl ether/PE). When TLC showed complete conversion of the aldehyde, the solvent was removed in vacuo. The product was purified on a flash-column (10% diethyl ether/PE), to yield ethyl 6-acetoxy-2-methyl-hexa-2,4-dienoate (**7**; 1.66 g, 7.8 mmol, 100%).

^{1}H NMR (300 MHz, $CDCl_3$) δ (ppm) = 1.31 (t, *J* =7.1 Hz, 3 H, OCH_2CH_3), 1.96 (s, 3 H, 2-CH_3), 2.10 (s, 3 H, CH_3 acetoxy), 4.21 (q, *J* = 7.1 Hz, 2 H, OCH_2CH_3), 4.69 (d, *J* = 6.0 Hz, 2 H, 6-H), 6.09 (dt, *J* = 6.0 Hz/15.2 Hz, 1 H, 5-H), 6.59 (dd, *J* = 11.4 Hz/15.2 Hz, 1 H, 4-H), 7.17 (d, *J* = 11.4 Hz, 1 H, 3-H).

^{13}C NMR (75 MHz, $CDCl_3$) δ (ppm) = 12.2 (2-CH_3), 13.8 (OCH_2CH_3), 20.3 (CH_3 acetoxy), 60.1 (OCH_2CH_3), 63.7 (C-6), 128.1 (C-2), 131.5 (C-5), 133.2 (C-3), 136.0 (C-4), 167.4 (C-1), 169.8 (C=O acetoxy).

Ethyl 6-Oxo-2-methyl-2,4-hexadienoate (8)

K_2CO_3 (2g) was addes to a solution of **7** (1.66 g, 7.8 mmol) in ethanol. After 2 hours at RT, TLC (diethyl ether) showed complete conversion of the starting material. The solution was concentrated to a volume of 20 mL, and NaCl-solution (50 mL, sat) was added. The water layer was extracted three times with diethyl ether, and the combined organic layers were dried with $MgSO_4$, which was removed by filtration. After evaporation of the solvent, the desired ethyl 6-hydroxy-2-methyl-2,4-hexadienoate (1.28 g, 7.5 mmol, 96%) was obtained. No further purification was necessary.

^{1}H NMR (300 MHz, $CDCl_3$) δ (ppm) = 1.31 (t, *J* = 7.1 Hz, 3 H, OCH_2CH_3), 1.94 (s, 3 H, 2-CH_3), 4.21 (q, *J* = 7.1 Hz, 2 H, OCH_2CH_3), 4.28 (d, *J* = 5.1 Hz, 2 H, 6-H), 6.17 (dt, *J* = 5.1 Hz/15.2 Hz, 1 H, 5-H), 6.59 (dd, *J* = 11.4 Hz/15.2 Hz, 1 H, 4-H), 7.18 (d, *J* = 11.4 Hz, 1 H, 3-H).

^{13}C NMR (75 MHz, $CDCl_3$) δ (ppm) = 12.4 (2-CH_3), 14.1 (OCH_2CH_3), 60.7 (OCH_2CH_3), 62.7 (C-6), 125.2 (C-4), 127.1 (C-2), 137.3 (C-5), 139.7 (C-3), 168.5 (C-1).

Ethyl 6-hydroxy-2-methylhexa-2,4-dienoate (1.28 g, 7.5 mmol) was added at 0ºC to a solution of PCC/Al (20 wt%; 10.5 g, 9.8 mmol) in dry DCM. The mixture was stirred for 16 hours, until TLC analysis (50% diethyl ether/PE) showed complete conversion of the starting material. PCC was removed by filtration through silica and washed with diethyl ether. The organic solvents were removed in vacuo to yield ethyl 6-oxo-2-methyl-2,4-hexadienoate (**8**; 1.0 g, 6.0 mmol, 80%).

^{1}H NMR (300 MHz, $CDCl_3$) δ (ppm) = 1.34 (t, *J* = 7.2 Hz, 3 H, OCH_2CH_3), 2.13 (s, 3 H, 2-CH_3), 4.27 (q, *J* = 7.2 Hz, 2 H, OCH_2CH_3), 6.39 (dd, *J* = 7.9 Hz/14.4 Hz, 1 H, 5-H), 7.33 (d, *J* = 12.0 Hz, 1 H, 3-H), 7.48 (dd, *J*=12.0 Hz/14.4 Hz, 1 H, 4-H), 9.61 (d, *J* = 7.9 Hz, 1 H, 6-H).

^{13}C NMR (75 MHz, $CDCl_3$) δ (ppm) = 13.3 (2-CH_3), 14.0 (OCH_2CH_3), 61.1 (OCH_2CH_3), 133.8 (C-2), 135.8 (C-5), 136.9 (C-3), 144.8 (C-4), 166.8 (C-1), 192.9 (C-6).

Diethyl 2,7-dimethylocta-2,4,6-triene-1,8-oate (4)

Method A:

But-2-ene-1,4-diol (**2**; 0.56 g, 6.3 mmol) in DCM (10 mL) was added to a suspension of activated MnO_2 (10 g) in DCM (25 mL) at 0°C. C_3-phosphorane 3 (5.5 g, 15.2 mmol) in DCM (15 mL) was added and the mixture was followed by TLC (50% diethyl ether/PE). The mixture was stirred overnight and MnO_2 was removed by filtration through Hyflo™. The filtrate was concentrated in vacuo and triphenylphosphonium oxide was removed by flash chromatography through silica gel (50% diethyl ether/PE). After a second purification on a short silica-gel column diethyl 2,7-dimethylocta-2,4,6-triene-1,8-oate (**4**; 1.5 g, 5.8 mmol, 92%) was obtained.

Method B:

Ethyl 2-methyl-6-oxo-2,4-hexadienoate (**8**; 1.0 g, 6.0 mmol) was dissolved in DCM (10 mL), and C_3-phosphorane **3** (2.2 g, 6.0 mmol) in DCM was added. The reaction was stirred at RT for 5 hours, until TLC (diethyl ether) showed completion of the reaction. The solvent was evaporated in vacuo and the triphenylphosphine oxide formed was removed on a short flash column (50 % ether/PE) to yield the C_{10}-diester (**4**; 1.5 g, 5.9 mmol, 99%) as a pure, white solid.

^{1}H NMR (300 MHz, $CDCl_3$) δ (ppm) = 1.32 (t, *J* = 7.1 Hz, 6 H, 2×$OCH_2\mathit{CH}_3$), 2.02 (s, 6 H, 2-CH_3/7-CH_3), 4.23 (q, *J* = 7.1 Hz, 4 H, 2×$OC\mathit{H}_2CH_3$), 6.81 (dd, *J* = 3.1 Hz/7.8 Hz, 2 H, 3-H/6-H), 7.29 (m, 2 H, 4-H/ 5-H).

^{13}C NMR (75 MHz, $CDCl_3$) δ (ppm) = 12.8 (2-CH_3/7-CH_3), 14.1 (2×$OCH_2\mathit{CH}_3$), 60.6 (2×OCH_2CH_3), 129.9 (C-2/C-7), 133.2 (C-4/C-5), 136.8 (C-3/C-6), 167.5 (C-1/C-8).

2,7-Dimethylocta-2,4,6-triene-1,8-dial (5)

A solution of **4** (1.5 g, 5.8 mmol) in dry PE was cooled to -80°C, and 4.4 equiv. Dibal-H (25.9 mL of a 1 M solution in hexanes, 25.9 mmol) was added with a syringe. The yellow-orange mixture was allowed to warm to -20°C in 1 hour. When TLC showed complete conversion of the diester, SiO_2/H_2O (45.4 g) was added, and the mixture was stirred at 0°C for 1 hour. K_2CO_3 and $MgSO_4$ were added, and the solids were removed by filtration and washed with DCM. The product was concentrated in vacuo, and the resulting diol was oxidized, without further purification.

2,7-Dimethylocta-2,4,6-triene-1,8-diol was dissolved in acetone (10 mL), and MnO_2 (10 g) was added at 0°C. The reaction was stirred overnight, and followed by TLC (diethyl ether). When the reaction was complete, the Mn salts were removed by filtration through Hyflo™, washed with DCM and the product was concentrated in vacuo. After purification on a silica-gel column, pure all-*trans*-C_{10}-dialdehyde (**5**; 0.77 g, 4.7 mmol, 80%) was obtained.

^{1}H NMR (300 MHz, $CDCl_3$) δ (ppm) = 1.95 (s, 6 H, 2-CH_3/7-CH_3), 7.06 (m, 4 H, 3-H/4-H/5-H/6-H), 9.55 (s, 2 H, 1-H/8-H).

^{13}C NMR (75 MHz, $CDCl_3$) δ (ppm) = 9.7 (2-CH_3/7-CH_3), 134.2 (C-4/C-5), 141.0 (C-2/C-7), 146.0 (C-3/C-6), 194.3 (C-1/C-8).

REFERENCES

[1] German JB, Bauman DE, Burrin DG, Failla ML, Freake HC, King JC, Klein S, Milner JA, Pelto GH, Rasmussen KM, Zeisel SH, *J. Nutr.* **2004**, *134*, 2729-2732.
[2] Vivant MR, Rosenblum ES, Tjeerdema RS, *Environ. Sci. Technol.* **2003**, *21*, 4982-4989.
[3] Van der Greef J, Stroobant P, Van der Heijden R, *Current Opinion in Chemical Biology* **2004**, *8*, 559-565.
[4] Lindon JC, Holmes E, Nicholson JK, *Progress in Nuclear Magnetic Resonance Spectroscopy* **2004**, *45*, 109-143.
[5] Mashego MR, Wu L, Van Dam JC, Ras C, Vinke JL, Van Winden WA, Van Gulik WM, Heijen JJ, *Biotechnology and Bioengineering* **2004**, *85*(6), 620-628.
[6] Kikuchi J, Shinozaki K, Hirayama T, *Plant Cell Physiol.* **2004,** *45*(8), 1099-1104.
[7] VanBreemen RB, *Analytical Chemistry News & Features* **1996**, 299A-304A.
[8] *Key to Carotenoids*; Pfander H; Ed. Birkhäuser Verlag: Basel, 1995.
[9] Britton G in *Carotenoids, Volume 1B: Spectroscopy*; Britton G, Liaaen-Jensen S, Pfander H; Eds. Birkhäuser Verlag: Basel, 1995.
[10] Nishino H, Tokuda H, Satomi Y, Masuda M, Bu P, Onozuka M, Yamaguchi S, Okuda Y, Takayasu J, Tsuruta J, Okuda M, Ichiishi E, Murakoshi M, Kato T, Misawa N, Narisawa T, Takasuka N, Yano M, *Pure Appl. Chem.* **1999**, *71* (12), 2273-2278.
[11] Van Dam RM, Huang Z, Giovanucci E, Stampfer M, Rosner B, Cook NR, Belanger C, LaMotte F, Gaziano JM, Ridker PM, Willett W, Peto R, *Am. J. Clin. Nutr*. **2000**, *71*, 135-141.
[12] Frieling UM, Schaumberg DA, Kupper TS, Muntwyler J, Hennekens CH, *Arch. Dermatol.* **2000**, *136*, 179-184.
[13] King TJ, Khachik F, Bortkiewicz H, Fukushima LH, Morioka S, Betram JS, *Pure Appl. Chem.* **1997**, *69* (10), 2135-2140.
[14] Hennekens CH, *Pure Appl. Chem.* **1997**, *69* (10), 2141-2144.
[15] Deming DM, Erdman JW, *Pure Appl. Chem.* **1999**, *71* (12), 2213-2223.
[16] Khachik F, Bernstein PS, Garland DL, *Invest. Opthalmol. Vis. Sci.* **1997**, *38*(9), 1802-1811.
[17] Street DA, Comstock GW, Salkeld RW, Schuep W, Klag MJ, *Circulation* **1994,** *90* 1154-1161.
[18] Hennekens CH, Buring JE, Manson JE et al., *N. Engl. J. Med.* **1996**, *334*, 1145-1149.
[19] Liu S, Manson JE, Lee IM, Cole SR, Hennekens CH, Willett WC, Buring JE, *Am. J. Clin. Nutr.* **2000,** *72,* 922-928.
[20] Broekmans WMR, *PhD Thesis*, Wageningen University, 2002.
[21] Wang Y, Xu X, Van Lieshout M, West CE, Lugtenburg J, Verhoeven MA, Creemers AFL, Muhilal, Van Breemen RB, *Anal. Chem.* **2000**, *72*, 4999-5003.
[22] Van Lieshout M, West CE, Muhilal, Permaeshi D, Wang Y, Xu X, Van Breemen RB, Creemers AFL, Verhoeven MA, Lugtenburg J, *Am. J. Clin. Nutr.* **2001**, *73*, 949-958.
[23] Ermakov IV, McClane RW, Gellermann W, *Optics Letters* **2001**, *26*(4), 202-204.
[24] Ermakov IV, Ermakova MR, McClane RW, Gellermann W, *Optics Letters* **2001**, *26*(15), 1179-1181.
[25] Hata TR, Scholz TA, Ermakov IV, McClane RW, Khackik F, Gellermann W, Pershing LK, *Journ. Invest. Dermatol.* **2000**, *115*(3), 441-447.
[26] Ramanauskaite RB, Segers-Nolten IGMJ, De Grauw KJ, Sijtsema NM, Van der Maas L, Greve J, Otto C, Figdor CG, *Pure Appl. Chem.* **1997**, *69*(10), 2131-2134.
[27] Weesie RJ, Merlin JC, Lugtenburg J, Britton G, Jansen FJHM, Cornard JP, *Biospectroscopy* **1999**, *5*, 19-33.
[28] Weesie RJ, Merlin JC, De Groot HJM, Britton G, Lugtenburg J, Jansen FJHM, Cornard JP, *Biospectroscopy* **1999**, *5*, 358-370.
[29] *Carotenoids, Volume 2: Synthesis*; Britton G, Liaaen-Jensen S, Pfander H; Eds. Birkhäuser Verlag: Basel, 1996.
[30] Mayer H, *Pure Appl. Chem.* **1994**, *66* (5), 931-938.
[31] Ito M, Yamano Y, Sumiya S, Wada A, *Pure Appl. Chem.* **1994**, *66* (5), 939-946.
[32] Pommer H, *Angew. Chem.* **1960**, *72*(23), 911-915.
[33] Azim E, Auzeloux P, Maurizis J-C, Braesco V, Grolier P, Veyre A, Madelmont J-C, *J. Lab. Comp. Radiopharm.* **1996**, *38*(5), 441-451.
[34] Inhoffen HH, Isler O, Von der Bey G, Raspé G, Zeller P, Ahrens R, *Ann. Chem.* **1953**, *580*, 7-19.
[35] Inhoffen HH, Von der Bey G, *Ann. Chem.* **1953**, *583*, 100-109.

[36] Jansen FJHM, Lugtenburg J in *Carotenoids, Volume 2: Synthesis;* Britton G, Liaaen-Jensen S, Pfander H; Eds. Birkhäuser Verlag: Basel, 1996, 233-258.
[37] Jansen FJHM, Kwestro M, Schmitt D, Lugtenburg J, *Recl. Trav. Chim. Pays-Bas* **1994**, *113*, 552-562.
[38] Jansen FJHM, Lugtenburg J, *Pure Appl. Chem*. **1994**, *113,* 963-972.
[39] Khachik F, Beecher GR, Li BW, Englert G, *J. Lab. Comp. Radiopharm.* **1995**, 35(12), 1157-1172.
[40] Heinen W, Rosenmöller CH, Wenzel CB, De Groot HJM, Lugtenburg J, *Macromolecules* **1996**, *29*, 1151-1157.
[41] Ouwerkerk N, Van Boom JH, Lugtenburg J, Raap J, *Eur. J. Org. Chem.* **2000**, 861-866.
[42] Werkhoven TM, Van Nispen R, Lugtenburg J, *Eur. J. Org. Chem*. **1999**, 2909-2914.
[43] Lang RW, Hansen H-J, *Helv. Chim. Acta* **1980**, *63*(44), 438-455.
[44] Broek AD, Muradin-Szweykowska M, Courtin JML, Lugtenburg J, *Recl. Trav. Chim. Pays-Bas* **1983**, *102*, 46-51.
[45] Van den Berg EMM, Van Liemt WBS, Heemskerk B, Lugtenburg J, *Recl. Trav. Chim. Pays-Bas* **1989**, *108*, 301-314.
[46] Wasserman HH, Vu CB, *Tetrahedron Lett.* **1990**, *31*, 5205-5208.

CHAPTER 5

SYNTHETIC SCHEME FOR THE PREPARATION OF ^{13}C-LABELED 3,4-DIDEHYDRO-RETINAL, 3-HYDROXYRETINAL AND 4-HYDROXYRETINAL UP TO UNIFORM ^{13}C-ENRICHMENT

Published in *Eur. J. Org. Chem*. 2003, 863-868.

A modular synthetic scheme has been developed for the synthesis of ^{13}C-labeled naturally occuring visual pigment chromophores; 3,4-didehydroretinal, 3-hydroxyretinal, and 4-hydroxyretinal. These compounds can now be made with >99% ^{13}C enrichment at any position or combination of positions. The common C_{10}+C_5+C_5 scheme for the synthesis of retinals was used, and by making variations in the C_{10} part, the desired retinal derivatives can now be prepared with selective or uniform ^{13}C enrichment.

The McMurry-dimerization of retinal-derivatives was explored, to develop an efficient method for the synthesis of ^{13}C-labeled carotenoids. Pure zeaxanthin was obtained from 3-hydroxyretinal and 3,4,3′,4′-tetradehydro-β,β-carotene from 3,4-didehydroretinal, indicating the potential of this method.

5.1 INTRODUCTION

Light is essential for living organisms as it provides the energy for life through photosynthesis as well as the means to efficiently interact with the outside world through visual sensation. In the eyes of animals - vertebrates, mollusks and anthropoids - light from the environment is converted into neural information by pigmented membrane proteins called rhodopsins, that start the visual process. Rhodopsin is the photosensitive protein of the rod photoreceptor in the vertebrate retina that mediates dim-light vision. Rhodopsin serves as a paradigm for the superfamily of seven-transmembrane-helix G-protein-coupled receptors (GPCRs).[1] The GPCRs mediate a broad array of important physiological and pharmacological signal-transduction processes that involve signalling by neurotransmitters, hormones, and neuropeptides.[2] Consequently, GPCRs are major pharmaceutical targets for pharmacological intervention in human (and veterinary) pathology.

In the majority of the known visual pigments 11*Z*-retinal is covalently bound in the interior of the protein via a protonated Schiff-base linkage with a lysine residue to form the retinylidene chromophore.[3] Absorption of a photon leads to the ultrafast isomerization of the C11=C12 bond of the retinylidene ligand from the 11*Z* to the all-*E* configuration in only ~200 fs, the fastest photochemical reaction known.[4,5]

The chromophores of the visual pigments of important groups of animals are derived from systems closely related to retinal. These chromophores include, for example, 3,4-didehydroretinal (also known as vitamin A_2-aldehyde), in amphibians and fresh-water fish,[6,7] (*R*)-3-hydroxyretinal in flies and butterflies,[8-10] and (*R*)-4-hydroxyretinal in squid.[11-13] These retinal derivatives are shown in Figure 1.

Recently the first ultra high-field ^{1}H and ^{13}C solid state NMR study of bovine rhodopsin with uniformly ^{13}C-enriched retinal was published.[14] Besides detailed chemical shift information of each carbon and hydrogen atom of the chromophore, unique information about the non-bonding interactions between hydrogen atoms of the methyl groups of the six-membered ring and the protein was obtained. These non-bonding interactions are attributed to nearby

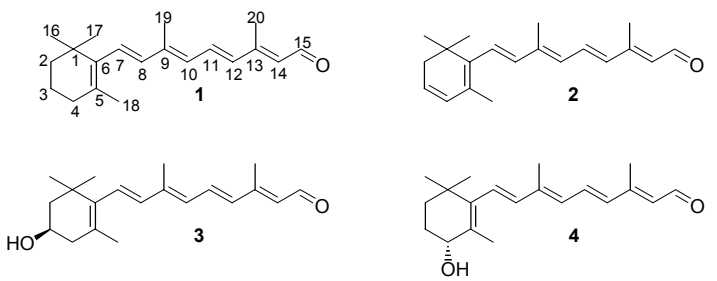

Figure 1. *(all-E) retinal (**1**) with IUPAC numbering, (all-E)-3,4-didehydroretinal (**2**), (3R, all-E)-3-hydroxyretinal (**3**) and (4R, all-E)-4-hydroxyretinal (**4**).*

aromatic amino acid residues Phe-208, Phe-212 and Trp-265 that are in close contact with respectively, CH_3-16, CH_3-17 and CH_3-18.[15] The chromophore occurs in one conformation only with a non-planar 6s-*cis* conformation with negative helicity and a non-planar 12s-*trans* conformation with positive helicity.[14] Surprisingly, in the case of isorhodopsin the interaction of the aromatic side chains of the active site of the protein with the six-membered ring, is substantially different from that of rhodopsin.[16] A similar solid-state ^1H and ^{13}C NMR study of rhodopsins and isorhodopsins regenerated with the uniformly ^{13}C-enriched 3,4-didehydro-, (*R*)-3-hydroxy- and (*R*)-4-hydroxyretinals will give access to as yet unavailable information about the factors that contribute to the nonbonding interactions of the CH_3-16, CH_3-17 and CH_3-18 groups with the aromatic amino-acids in the active site of visual pigments and about the effects of modifications in the ring on the binding to the active site.

In addition to the results obtained via uniformly ^{13}C-labeled rhodopsin, also very precise distance information between atoms C8 and C18, C10 and C20, and C11 and C20 in the chromophore has been obtained via rotational-resonance solid-state ^{13}C NMR measurements of $^{13}C_2$-labeled rhodopsins. This distance information is an order of magnitude more accurate than distances obtained via X-ray crystallography.[17-19] Also, information on the torsion around the 10-11 single bond in the chromophore has been obtained via double-quantum solid-state ^{13}C NMR, using ^{13}C-labeled retinal.[20,21] In addition, the full vibrational analysis of the chromophore of rhodopsin, isorhodopsin and bathorhodopsin was based on a set of ^{13}C isotopomers.[22,23]

To obtain the ^1H and ^{13}C NMR solid-state NMR data, distance measurements and vibrational analysis of 3,4-didehydro-, (*R*)-3-hydroxy- and (*R*)-4-hydroxyrhodopsin and isorhodopsin with ^{13}C-enriched chromophores, the corresponding ^{13}C isotopomers of these chemically modified retinoids have to be prepared.

The basis for these syntheses is the chemistry that is explored for the preparation of uniformly ^{13}C-labeled retinal via a modular total organic synthetic strategy that allows the preparation of any ^{13}C isotopomer up to the uniformly labeled form.[24] The central modules in this synthesis are [$^{13}C_{10}$]-α-cyclocitronitrile (**5**, Scheme 1) and [$^{13}C_5$]-4-(diethylphosphono)-3-methyl-2-butenenitrile (**12**, Scheme 2). In this chapter the efficient conversion of **5** into racemic 4-hydroxy-

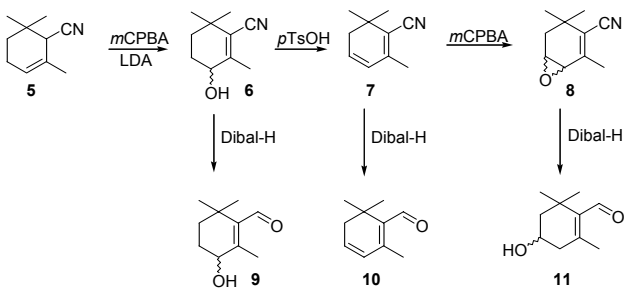

Scheme 1. *Synthesis of racemic 4-hydroxy-β-cyclocitral (**9**), safranal (**10**) and racemic 3-hydroxy-β-cyclocitral (**11**).*

cyclocitral (**9**), safranal (**10**) and racemic 3-hydroxycyclocitral (**11**) is discussed. The cyclocitral derivatives serve as C_{10}-building blocks for the synthesis of the corresponding retinal derivatives 3,4-didehydroretinal (**2**), (*R*)-3-hydroxyretinal (**3**) and (*R*)-4-hydroxyretinal (**4**) (see Figure 1). The resolution of **3** and **4** into the optically pure forms has been reported in the literature.[8,25-28]

These C_{10}-cyclocitral derivatives fit perfectly in the synthetic scheme for the synthesis of ^{13}C-labeled retinals, and by making variations in the C_{10}-part, retinal derivatives with ^{13}C enrichment at the desired positions can easily be obtained.

This chapter ends with the McMurry-dimerization of functionalized retinals. This reaction is commonly used for the synthesis of β-carotene from retinal. The exploration of the McMurry-dimerization of 3,4-didehydroretinal, 3-hydroxyretinal and 4-hydroxyretinal to the corresponding carotenoids is described here.

5.2 RESULTS AND DISCUSSION

In this chapter the synthetic scheme for the synthesis of ^{13}C-enriched 3,4-didehydroretinal (**2**), (*RS*)-3-hydroxyretinal (**3**) and (*RS*)-4-hydroxyretinal (**4**) (see Figure 1) is worked out at the natural abundance level. The scheme (see Scheme 1) starts with the easily accesible α-cyclonitrile (**5**),[24] which is converted into racemic 4-hydroxy-β-cyclocitral (**6**) by treatment with *meta*-chloroperbenzoic acid (*m*CPBA) and subsequent opening of the formed epoxide with base.[29] Acid-catalyzed dehydration of **6** gives safronitrile (**7**) in high yield.[30] It was found that subsequent epoxidation with *m*CPBA gives 3,4-epoxy-β-cyclocitronitrile (**8**) in good yield. It is interesting that the C5=C6 double bond, conjugated with the nitrile group, is sufficiently deactivated that only the C3=C4 double bond of safronitrile (**7**) reacts. The β-cyclocitronitriles **6**,**7** and **8** are converted in high yield into the corresponding aldehydes by reduction with Dibal-H. Safronitrile (**7**) is treated with 1.3 equivalents of Dibal-H to give safranal (**10**). For the reduction of 4-hydroxy-β-cyclonitrile (**6**), an additional equivalent of Dibal-H is required to give 4-hydroxy-β-cyclocitral (**9**). Similar reduction of 3,4-epoxy-β-cyclocitronitrile (**8**) with 2.3 equivalents of Dibal-H converts the nitrile to an aldehyde in one step, and the epoxide opens in the same step to give the hydroxyl group selectively at the 3-position, yielding a racemic mixture of 3-hydroxy-β-cyclocitral (**11**).

The β-cyclocitral derivatives **9**, **10**, and **11** can easily be converted into the corresponding retinals **2**, **3**, and **4** by a Horner-Wadsworth-Emmons (HWE) coupling with phosphonate **12** and subsequent Dibal-H reduction to obtain the intermediate β-ionylidene acetaldehydes. Repetition of the phosphonate coupling reaction and reduction gives the retinal derivatives **2**, **3**, and **4** as depicted in Scheme 2.

This sequence worked without problems for safranal (**10**). However, the presence of the hydroxyl groups in **9** and **11** interferes with the HWE-coupling reaction. For this reason, the hydroxyl derivatives were treated with NaH first, to convert the hydroxyl groups to alkoxides.

Using another equivalent NaH to deprotonate the phosphonate **12**, these alkoxides reacted in the HWE-coupling reactions without difficulties.

The retinals were obtained as a mixture of 13*Z* and all-*E* isomers, with the all-*E* isomers as the predominant products (60/40).[31] The all-*E* retinals can be isolated by purification of the mixture of isomers via column chromatography or HPLC, according to literature.[8,26,32,33] The final products were characterized using ^{1}H and ^{13}C NMR spectroscopy; the analytical data proved to be identical to the data presented in literature of the authentic compounds.[8,26,34,35]

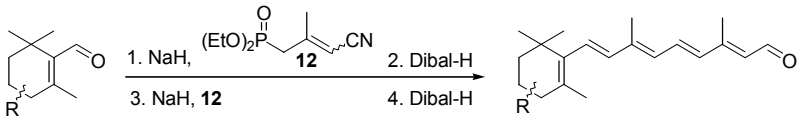

9 = 4-hydroxy-β-cyclocitral
10 = safranal
11 = 3-hydroxy-β-cyclocitral

2 = 3,4-didehydroretinal
3 = 3-hydroxyretinal
4 = 4-hydroxyretinal

Scheme 2. *Synthesis of C_{20}-retinal derivatives.*

5.3 SYNTHESIS OF ^{13}C-LABELED CAROTENOIDS USING THE REDUCTIVE MCMURRY-DIMERIZATION

Most C_{40}-carotenoids are synthesized using the $C_{15} + C_{10} + C_{15}$ scheme, where the final step is the double Wittig-coupling of the C_{15}-Wittig salt to the central C_{10}-dialdehyde. However, it is known that β-carotene can easily be synthesized by reductive dimerization of retinal with a $TiCl_4/LiAlH_4$ mixture, $TiCl_2$ being the actual reducing agent. Via this so-called McMurry dimerization, all-*E* β-carotene can be obtained in good yield (50% after recrystallization) from retinal.[36-40]

Starting from the above described retinal-derivates, the McMurry-dimerization was used to prepare the corresponding C_{40}-carotenoids in a similar $C_{20} + C_{20}$ scheme, as depicted in Scheme 3.

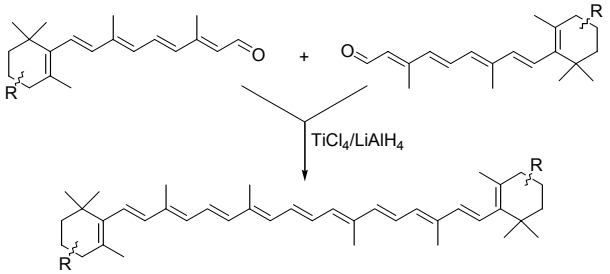

Scheme 3. *Synthesis of C_{40}-carotenoids, via the reductive McMurry dimerization of two C_{20}-retinal derivatives.*

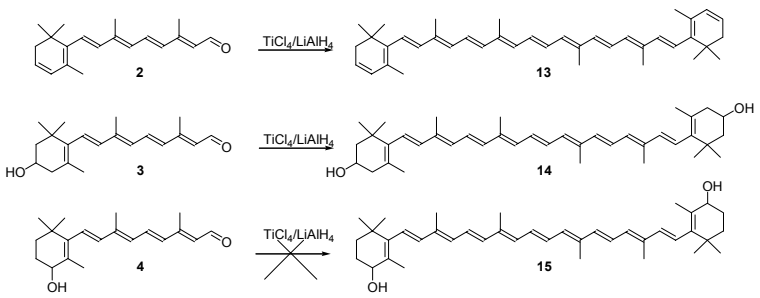

Scheme 4. *McMurry dimerization of 3,4-didehydroretinal (**2**), 3-hydroxyretinal (**3**) and 4-hydroxyretinal (**4**) to obtain the corresponding C_{40}-carotenoids **13**, **14** and **15**.*

This scheme can be an improvement to the C_{15}+C_{10}+C_{15} synthetic scheme for carotenoids when ^{13}C labels are desired in the central polyene-chain. As described above for the synthesis of retinal derivatives **9**, **10**, and **11**, the carbons of the central polyene chain are introduced at the end of the synthetic scheme, by two consecutive HWE-coupling reactions to C_5-phosphonate **12** (see Scheme 2). This C_5-phosphonate can easily be made with ^{13}C enrichment at any position or combination of positions.[24] In contrast to the C_{15}+C_{10}+C_{15} synthetic scheme, the desired C_{40}-carotenoid can be obtained using the C_{20}+C_{20} McMurry reaction by carrying out only a limited number of reactions after the ^{13}C labels are introduced, which improves the yield compared to the relatively expensive ^{13}C labeled starting compounds.

The retinal-derivatives **9**, **10**, and **11** were subjected to a McMurry-dimerization for synthesis of the corresponding C_{40}-carotenoids 3,4,3',4'-tetradehydro-β,β-carotene (**13**) (also known as dehydrocarotene III), zeaxanthin (**14**) and isozeaxanthin (**15**), as shown in Scheme 4.[41]

The results of the coupling reactions varied for the different retinal derivatives. As expected, 3,4-didehydroretinal reacted without difficulties to give the corresponding all-*E* dehydrocarotene III (**13**), in good yield (50% after recrystallization), similar to the synthesis of all-*E* β,β-carotene from retinal.

In the literature is described that McMurry-dimerization of aldehydes can be performed in the presence of a free hydroxyl-function.[42,43] However, the dimerization of 3-hydroxyretinal is very sensitive to oxygen, good quality reagents have to be used, and good practical skills are required. When the reaction was carried out carefully, pure all-*E* zeaxanthin (**14**) was obtained after recrystallization. The reaction should be optimized to increase the yield, which was now only 10%. However, these results indicate that the developed reaction scheme leads to the desired products and is promising as an efficient method for the introduction of ^{13}C labels in the polyene chain of carotenoids.

Reductive coupling of 4-hydroxyretinal (**11**) did not give the desired product (**15**), but only degradation of the starting material. Therefore, a suitable protection group for the hydroxyl function was needed. First, it was tried to convert the hydroxyl group to a THP-ether. However, treatment with a trace of *p*TsOH at room temperature quickly led to the dehydration of (**11**),

giving 3,4-didehydroretinal (**9**) instead of the desired THP-ether of **11**. It was expected that the allylic alcohol-group would be acid-sensitive, since a similar acid-catalyzed dehydration is used to obtain 3,4-didehydrocyclocitral (**10**). This latter reaction requires heating overnight with removal of water to obtain the desired product. Due to the longer polyene chain in **11**, the allylic alcohol is more easily dehydrated. To circumvent this problem a base-catalyzed protection group was introduced, a *t*-butyldimethylsilyl (TBDMS) ether. Unfortunately, this reaction only gave degradation of the starting compound.

If in the future the above-mentioned problems with the McMurry-dimerization of 4-hydroxyretinal can be overcome, this can lead to an improved synthetic scheme for the synthesis of (^{13}C labeled) carotenoids like isozeaxanthin. Isozeaxanthin can be converted to cantaxanthin according to literature,[44-46] which in turn can be converted to astaxanthin.[47-49]

A suitable synthetic method would lead to a new and efficient scheme for the synthesis of these carotenoids, that play an important role in food and feed industry, with ^{13}C enrichment at the desired positions.

5.4 CONCLUSION

Based on our modular strategy to prepare ^{13}C isotopomers of all-*E* retinal, we have described the chemical modification of the α-cyclocitral module to prepare 3,4-didehydro-, 3-hydroxy- and 4-hydroxyretinal. The McMurry-dimerization of retinal-derivatives to obtain the corresponding carotenoids was explored, to develop an efficient method for the synthesis of ^{13}C-labeled carotenoids. Using this method, pure zeaxanthin was obtained from 3-hydroxyretinal and 3,4,3′,4′-tetradehydro-β,β-carotene from 3,4-didehydroretinal, indicating the potential of this scheme. The synthesis of other carotenoids via this method requires further investigation.

EXPERIMENTAL

3-Hydroxy-2,6,6-trimethylcyclohex-1-enecarbonitrile (6)

A solution of α-cyclocitronitrile **5** (5.76 g, 38.6 mmol) in ethyl acetate (30 mL) was slowly added to a solution of 70% *m*CPBA (11.4 g, 46.3 mmol) in ethyl acetate (30 mL) at 0°C. The reaction mixture was stirred overnight at room temperature. The solvent was removed in vacuo and PE (100 mL) was added. The solution was cooled to 0°C and triethylamine (TEA, 10 mL) was slowly added. After stirring for 10 min a white precipitate was formed, which was removed by filtration through silica gel. The silica was washed (25% diethyl ether/3% TEA/PE) and the filtrate was concentrated in vacuo, to obtain 2,3-epoxy-2,6,6-trimethyl-2-cyclohexanecarbonitrile (5.46 g, 33.0 mmol, 88%) as a mixture of isomers.

^{1}H NMR (300 MHz, $CDCl_3$) δ (ppm) = 1.05 (s, 3 H, 1-CH_3), 1.09 (s, 3 H, 1-CH_3), 1.2-1.3 (m, 2 H, 2-H), 1.55 (s, 3 H, 5-CH_3), 2.00 (m, 2 H, 3-H), 2.75 (s, 1 H, 6-H), 3.05 (br. s, 1 H, 4-H).

^{13}C NMR (75 MHz, $CDCl_3$) δ (ppm) = 20.7/21.5 (5-CH_3), 23.3 (C-3), 28.4 (C-1), 29.3/30.3 (1-CH_3), 31.3 (C-2), 44.7 (C-6), 55.3 (C-5), 58.6 (C-4), 118.5 (CN).

Lithium diisopropylamide (LDA) was prepared at -20°C by adding *n*-BuLi (1.6 M solution in hexane, 24.8 mL, 39.6 mmol) to a solution of diisopropylamine (DIPA, 6.0 mL, 43.0 mmol) in dry THF. A solution of 2,3-epoxy-2,6,6-trimethyl-2-cyclohexanecarbonitrile (5.46 g, 33.0 mmol) in dry THF (10 mL) was slowly added at -40°C, and the reaction mixture was allowed to warm to RT overnight. The mixture was neutralized by adding NH_4Cl (sat), and the mixture was extracted three times with diethyl ether. The combined organic layers were washed with NaCl (sat) and dried with $MgSO_4$. After filtration and concentration in vacuo of the crude product 3-hydroxy-2,6,6-trimethylcyclohex-1-enecarbonitrile **6** (5.05 g, 30.6 mmol, 93%) was obtained.

^{1}H NMR (300 MHz, $CDCl_3$) δ (ppm) = 1.15 (s, 3 H, 1-CH_3), 1.20 (s, 3 H, 1-CH_3), 1.3-2.0 (m, 4 H, 2-H/3-H), 2.10 (s, 3 H, 5-CH_3), 2.45 (br. s, 1 H, OH), 4.06 (t, *J* = 6.0 Hz, 1 H, 3-H).

^{13}C NMR (75 MHz, $CDCl_3$) δ (ppm) = 19.8 (5-CH_3), 27.9 (1-CH_3), 28.2 (C-3), 33.0 (C-2), 33.7 (C-1), 68.2 (C-4), 117.1 (CN), 119.7 (C-6), 152.5 (C-5).

2,6,6-Trimethylcyclohexa-1,3-dienecarbonitrile (7)

4-Hydroxy-β-cyclocitronitrile **6** (5.0 g, 30.5 mmol) was dissolved in toluene and *p*-toluenesulfonic acid (*p*TsOH, 2.0 g) was added. The mixture was refluxed overnight and the water formed during the reaction was trapped with a Dean-Stark apparatus. Workup was carried out by adding diethyl ether (100 mL) and $NaHCO_3$ (75 mL, sat). The organic layer was collected and washed again with $NaHCO_3$ (sat) and NaCl (sat), dried with $MgSO_4$ and concentrated in vacuo to give 2,6,6-trimethylcyclohexa-1,3-dienecarbonitrile **7** (3.46 g, 23.5 mmol, 77%).

^{1}H NMR (300 MHz, $CDCl_3$) δ (ppm) = 1.15 (s, 6 H, 1-CH_3), 2.05 (s, 3 H, 5-CH_3), 2.19 (dd, *J* = 1.9 Hz/4.4 Hz, 2 H, 2-H), 5.92 (dt, *J* = 1.9 Hz/9.5 Hz, 1 H, 4-H), 6.06 (dt, *J* = 4.4 Hz/9.6 Hz, 1 H, 3-H).

^{13}C NMR (75 MHz, $CDCl_3$) δ (ppm) = 21.2 (5-CH_3), 26.6 (1-CH_3), 31.2 (C-1), 37.3 (C-2), 113.6 (CN), 117.5 (C-6), 126.1 (C-4), 131.3 (C-3), 145.5 (C-5).

3,4-Epoxy-2,6,6-trimethylcyclohex-1-enecarbonitrile (8)

2,6,6-Trimethylcyclohexa-1,3-dienecarbonitrile **7** (2.09 g, 14.2 mmol) was dissolved in ethyl acetate (30 mL) and *m*CPBA (4.2 g, 17 mmol) in ethyl acetate (30 mL) was added at RT and the mixture was refluxed overnight. The solvent was removed by evaporation in vacuo, and PE (150 mL) was added. The suspension was cooled to 0°C and TEA (9 mL) was added. After stirring for 15 min the white precipitate of *m*-chlorobenzoic acid was removed by filtration through silica gel. The silica was washed (25% ether/3% TEA/PE) and the filtrate concentrated in vacuo, to yield 3,4-epoxy-2,6,6-trimethylcyclohex-1-enecarbonitrile **8** (2.04 g, 12.1 mmol, 85%) as a mixture of isomers.

^{1}H NMR (300 MHz, $CDCl_3$) δ (ppm) = 1.19/1.21 (2s, 6 H, 1-CH_3), 1.63/1.71 (m, 1 H, 2-H), 2.12/2.21 (d, *J* = 2.4 Hz, 1 H, 2-H), 2.25 (s, 3 H, 5-CH_3), 3.23/3.25 (m, 1 H, 3-H), 3.59 (m, 1 H, 4-H).

^{13}C NMR (75 MHz, $CDCl_3$) δ (ppm) = 22.0 (5-CH_3), 29.6/31.4 (1-CH_3), 32.9 (C-6), 35.2 (C-2), 49.6 (C-3), 55.2 (C-4), 116.3 (CN), 119.6 (C-1), 147.5 (C-5).

3-Hydroxy-2,6,6-trimethylcyclohex-1-enecarbaldehyde (9)

A solution of 3-hydroxy-2,6,6-trimethylcyclohex-1-enecarbonitrile **6** (1.0 g, 6.1 mmol) in dry toluene was cooled to -60°C and Dibal-H (14 mL, 14.0 mmol) was added. The solution was allowed to warm to RT and the reaction was followed on TLC. After 30 min at RT the mixture was cooled to -20°C and SiO_2/H_2O (24.4 g) was added. The suspension was stirred for another hour at 0°C, K_2CO_3 and $MgSO_4$ were added, and after stirring for 15 min the solids were removed by filtration, washed with diethyl ether and the filtrate was concentrated in vacuo to yield, after flash column chromatography (60% diethyl ether/PE) 3-hydroxy-2,6,6-trimethylcyclohex-1-enecarbaldehyde **9** (0.74 g, 4.4 mmol, 73%).

^{1}H NMR (300 MHz, $CDCl_3$) δ (ppm) = 1.16/1.21 (2s, 6 H, 1-CH_3), 1.3-2.0 (m, 4 H, 2-H/3-H), 2.20 (s, 3 H, 5-CH_3), 3.72 (br. s, 1 H, OH), 4.07 (t, *J* = 6.2 Hz, 1 H, 4-H), 10.11 (s, 1 H, CHO).

^{13}C NMR (75 MHz, $CDCl_3$) δ (ppm) = 15.2 (5-CH_3), 27.0 (1-CH_3), 27.6 (C-3), 33.1 (C-1), 35.7 (C-2), 70.2 (C-4), 140.8 (C-6), 154.4 (C-5), 193.5 (CHO).

2,6,6-Trimethylcyclohexa-1,3-dienecarbaldehyde (10)

2,6,6-Trimethylcyclohexa-1,3-dienecarbonitrile **7** (2.0 g, 13.6 mmol) was dissolved in dry PE (75 mL) and Dibal-H (17.7 mL, 17.7 mmol) was added at -60°C. The solution was allowed to warm to RT and stirred for 30 min at RT. The mixture was cooled to -20°C, SiO_2/H_2O (30.9 g) was added and the suspension was stirred for 1 h at 0°C. K_2CO_3 and $MgSO_4$ were added, the solids were removed by filtration and the filtrate was concentrated in vacuo. Flash-column purification (10% diethyl ether/PE) yielded aldehyde **10** (2.04 g, 12.1 mmol, 92%).

^{1}H NMR (300 MHz, $CDCl_3$) δ (ppm) = 1.19 (s, 6 H, 1-CH_3), 2.15 (dd, *J* = 1.9 Hz/4.5 Hz, 2 H, 2-H), 2.17 (s, 3 H, 5-CH_3), 5.91 (dt, *J* = 1.9 Hz/9.5 Hz, 2 H, 4-H), 6.15 (dt, *J* = 4.5 Hz/9.5 Hz, 1 H, 3-H), 10.14 (s, 1 H, CHO).

^{13}C NMR (75 MHz, $CDCl_3$) δ (ppm) = 17.6 (5-CH_3), 26.2 (1-CH_3), 32.6 (C-1), 40.9 (C-2), 129.8 (C-4), 134.4 (C-3), 137.4 (C-6), 146.8 (C-5), 191.7 (CHO).

4-Hydroxy-2,6,6-trimethylcyclohex-1-enecarbaldehyde (11)

Dibal-H (36.3 mL, 36.3 mmol) was added to a solution of 3,4-epoxy-2,6,6-trimethyl-cyclohex-1-enecarbonitrile **8** (2.04 g, 12.1 mmol) in dry PE at -60°C. The solution was allowed to warm to RT in 1 h and stirred for another 2 h at RT. It was cooled to -20°C, SiO_2/H_2O (63.6 g) was added and the suspension was stirred at 0°C for 1 h, after which $MgSO_4$ and K_2CO_3 were added. The solids were removed by filtration and the solvent removed by evaporation in vacuo. After flash-chromatography (60% diethyl ether/PE) 3-hydroxy-β-cyclocitral **11** (1.60 g, 9.53 mmol, 79%) was obtained.

^{1}H NMR (300 MHz, $CDCl_3$) δ (ppm) = 1.23/1.25 (2s, 6 H, 1-CH_3), 1.47 (dt, *J* = 2.6 Hz/8.9 Hz, 1 H, 2-H_{ax}), 1.71 (d, *J* = 2.7 Hz, 1 H, 2-H_{eq}), 2.13 (s, 3 H, 5-CH_3), 2.25 (dd, *J* = 9.2 Hz/18.4 Hz, 4-H_{eq}), 2.53 (dd, *J* = 2.2 Hz/2.9 Hz, 4-H_{ax}), 3.3 (br. s, 1 H, OH), 3.98 (m, 1 H, 3-H), 10.10 (s, 1 H, CHO).

^{13}C NMR (75 MHz, $CDCl_3$) δ (ppm) = 19.0 (5-CH_3), 27.5/28.6 (1-CH_3), 35.5 (C-1), 44.2 (C-4), 49.0 (C-2), 63.4 (C-3), 139.6 (C-6), 153.4 (C-5), 191.6 (CHO).

3,4-Didehydroretinal (2)

3-Methyl-5-(2,6,6-trimethylcyclohexa-1,3-dienyl)-penta-2,4-dienal

A suspension of NaH (60% in mineral oil, 0.43 g, 10.7 mmol) was washed three times with dry PE and transferred into a flame-dried flask. The suspension was once more washed with dry PE, PE was removed with a N_2-flow and dry THF (75 mL) was added. At 0°C, 4-(diethylphosphono)-3-methyl-2-butenenitrile **12** (2.14 g, 9.9 mmol) in THF was added and during 30 min of stirring at RT the phosphonate anion was formed. The solution was cooled to 0°C and 2,6,6-trimethyl-cyclohexa-1,3-dienecarbaldehyde **10** (1.23 g, 8.21 mmol) in THF was added. After stirring overnight at RT, the reaction was quenched by adding NH_4Cl (sat) and the mixture was extracted three times with diethyl ether. The combined organic layers were washed with NaCl (sat), dried with $MgSO_4$ and concentrated in vacuo. After purification on a silica-gel column (20% diethyl ether/PE) pure 3-methyl-5-(2,6,6-trimethylcyclohexa-1,3-dienyl)-penta-2,4-dienitrile (1.06 g, 5.0 mmol, 61%) was obtained as a mixture of isomers.

^{1}H NMR (300 MHz, $CDCl_3$) δ (ppm) = 1.04 (s, 6 H, 1-CH_3), 1.86 (s, 3 H, 5-CH_3), 2.09 (m, 2 H, 2-H), 2.21 (s, 3 H, 9-CH_3), 5.20 (s, 1 H, 10-H), 5.81 (dt, *J* = 4.2 Hz/9.7 Hz, 1 H, 3-H), 5.86 (d, *J* = 9.7 Hz, 1 H, 4-H), 6.27 (d, *J* = 16.1 Hz, 1 H, 8-H), 6.56 (d, *J* = 16.1 Hz, 1 H, 7-H).

^{13}C NMR (75 MHz, $CDCl_3$) δ (ppm) = 16.3 (9-CH_3), 20.1 (5-CH_3), 26.5 (1-CH_3), 33.8 (C-1), 39.7 (C-2), 96.3 (C-10), 117.9 (C-11), 122.0 (C-3), 126.7 (C-5), 129.4 (C-4), 131.7 (C-7), 134.2 (C-8), 140.3 (C-6), 156.8 (C-9).

A solution of 3-methyl-5-(2,6,6-trimethylcyclohexa-1,3-dienyl)-penta-2,4-dienitrile (1.06 g, 5.0 mmol) in dry PE was cooled to -60°C and Dibal-H (6.5 mL, 6.5 mmol) was added. The mixture was warmed to RT in 1 h, and stirred for another 30 min at RT. After cooling to -20°C, SiO_2/H_2O (11.3 g) was added, and the mixture was stirred for 1 h at 0°C. K_2CO_3 and $MgSO_4$ were added, the solids were removed by filtration and washed with diethyl ether. The solvents were removed in vacuo, and the product was purified on a silica-gel column (20% diethyl ether/PE) to give 3-methyl-5-(2,6,6-trimethylcyclohexa-1,3-dienyl)-penta-2,4-dienal (1.03 g, 4.8 mmol, 96%) as a mixture of isomers.

^{1}H NMR (300 MHz, $CDCl_3$) δ (ppm) = 1.06 (s, 6 H, 1-CH_3), 1.88 (s, 3 H, 5-CH_3), 2.12 (d, *J* = 4.2 Hz, 2 H, 2-H), 2.33 (s, 3 H, 9-CH_3), 5.82 (dt, *J* = 4.2 Hz/9.6 Hz, 1 H, 3-H), 5.88 (d, *J* = 9.6 Hz, 4-H), 5.94 (d, *J* = 8.2 Hz, 1 H, 10-H), 6.33 (d, *J* = 16.5 Hz, 1 H, 8-H), 6.73 (d, *J* = 16.5 Hz, 1 H, 7-H), 10.13 (d, *J* = 8.2 Hz, 1 H, 11-H).
^{13}C NMR (75 MHz, $CDCl_3$) δ (ppm) = 12.4 (9-CH_3), 20.0 (5-CH_3), 26.4 (1-CH_3), 33.7 (C-1), 39.5 (C-2), 126.4 (C-3), 127.4 (C-5), 128.5 (C-10), 129.5 (C-4), 133.7 (C-7), 134.5 (C-8), 136.9 (C-6), 154.1 (C-9), 190.5 (C-11).

C_5-phosphonate **12** (1.24 g, 5.7 mmol) in dry THF (10 mL) was added to a suspension of washed NaH (0.25 g, 6.2 mmol) in dry THF at 0°C. After stirring at RT for 30 min the NaH had reacted with the phosphonate and 3-methyl-5-(2,6,6-trimethylcyclohex-1,3-dienyl)-penta-2,4-dienal (1.03 g, 4.8 mmol) in THF was added to the formed phosphonate anion at 0°C. The solution was stirred overnight, and NH_4Cl (sat) was added. The mixture was extracted three times with diethyl ether, the combined organic layers were washed with NaCl (sat) and dried with $MgSO_4$. The solid was removed by filtration and the filtrate concentrated in vacuo to give, after column purification (10% diethyl ether/PE) 3,7-dimethyl-9-(2,6,6-trimethylcyclohexa-1,3-dienyl)-nona-2,4,6,8-tetraenenitrile (1.3 g, 4.6 mmol, 96%) as a mixture of isomers.
^{1}H NMR (300 MHz, $CDCl_3$) δ (ppm) = 1.04 (s, 6 H, 1-CH_3), 1.86 (s, 3 H, 5-CH_3), 2.02 (s, 3 H, 9-CH_3), 2.09 (d, *J* = 4.4 Hz, 2 H, 2-H), 2.20 (s, 3 H, 13-CH_3), 5.17 (s, 1 H, 14-H), 5.75 (dt, *J* = 4.4 Hz/9.4 Hz, 1 H, 3-H), 5.85 (d, *J* = 9.4 Hz, 1 H, 4-H), 6.15 (d, *J* = 11.4 Hz, 1 H, 10-H), 6.29 (d, *J* = 15.0 Hz, 1 H, 12-H), 6.31 (2s, 2 H, 7-H/8-H), 6.95 (dd, *J* = 11.4 Hz/15.0 Hz, 1 H, 11-H).
^{13}C NMR (75 MHz, $CDCl_3$) δ (ppm) = 12.6 (9-CH_3), 16.3 (13-CH_3), 20.1 (5-CH_3), 26.5 (1-CH_3), 33.7 (C-1), 39.7 (C-2), 96.3 (C-14), 117.8 (C-15), 125.3 (C-3), 127.4 (C-5), 128.1 (C-7), 129.2 (C-10), 129.6 (C-4), 132.2 (C-11), 133.8 (C-12), 136.8 (C-8), 137.9 (C-6), 140.8 (C-9), 156.6 (C-13).

The 3,4-didehydro-C_{20}-nitrile (1.27 g, 4.6 mmol) was dissolved in dry toluene and Dibal-H (6.0 mL, 6.0 mmol) was added at -80°C. The mixture was allowed to warm to -50°C in 20 min and SiO_2/H_2O (10.5 g) was added. The suspension was stirred for 1 h at 0°C and K_2CO_3 and $MgSO_4$ were added. The solids were removed by filtration, washed with diethyl ether and the solvents were removed in vacuo. After column chromatography (20% diethyl ether/PE) 3,4-didehydroretinal **2** (1.2 g, 4.3 mmol, 94%) was obtained as a mixture of isomers.
^{1}H NMR (400 MHz, $CDCl_3$) δ (ppm) = 1.05 (s, 6 H, 1-CH_3), 1.88 (s, 3 H, 5-CH_3), 2.04 (s, 3 H, 9-CH_3), 2.09 (dd, *J* = 4.3 Hz, 2 H, 2-H), 2.33 (s, 3 H, 13-CH_3), 5.76 (dt, *J* = 4.3 Hz/9.5 Hz, 1 H, 3-H), 5.86 (d, *J* = 9.5 Hz, 1 H, 4-H), 5.97 (d, *J* = 8.1 Hz, 14-H), 6.23 (d, *J* = 11.5 Hz, 1 H, 10-H), 6.33 (2s, 2 H, 7-H/8-H), 6.38 (d, *J* = 15.1 Hz, 1 H, 12-H), 7.15 (dd, *J* = 11.5 Hz/15.1 Hz, 1 H, 11-H), 10.11 (d, *J* = 8.1 Hz, 1 H, 15-H).
^{13}C NMR (100 MHz, $CDCl_3$) δ (ppm) = 12.8 (9-CH_3), 13.0 (13-CH_3), 20.2 (5-CH_3), 26.7 (1-CH_3), 33.9 (C-1), 39.8 (C-2), 125.5 (C-3), 127.7 (C-5), 128.4 (C-7), 128.9 (C-14), 129.8 (C-4), 129.8 (C-10), 132.4 (C-11), 134.6 (C-12), 136.4 (C-8), 138.1 (C-6), 141.0 (C-9), 154.6 (C-13), 190.9 (C-15).

(3*RS*)-Hydroxyretinal (3)

3-Methyl-5-(4-hydroxy-2,6,6-trimethylcyclohex-1-enyl)-penta-2,4-dienal

In a procedure similar to the one described above, C_5-phosphonate **12** (2.59 g, 11.9 mmol) in THF was added to a suspension of washed NaH (0.91 g, 22.8 mmol) in dry THF at 0°C. After 30 min at RT, the suspension was cooled back to 0°C and 4-hydroxy-2,6,6-trimethylcyclohex-1-enecarbaldehyde **11** (1.67 g, 9.9 mmol) in THF (10 mL) was added. After stirring overnight at RT, NH_4Cl (sat) was added and the mixture was extracted three times with diethyl ether. The organic layer was washed with NaCl (sat), dried with $MgSO_4$, filtered and concentrated. Column purification (60% diethyl ether/PE) yielded 3-methyl-5-(4-hydroxy-2,6,6-trimethyl-cyclohex-1-enyl)-penta-2,4-dienitrile (0.96 g, 4.2 mmol, 42%) as a mixture of isomers.

^{1}H NMR (300 MHz, $CDCl_3$) δ (ppm) = 1.06/1.07 (2s, 6 H, 1-CH_3), 1.4 (m, 1 H, 2-H_{ax}), 1.72 (s, 3 H, 5-CH_3), 1.8 (m, 1 H, 2-H_{eq}), 2.0 (m, 1 H, 4-H_{ax}), 2.20 (s, 3 H, 9-CH_3), 2.4 (m, 1 H, 4-H_{eq}), 2.72 (br. s, 1 H, OH), 3.96 (m, 1 H, 3-H), 5.19 (s, 1 H, 10-H), 6.15 (d, *J* = 16.1 Hz, 1 H, 8-H), 6.69 (d, *J* = 16.1 Hz, 1 H, 7-H).

^{13}C NMR (75 MHz, $CDCl_3$) δ (ppm) = 16.2 (9-CH_3), 22.7 (5-CH_3), 28.1/29.5 (1-CH_3), 35.2 (C-1), 40.6 (C-4), 45.1 (C-2), 64.0 (C-3), 96.4 (C-10), 117.1 (C-11), 126.3 (C-5), 134.7 (C-7), 136.1 (C-8), 139.2 (C-6), 156.9 (C-9).

In a similar Dibal-H reduction to the one described earlier, 3-methyl-5-(4-hydroxy-2,6,6-trimethylcyclohex-1-enyl)-penta-2,4-dienitrile (0.82 g, 3.6 mmol) was reduced with Dibal-H (8.2 mL, 8.2 mmol) in dry toluene to give, after column purification (60% diethyl ether/PE), the corresponding 3-methyl-5-(4-hydroxy-2,6,6-trimethylcyclohex-1-enyl)-penta-2,4-dienal (0.75 g, 3.2 mmol, 90%) as a mixture of isomers.

^{1}H NMR (300 MHz, $CDCl_3$) δ (ppm) = 1.09/1.10 (2s, 6 H, 1-CH_3), 1.5 (m, 1 H, 2-H_{ax}), 1.75 (s, 3 H, 5-CH_3), 1.8 (m, 1 H, 2-H_{eq}), 2.0 (m, 1 H, 4-H_{ax}), 2.33 (s, 3 H, 9-CH_3), 2.4 (m, 1 H, 4-H_{eq}), 3.15 (br. s, 1 H, OH), 3.98 (m, 1 H, 3-H), 5.95 (d, *J* = 8.4 Hz, 1 H, 10-H), 6.22 (d, *J* = 16.1 Hz, 1 H, 8-H), 6.73 (d, *J* = 16.1 Hz, 1 H, 7-H), 10.10 (d, *J* = 8.4 Hz, 1 H, 11-H).

^{13}C NMR (75 MHz, $CDCl_3$) δ (ppm) = 12.4 (9-CH_3), 21.1 (5-CH_3), 28.2/30.1 (1-CH_3), 36.5 (C-1), 42.1 (C-4), 47.7 (C-2), 63.7 (C-3), 128.6 (C-10), 129.4 (C-5), 134.8 (C-7), 136.7 (C-8), 139.6 (C-6), 154.8 (C-9), 191.2 (C-11).

By using a similar method as described above for (**2**), the anion of C_5-phosphonate **12**, formed by adding **12** (0.83 g, 3.8 mmol) to a suspension of washed NaH (0.29 g, 7.3 mmol) in dry THF at 0°C, reacted with 3-methyl-5-(4-hydroxy-2,6,6-trimethylcyclohex-1-enyl)-penta-2,4-dienal (0.75 g, 3.2 mmol). After workup and purification (silica gel, 60% diethyl ether/PE), 3,7-dimethyl-9-(4-hydroxy-2,6,6-trimethylcyclohex-1-enyl)-nona-2,4,6,8-tetraenenitrile (0.65 g, 2.2 mmol, 69%) was obtained as a mixture of isomers.

^{1}H NMR (300 MHz, $CDCl_3$) δ (ppm) = 1.03/1.08 (2s, 6 H, 1-CH_3), 1.4 (m, 1 H, 2-H_{ax}), 1.73 (s, 3 H, 5-CH_3) 1.8 (m, 1 H, 2-H_{eq}), 2.01 (s, 3 H, 9-CH_3), 2.1 (m, 1 H, 4-H_{ax}), 2.20 (s, 3 H, 13-CH_3), 2.4 (m, 1 H, 4-H_{eq}), 2.99 (br. s, 1 H, OH), 3.96 (m, 1 H, 3-H), 5.20 (s, 1 H, 14-H), 6.13 (d, *J* = 11.6 Hz, 1 H, 10-H), 6.14 (d, *J* = 16.0 Hz, 1 H, 8-H), 6.27 (d, *J* = 16.0 Hz, 1 H, 7-H), 6.31 (d, *J* = 15.0 Hz, 1 H, 12-H), 6.96 (dd, *J* = 11.6 Hz/15.0 Hz, 1 H, 11-H).

^{13}C NMR (75 MHz, $CDCl_3$) δ (ppm) = 12.8 (9-CH_3), 16.4 (13-CH_3), 21.4 (5-CH_3), 28.5/30.0 (1-CH_3), 36.8 (C-1), 42.2 (C-4), 48.0 (C-2), 64.2 (C-3), 96.3 (C-14), 117.2 (C-15), 127.1 (C-5), 128.4 (C-7), 131.3 (C-10), 132.3 (C-11), 133.2 (C-12), 137.1 (C-6), 137.5 (C-8), 140.8 (C-9), 156.9 (C-13).

The C_{20}-nitrile (0.54 g, 1.8 mmol) was reduced to the corresponding aldehyde **3** with Dibal-H (4.5 mL, 4.5 mmol) in dry toluene, using the same procedure as described before. After purification on a silica-gel column (60% diethyl ether/PE) 3-hydroxy-retinal (**3**) (0.48 g, 1.6 mmol, 89%) was obtained as a mixture of isomers.

^{1}H NMR (600 MHz, $CDCl_3$) δ (ppm) = 1.03/1.08 (2s, 6 H, 1-CH_3), 1.50 (t, *J* = 12.0 Hz, 1 H, 2-H_{ax}), 1.74 (s, 3 H, 5-CH_3), 1.79 (t, *J* = 4.1 Hz, 1 H, 2-H_{eq}), 2.03 (s, 3 H, 9-CH_3), 2.08 (t, *J* = 10.3 Hz, 1 H, 4-H_{ax}), 2.33 (s, 3 H, 13-CH_3), 2.40 (d, *J* = 5.2 Hz, 1 H, 4-H_{eq}), 2.90 (br. s, 1 H, OH), 4.00 (m, 1 H, 3-H), 5.97 (d, *J* = 8.2 Hz, 1 H, 14-H), 6.16 (d, *J* = 16.1 Hz, 1 H, 8-H), 6.20 (d, *J* = 11.5 Hz, 1 H, 10-H), 6.29 (d, *J* = 16.1 Hz, 1 H, 7-H), 6.38 (d, *J* = 15.0 Hz, 1 H, 12-H), 7.15 (dd, *J* = 11.5 Hz/15.0 Hz, 1 H, 11-H), 10.08 (d, *J* = 8.2 Hz, 1 H, 15-H).

^{13}C NMR (150 MHz, $CDCl_3$) δ (ppm) = 12.7 (9-CH_3), 12.9 (13-CH_3), 21.4 (C-18), 28.5/30.0 (1-CH_3), 36.8 (C-1), 42.3 (C-4), 48.0 (C-2), 64.3 (C-3), 127.3 (C-5), 128.5/128.7 (C-7/C-14), 129.6 (C-10), 132.3 (C-11), 134.5 (C-12), 137.1 (C-6), 137.4 (C-8), 140.8 (C-9), 154.8 (C-13), 191.0 (C-15)

(4*RS*)-Hydroxyretinal (4)

3-Methyl-5-(3-hydroxy-2,6,6-trimethylcyclohex-1-enyl)-penta-2,4-dienal

In a similar way to that described above, C_5-phosphonate **12** (1.14 g, 5.3 mmol) was deprotonated with NaH (0.4 g, 10.1 mmol) and coupled to 3-hydroxy-2,6,6-trimethylcyclohex-1-enecarbaldehyde **9** (0.74 g, 4.4 mmol). After purification (50% diethyl ether/PE), 3-methyl-5-(3-hydroxy-2,6,6-trimethylcyclohex-1-enyl)-penta-2,4-dienitrile (0.82 g, 3.6 mmol, 81%) was obtained as a mixture of isomers.

^{1}H NMR (300 MHz, $CDCl_3$) δ (ppm) = 1.01/1.04 (2s, 6 H, 1-CH_3), 1.4 (m, 1 H, 2-H_{eq}), 1.7 (m, 2 H, 2-H_{ax}/3-H_{ax}), 1.81 (s, 3 H, 5-CH_3), 1.9 (m, 1 H, 3-H_{eq}), 2.20 (s, 3 H, 9-CH_3), 2.64 (br. s, 1 H, OH), 3.99 (br. s, 1 H, 4-H), 5.21 (s, 1 H, 10-H), 6.17 (d, *J* = 16.0 Hz, 1 H,8-H), 6.52 (d, *J* = 16.0 Hz, 1 H, 7-H).

^{13}C NMR (75 MHz, $CDCl_3$) δ (ppm) = 15.9 (9-CH_3), 18.0 (5-CH_3), 27.0/27.8 (1-CH_3), 28.3 (C-3), 34.0 (C-2), 34.0 (C-1), 69.1 (C-4), 96.6 (C-10), 117.1 (C-11), 131.8 (C-5), 133.1 (C-7), 134.5 (C-8), 139.4 (C-6), 156.3 (C-9).

By using the same procedure as described before, 3-methyl-5-(3-hydroxy-2,6,6-trimethylcyclohex-1-enyl)-penta-2,4-dienitrile (0.60 g, 2.6 mmol) in dry toluene was reduced with Dibal-H (6 mL, 6.0 mmol). After purification on a silica-gel column (60% diethyl ether/PE) 3-methyl-5-(3-hydroxy-2,6,6-trimethylcyclohex-1-enyl)-penta-2,4-dienal (0.57 g, 2.4 mmol, 94%) was obtained as a mixture of isomers.

^{1}H NMR (300 MHz, $CDCl_3$) δ (ppm) = 1.03/1.06 (2s, 6 H, 1-CH_3), 1.4 (m, 1 H, 2-H_{eq}), 1.7 (m, 2 H, 2-H_{ax}/3-H_{ax}), 1.84 (s, 3 H, 5-CH_3), 1.9 (m, 1 H, 3-H_{eq}), 2.32 (s, 3 H, 9-CH_3), 2.70 (br. s, 1 H, OH), 3.99 (br. s, 1 H, 4-H), 5.92 (d, *J* = 7.9 Hz, 1 H, 10-H), 6.23 (d, *J* = 16.0 Hz, 1 H, 8-H), 6.70 (d, *J* = 16.0 Hz, 1 H, 7-H), 10.11 (d, *J* = 7.9 Hz, 1 H, 11-H).

^{13}C NMR (75 MHz, $CDCl_3$) δ (ppm) = 12.8 (9-CH_3), 18.4 (5-CH_3), 27.4/28.2 (1-CH_3), 28.7 (C-3), 34.4 (C-2), 34.6 (C-1), 69.6 (C-4), 129.0 (C-10), 132.3 (C-5), 134.8 (C-7), 136.6 (C-8), 140.3 (C-6), 154.5 (C-9), 191.3 (C-11).

C_5-phosphonate **12** (0.63 g, 2.9 mmol) in dry THF (10 mL) was added to a suspension of NaH (0.22 g, 5.6 mmol) in dry THF at 0°C. After 30 min at RT, 3-methyl-5-(3-hydroxy-2,6,6-trimethylcyclohex-1-enyl)-2,4-pentadienal (0.57 g, 2.4 mmol) in THF was added and the mixture was stirred overnight at RT. After workup

and purification by column chromatography (60% diethyl ether/PE), 3,7-dimethyl-9-(3-hydroxy-2,6,6-trimethylcyclohex-1-enyl)-nona-2,4,6,8-tetraenenitrile (0.60 g, 2.0 mmol, 83%) was obtained as a mixture of isomers.

^{1}H NMR (300 MHz, $CDCl_3$) δ (ppm) = 1.02/1.06 (2s, 6 H, 1-CH_3), 1.43 (m, 1 H, 2-H_{eq}), 1.69 (m, 1 H, 2-H_{ax}), 1.72 (m, 1 H, 3-H_{ax}), 1.84 (s, 3 H, 5-CH_3), 1.90 (m, 1 H, 3-H_{eq}), 2.01 (s, 3 H, 9-CH_3), 2.20 (s, 3 H, 13-CH_3), 3.12 (br. s, 1 H, OH), 4.00 (m, 1 H, 4-H), 5.20 (s, 1 H, 14-H), 6.09 (d, *J* = 11.5 Hz, 1 H, 10-H), 6.18 (d, *J* = 16.3 Hz, 1 H, 8-H), 6.28 (d, *J* = 16.3 Hz, 1 H, 7-H), 6.31 (d, *J* = 15.1 Hz, 1 H, 12-H), 6.95 (dd, *J* = 11.5 Hz/15.1 Hz, 1 H, 11-H).

^{13}C NMR (75 MHz, $CDCl_3$) δ (ppm) = 12.7 (9-CH_3), 16.3 (13-CH_3), 20.7 (5-CH_3), 27.3/28.7 (1-CH_3), 28.2 (C-3), 34.4 (C-2), 34.5 (C-1), 69.7 (C-4), 96.4 (C-14), 117.8 (C-15), 128.5 (C-7), 129.2 (C-10), 129.2 (C-12), 130.5 (C-5), 131.4 (C-11), 137.7 (C-8), 140.6 (C-9), 140.9 (C-6), 156.7 (C-13).

By using the same procedure as described above for (**2**), reduction of the 4-hydroxy-C_{20}-nitrile (0.60 g, 2.0 mmol) in dry toluene with Dibal-H (5 mL, 5 mmol) gave, after purification (60% diethyl ether/PE), the corresponding 4-hydroxy-retinal **4** (0.53 g, 1.8 mmol, 87%) of as a mixture of isomers.

^{1}H NMR (400 MHz, $CDCl_3$) δ (ppm) = 1.03/1.06 (2s, 6 H, 1-CH_3), 1.43 (m, 1 H, 2-H_{eq}), 1.68 (m, 1 H, 2-H_{ax}), 1.73 (m, 1 H, 3-H_{ax}), 1.85 (s, 3 H, 5-CH_3), 1.89 (m, 1 H, 3-H_{eq}), 2.03 (s, 3 H, 9-CH_3), 2.33 (s, 3 H, 13-CH_3), 2.90 (br. s, 1 H, OH), 4.02 (m, 1 H, 4-H), 5.97 (d, *J* = 8.1 Hz, 1 H, 14-H), 6.19 (d, *J* = 16.0 Hz, 1 H, 8-H), 6.21 (d, *J* = 11.3 Hz, 1 H, 10-H), 6.31 (d, *J* = 16.0 Hz, 1 H, 7-H), 6.38 (d, *J* = 15.1 Hz, 1 H, 12-H), 7.14 (dd, *J* = 11.3 Hz/15.1 Hz, 1 H, 11-H), 10.07 (d, *J* = 8.1 Hz, 1 H, 15-H).

^{13}C NMR (100 MHz, $CDCl_3$) δ (ppm) = 12.7 (9-CH_3), 12.8 (13-CH_3), 18.4 (5-CH_3), 27.4/28.7 (1-CH_3), 28.2 (C-3), 34.4 (C-2), 34.4 (C-1), 69.6 (C-4), 128.6/128.7 (C-7/C-14), 129.5 (C-10), 130.7 (C-5), 132.2 (C-11), 134.6 (C-12), 137.7 (C-8), 140.5/140.7 (C-6/C-9), 154.7 (C-13), 190.9 (C-15).

3,4,3′,4′-Didehydro-β,β-carotene (13)

$TiCl_3$ (0.3 g, 1.6 mmol) was added to dry THF under argon, $LiAlH_4$ (0.03 g, 0.8 mmol) was added to the suspension and the mixture was stirred for 2 h at RT. 3,4-Didehydro-retinal (0.23 g, 0.8 mmol) in THF was slowly added and the mixture was stirred overnight at RT. The reaction was quenched by adding HCl (1 M) and the mixture was extracted twice with diethyl ether. The combined organic layers were washed with NaCl (sat), dried with $MgSO_4$ and concentrated in vacuo. After purification on a silica-gel column (10% diethyl ether/PE) 3,4,3′,4′-didehydro-β,β-carotene **13** (0.1 g, 0.2 mmol, 50%) was obtained.

^{1}H NMR (600 MHz, $CDCl_3$) δ (ppm) = 1.04 (s, 12 H, 16-H/16′-H/17-H/17′-H), 1.88 (s, 6 H, 18-H/18′-H), 1.98 (s, 12 H, 19-H/19′-H/20-H/20′-H), 2.08 (2d, *J* = 4.6 Hz, 4 H, 2-H/2′-H), 5.72 (dt, *J* = 4.6 Hz/9.5 Hz, 2 H, 3-H/3′-H), 5.86 (d, *J* = 9.5 Hz, 2 H, 4-H/4′-H), 6.16 (m, 2 H, 10-H/10′-H), 6.18 (d, *J* = 15.1 Hz, 2 H, 7-H/7′-H), 6.30 (m, 4 H, 12-H/12′-H/14-H/14′-H), 6.37 (d, *J* = 15.1 Hz, 2 H, 8-H/8′-H), 6.64 (m, 4 H, 11-H/11′-H/15-H/15′-H).

^{13}C NMR (150 MHz, $CDCl_3$) (ppm) = 12.7 (C-19/C19′), 12.8 (C-20/C-20′), 20.3 (C-18/C-18′), 26.8 (C-16/C-16′/C-17/C-17′), 34.0 (C-1/C-1′), 39.9 (C-2/C-2′), 124.9 (C-3/C-3′/C-11/C-11′), 125.6 (C-7/C-7′), 126.7 (C-5/C-5′), 130.0 (C-4/C-4′/C-15/C-15′), 131.5 (C-10/C-10′), 132.6 (C-14/C-14′), 135.9 (C-9/C-9′), 135.9 (C-13/C-13′), 137.3 (C-8/C-8′), 137.5 (C-12/C-12′), 138.7 (C-6/C-6′).

Zeaxanthin (14)

$TiCl_3$ (0.22 g, 1.4 mmol) was added to dry THF under argon, $LiAlH_4$ (0.04 g, 1.1 mmol) was added to the suspension and the mixture was stirred for 2 h at RT. 3-Hydroxyretinal (0.21 g, 0.7 mmol) in THF was slowly added and the mixture was stirred overnight at RT. HCl (1 M) was added and the mixture was extracted twice with diethyl ether. The combined organic layers were washed with NaCl (sat), dried with $MgSO_4$ and concentrated in vacuo. After purification on a silica-gel column (50% diethyl ether/PE), and subsequent recrystallization (CH_2Cl_2/EtOH, -20°C), pure all-*E* zeaxanthin **14** (0.02 g, 0.04 mmol, 10%) was obtained.

^{1}H NMR (600 MHz, $CDCl_3$) δ (ppm) = 1.07 (s, 12 H, 16-H/16′-H/17-H/17′-H), 1.48 (m, 2 H, 2-H_{ax}/2′-H_{ax}), 1.74 (s, 6 H, 18-H/18′-H), 1.79 (m, 2 H, 2-H_{eq}/2′-H_{eq}), 1.97 (s, 12 H, 19-H/19′-H/20-H/20′-H), 2.05 (m, 2 H, 4-H_{ax}/4′-H_{ax}), 2.39 (m, 2 H, 4-H_{eq}/4′-H_{eq}), 4.00 (m, 2 H, 3-H/3′-H), 6.12 (s, 4 H, 7-H/7′-H/8-H/8′-H), 6.16 (d, *J* = 11.5 Hz, 2 H, 10-H/10′-H), 6.26 (d, *J* = 9.7 Hz, 2 H, 14-H/14′-H), 6.36 (d, *J* = 14.9 Hz, 2 H, 12-H/12′-H), 6.63 (m, 11-H/11′-H/15-H/15′-H).

^{13}C NMR (150 MHz, $CDCl_3$) δ (ppm) = 12.8 (C-19/C-19′/C-20/C-20′), 21.6 (C-18/C-18′), 28.7/30.3 (C-16/C-16′/C-17/C-17′), 37.1 (C-1/C-1′), 42.6 (C-4/C-4′), 48.5 (C-2/C-2′), 65.1 (C-3/C-3′), 124.9 (C-11/C-11′), 125.6 (C-7/C-7′), 126.2 (C-5/C-5′), 130.1 (C-15/C-15′), 131.3 (C-10/C-10′), 132.6 (C-14/C-14′), 135.7 (C-9/C-9′), 136.4 (C-13/C-13′), 137.6 (C-12/C-12′), 137.8 (C-6/C-6′), 138.5 (C-8/C-8′).

REFERENCES

[1] Baldwin JM, Schertler GFX, Unger VM, *J. Mol. Biol.* **1997**, *272*, 144-164.
[2] Ji TH, Grossmann M, Ji I, *J. Biol. Chem.* **1998**, *273*, 17299-17302.
[3] Wald G, *Nature* **1968**, *219*, 800-807.
[4] Schoenlein RW, Peteanu LA, Mathies RA, Shank CV, *Science* **1991**, *254*, 412-415.
[5] Peteanu LA, Mathies RA, Shank CV, *Proc. Natl. Acad. Sci.U.S.A.* **1993**, *90*, 11762-11766.
[6] Zechmeister L in *Cis-trans Isomeric Carotenoids, Vitamins A and Arylpolyenes*, Springer Verlag: Vienna, 1962.
[7] Isler O in *Carotenoids*, Birkhäuser Verlag: Basel, 1971.
[8] Katsuta Y, Yoshihara K, *Tet. Letters* **1994**, *35*(6), 905-908.
[9] Sedou M, Sugahara M, Uchiyama H, Hiraki K, Hamanaka T, Michinomae M,Yoshihara K, Kito Y, *J. Comp. Phys*. **1990**, *A166*, 769-773.
[10] Matsui S, Seidou M, Uchiyama I, Sekiya N, Hiraki K, Yoshihara K, Kito Y, *Biochim. Biophys. Acta* **1988**, *966*, 370-374.
[11] Vogt K, Kirschfeld K, *Naturwissenschaften* **1984**, *71*, 211-213.
[12] Ito M, Matsuoka N, Tsukida K, Seki T, *Chem. Pharm. Bull.* **1988**, *36*, 78-86.
[13] Ito M in *Chemistry and Biology of Synthetic Retinoids*; Dawson MI, Okamura WH; Eds. CRC Press: Boca Raton, 1990.
[14] Creemers AFL, Kiihne S, Bovee-Geurts PHM, De Grip WJ, Lugtenburg J, De Groot HJM, *Proc. Natl. Acad. Sci. U.S.A.* **2002**, *99*(14), 9101-9106.
[15] Palczewski K, Kumasaka T, Hori T, Behnke CA, Motoshima H, Fox BA, Le-Trong I, Teller DC, Okada T, Stenkamp RE, Yamamoto M, Miyano M, *Science* **2000**, *289,* 739-745.
[16] Creemers AFL, Bovee-Geurts PHM, De Grip WJ, Lugtenburg J, De Groot HJM, *Biochem.* **2004**, *43*, 16011-16018.
[17] Verdegem PJE, Bovee-Geurts PHM, De Grip WJ, Lugtenburg J, De Groot HJM, *Biochem.* **1999**, 38, 11316-11324.
[18] Verdegem PJE, Helme M, Lugtenburg J, De Groot HJM, *J. Am. Chem. Soc.* **1998**, *119*, 169-174.
[19] Spooner PJR, Sharpless JM, Verhoeven MA, Lugtenburg J, Gaubitz C, Watts A, *Biochem.* **2002**, *41*, 7549-7555.
[20] Feng X, Verdegem PJE, Lee YK, Sandström D, Edén M, Bovee-Geurts P, De Grip WJ, Lugtenburg J, De Groot HJM, Levitt MH, *J. Am. Chem. Soc.* **1997**, *119*, 6853-6857.
[21] Feng X, Verdegem PJE, Edén M, Sandström D, Lee YK, Bovee-Geurts PHM, de Grip WJ, Lugtenburg J, De Groot HJM, Levitt MH, *J. Biomol. NMR* **2000**, *16*, 1-8.
[22] Palings I, Pardoen JA, Van den Berg EMM, Winkel C, Lugtenburg J, Mathies RA, *Biochem.* **1987**, *26*, 2544-2556.
[23] Palings I, Van den Berg EMM, Lugtenburg J, Mathies RA, *Biochem.* **1989**, *28*, 1498-1507.
[24] Creemers AFL, Lugtenburg J, *J. Am. Chem. Soc.* **2002**, *124*, 6324-6334.
[25] Rüttimann A, Mayer H, *Helv. Chim. Acta* **1980**, *63*(6), 1456-1462.
[26] Mayer H, Santer J-M, *Helv. Chim. Acta* **1980**, *63*(6), 1467-1472.
[27] Brown HC, Chandrasekharan J, Ramachandran PV, *J. Am. Chem. Soc.* **1988**, *110*, 1539-1546.
[28] Liu RSH, Asato AE, Denny M, *J. Am. Chem. Soc.* **1977**, *99*(23), 8095-8097.
[29] Jansen FJHM, Lugtenburg J, *Eur. J. Org. Chem.* **2000**, 829-836.
[30] Kutney JP, Gunning PJ, Clewley RG, Somerville J, Rettig SJ, *Can. J. Chem*. **1992**, *70*, 2094-2114.
[31] Liu RSH, Asato AE, *Tetrahedron* **1984**, *40*(11), 1931-1969.
[32] Chen R-L, Liu RSH, *Tetrahedron* **1996**, *52*(23), 7809-7816.
[33] Schwieter U, Saucy G, Montavon M, Von Planta C, Rüegg R, Isler O, *Helv. Chim. Acta* **1962**, *XLV*(61-62), 517-561.
[34] Englert G, *Helv. Chim. Acta* **1975**, *58*(8), 2367-2390.
[35] Englert G in *Carotenoids. Volume 1B: Spectroscopy*; Britton G, Liaaen-Jensen S, Pfander H; Eds. Birkhäuser Verlag: Basel, 1995, 147-260.
[36] Jansen FJHM, Lugtenburg J in *Carotenoids*, *Volume 2: Synthesis*; Britton G, Liaaen-Jensen S, Pfander H; Eds. Birkhäuser Verlag: Basel, 1996, 233-258.
[37] McMurry JE, Silvestri M, *J. Org. Chem.* **1975**, *40*(18), 2687-2688.

[38] McMurry JE, *Chem. Rev.* **1989**, *89*, 1513-1524.
[39] Ephritikhine M, *Chem. Comm.* **1998**, 2549-2554.
[40] Daik R, Feast WJ, Batsanov AS, Howard JAK, *New J. Chem.* **1998**, 1047-1049.
[41] Straub O in *Carotenoids*; Isler O; Ed. Birkhäuser Verlag: Basel, 1971, 772-850.
[42] Li W-DZ, Li Y, Li Y, *Tetrahedron Letters* **1999**, *40*, 965-968.
[43] Gauthier S, Sancéau J-Y, Mailhot J, Caron B, Cloutier J, *Tetrahedron* **2000**, *56*, 703-709.
[44] Paust J in *Carotenoids, Volume 2: Synthesis*; Britton G, Liaaen-Jensen S, Pfander H; Eds. Birkhäuser Verlag: Basel, 1996, 267.
[45] Entschell R, Karrer P, *Helv. Chim. Acta* **1958**, *41*, 402.
[46] Liaaen-Jensen S, *Acta Chem. Scand.* **1965**, *19*, 1166.
[47] Paust J in *Carotenoids, Volume 2: Synthesis*; Britton G, Liaaen-Jensen S, Pfander H; Eds. Birkhäuser Verlag: Basel, 1996, 268.
[48] Bernard K, Müller RK, Spruijtenburg R, Roche, US Pat. 4585 885 (**1986**)
[49] Moldt P, Neurosearch, US Pat. 5166 441 (**1990**) and 5225 604 (**1993**)

CHAPTER 6

CONCLUSIONS AND PROSPECTS

6.1 α-CRUSTACYANIN

α-Crustacyanin is the carotenoprotein complex that is responsible for the blue color of the living lobster (λ_{max} = 632 nm). When the lobster is cooked the denaturation of this protein complex leads to the release of free astaxanthin that gives a deep red color (λ_{max} = 472 nm). α-Crustacyanin can be irreversibly dissociated in eight β-crustacyanin units (λ_{max} = 586 nm).

Recently the X-ray structure of β-crustacyanin has been published at 3.2 Å resolution.[1] The X-ray structure reveals that two astaxanthin units are situated in parallel planes in β-crustacyanin. They cross off-center at a distance of 7Å with an angle of 120° of the axes of the astaxanthin units. In contrast to free astaxanthin, which occurs in a non-planar 6s,6′s-*cis* conformation, astaxanthin in β-crustacyanin has a planar 6s,6′s-*trans* conformation. The 3,3′ hydroxyl and 4,4′ carbonyl groups are positioned such that they can form hydrogen bonds with nearby histidines.

α-Crustacyanin can be irreversibly dissociated in eight β-crustacyanin units. In β-crustacyanin the bathochromic shift is two-thirds of the value found for α-crustacyanin. The simplest assumption is that the structure of α-crustacyanin corresponds to the known structure of β-crustacyanin and that the bathochromic shift from 586 nm to 632 nm should be explained by the aggregation of the eight β-crustacyanin dimers to form α-crustacyanin. The bathochromic shift of astaxanthin in β- and α-crustacyanin compared to free astaxanthin can be due to (i) astaxanthin-protein interactions in the electronic ground state or (ii) interactions between the excited singlet state of astaxanthin and the protein or (iii) exciton interactions between the two excited states or (iv) combinations of these interactions.

Earlier investigations with solid-state ^{13}C NMR spectroscopy on α-crustacyanin with ^{13}C-enriched astaxanthin have given an indication that double protonation of the 4,4′ carbonyl groups of astaxanthin in the ground state, caused by the protein, might be the basis of the bathochromic shift. Based on the protonation hypothesis the positive charge should be delocalized mostly on the sp^2 carbon atoms near the six-membered rings of astaxanthin. The X-ray structure shows that presumably no acidic sites are present near the 4,4′ carbonyl groups of astaxanthin in β-crustacyanin, which makes the protonation model unlikely.

In this thesis the solid state ^{13}C NMR spectroscopy of [6,6′,7,7′]-$^{13}C_4$ and [8,8′,9,9′,10,10′,11,11′,19,19′]-$^{13}C_{10}$ α-crustacyanin as an essential complement to the earlier studies is described. The conclusion of the present work is that there is very little electronic perturbation of astaxanthin by the protein in the electronic ground state. This conclusion is nicely supported by Kildahl-Andersen et al.[2] who reported a ^{13}C NMR study of protonated canthaxanthins. In their system large changes in chemical shifts of 6,6′,8,8′ are clearly present when canthaxanthin is protonated at both carbonyl groups. Since this is not observed for astaxanthin in α-crustacyanin, it is now clear from our study that protonation of the 4,4′ carbonyl groups does not form an important contribution to the bathochromic shift of α- or β-crustacyanin.

The resonance Raman study of [8,8',9,9',10,10',11,11',19,19']-$^{13}C_{10}$ α-crustacyanin and the corresponding free astaxanthin has lead to the conclusion that the conjugation in α-crustacyanin should be more extended than in free astaxanthin, since in α-crustacyanin also vibrations of the conjugated part next to the central part contribute, which is not the case in any other carotenoid. This is can be explained by the extended conjugation of the 6s,6's-*trans* conformation of astaxanthin in β-crustacyanin.

Finally, time-dependent density functional theory has shown that hydrogen bonds to the nearby histidines and the planar 6s,6's-*trans* configuration that gives astaxanthin in β-crustacyanin its more extended conjugation are responsible for about 30% of the bathochromic shift of β-crustacyanin. The largest contribution (~70%) is the exciton splitting by the transition dipole-dipole interaction. The geometry of the pair of astaxanthin units in β-crustacyanin is in agreement with the strong negative exciton splitting in the CD-spectrum of β-crustacyanin. Compared to β-crustacyanin, the bathochromic shift of α-crustacyanin increases by 50%. In addition, the CD-spectrum of α-crustacyanin is more symmetric and shifts to longer wavelength.[3] This means that stacking of the eight β-crustacyanin units in α-crustacyanin gives additional positive exciton interactions.

Using the combination of techniques as described above, the basis for the bathochromic shift of astaxanthin in α-crustacyanin and β-crustacyanin has now been established.

6.2 SYNTHESIS OF ^{13}C-LABELED CAROTENOIDS

Several synthons are now available for the synthesis of compounds with site-directed ^{13}C labeling at any postion or combination of positions. Recently, Creemers et al.[4] have developed more efficient schemes for the synthesis of carotenoids and retinoids. The syntheses are based on a modular strategy, to efficiently introduce ^{13}C labels at the desired positions in carotenoids and retinoids. The presented synthetic routes were successfully applied for the synthesis of [8,8',9,9',10,10',11,11',19,19']-$^{13}C_{10}$ astaxanthin and [6,6',7,7']-$^{13}C_4$ astaxanthin.

A synthetic scheme was developed for the preparation of 2,7-dimethylocta-2,4,6-triene-1,8-dial, the C_{10}-dialdehyde that is the common synthetic building block for the central part of all carotenoids, with selective or uniform ^{13}C enrichment. Using the modular $C_{15} + C_{10} + C_{15}$ strategy, the presented synthetic scheme for the synthesis of the C_{10}-dialdehyde allows a quick and easy preparation of any carotenoid with symmetrical ^{13}C labeling in the central part.

Complementary to the development of a convergent synthesis for the labeling of the central part of carotenoids, methods were developed to efficiently introduce functionalities in the six-membered ring. This is essential for the synthesis of functionalised carotenoids like zeaxanthin and lutein, which are abundant in our food and are involved, for example in prevention of cancer, cardiovascular disease and age-related macular degeneration and cataract. With prevention being the only way to reduce health care costs in an aging population, the importance

of the chemistry and chemical technology behind such preventive nutrients is difficult to underestimate.

Based on our modular strategy to prepare ^{13}C isotopomers of all-*E* carotenoids, we investigated modification of the α-cyclocitral module for the synthesis of ^{13}C-labeled carotenoids with functionalities in the six-membered ring. An efficient strategy has been developed for the preparation of ^{13}C-enriched 3,4-didehydro-, 3-hydroxy- and 4-hydroxy cyclocitral. The functionalized cyclocitral modules were converted into the corresponding C_{15}- and C_{20}-synthons. Via the commonly used $C_{15} + C_{10} + C_{15}$ strategy the corresponding functionalized carotenoids can be prepared, with >99% ^{13}C enrichment at any position or combination of positions.

To obtain more flexibility for the specific introduction of ^{13}C-labels, we explored the $C_{20} + C_{20}$ McMurry-dimerization of retinal-derivatives to obtain the corresponding symmetrical carotenoids. This is complementary to the commonly used $C_{15} + C_{10} + C_{15}$ strategy, and can be the preferred method for the introduction of ^{13}C labels at specific positions in symmetrical carotenoids.

So far the McMurry-dimerization was mainly used for the synthesis of β-carotene, but recently it has also been used for the coupling of aldehydes with different functional groups.[5-7] In Chapter 5 is described the yet unpublished synthesis of zeaxanthin from 3-hydroxyretinal and 3,4,3′,4′-tetradehydro-β,β-carotene from 3,4-didehydroretinal, indicating the potential of this method for the synthesis of functionalized carotenoids.

In conclusion, more efficient methods for the synthesis of carotenoids with >99% ^{13}C enrichment at any position or combination of positions have been developed, both for ^{13}C labels in the central part of carotenoids as in the end-ring. The synthesis of different ^{13}C-labeled carotenoids via the same general scheme is now feasible, leading to reduction of labour and costs of ^{13}C-labeled starting materials. Our advances in the synthesis of ^{13}C-labeled carotenoids expand the possibilities to study the role of carotenoids in various essential aspects of the life processes in man, animals and plants.

6.3 PROSPECTS

6.3.1 The Study of Photochemical Processes in Nature

The research strategy discussed in this thesis for the elucidation of the factors that contribute to the bathochromic shift of α-crustacyanin can provide a general method for the study of chromophore-protein interactions. Using a combination of isotope-sensitive techniques and isotope labeling, can give information of chromophores in a natural system at the atomic level. However, most available analytical techniques only give structural information on the electronic ground-state of a system. Information of the electronically excited-state can be obtained from theoretical computations, although only for relatively small systems.

Just as we have found for the bathochromic shift of astaxanthin in the active site of β-crustacyanin, information on the structural properties of the excited state may be essential to understand photochemical processes. An example is the photochemistry of rhodopsin and isorhodopsin, retinal-containing proteins essential for vision. Very recently Matthies and co-workers have described femtosecond time resolved stimulated Raman spectroscopy as the first experimental method that has given time resolved vibrational information of electronically excited states.[8-10] Application of this technique after excitation with a femtosecond light-pulse will give time resolved vibrational information of electronically excited state on a femtosecond time-scale. Recently, Touw et al. have reported ab initio modelling of the spatial, electronic and vibrational structure of Schiff base models for visual photoreceptors. This method allows theoretical calculations of the vibrational frequencies, supplementary to the experimental results obtained by Raman spectroscopy.[11] In principle, the same method can be extended for ab initio calculation of the intensities of the vibrational modes, and vibrational analysis of the excited states formed during photochemical processes. For interpretation of a complete vibrational analysis a full set of ^{13}C-enriched isotopomers is necessary.

Combining these analytical and theoretical techniques gives structural information of both the ground state and electronically excited-states during chemical photochemical processes. This way, in the near future the photochemistry of rhodopsin and isorhodopsin can be unravelled in structural detail at the atomic level. There will be in principle no limitation to extend this approach to other photochemical processes.

6.3.2 The Use of ^{13}C-Labeled Carotenoids in Food and Health Studies

Carotenoids in the diet of humans show beneficial health effects, playing a role in prevention of cancer, cardiovascular diseases and eye degradation. Man and animals are unable to synthesize carotenoids *de novo*, and depend on food for their required carotenoids. Up to about 100 different carotenoids are present in a varied human diet, and, of these around 20 can be detected in human blood and tissue, e.g. α-carotene, β-carotene, lycopene, zeaxanthin, canthaxanthin, astaxanthin and lutein.[12] Based on the difference in mass between natural and ^{13}C-enriched compounds, a LC-MS method has recently been described that allows study of all aspects of the uptake of [12,12′,13,13′,14,14′,15,15′,19,19′,20,20′] $^{13}C_{10}$ β-carotene from food and the metabolism in living persons at the physiological level in real time.[13,14] This study shows that the conversion of β-carotene to vitamin A is more efficient than formerly assumed. Expanding this method to all carotenoids that are available from food will give essential information about the role of the various carotenoids in humans and animals.

Via resonance Raman studies the food-derived carotenoid levels in single living lymphocytes have been quantified.[15] It has been found that the carotenoid concentration in lymphocyte gall bodies is lower in older persons. The carotenoid levels from lung cancer patients are even lower than those in healthy elderly people. These studies have been carried out with carotenoids with natural abundant isotopes. However, all nutritional important carotenoids show within

experimental error the same resonance Raman spectrum. Carotenoids with 99% $^{13}C_{10}$ labeling in the central part show resonance Raman spectra which are clearly distinct from unlabeled carotenoids. Adding one of the nutritionally important carotenoids with central 99% $^{13}C_{10}$ labeling at the 1%-10% level of the normal physiological amount will allow, via a combined study with LC-MS and resonance Raman spectroscopy, a quantitative study of the dynamics of carotenoid uptake from food, its metabolism and dynamic uptake in various living cells. Performing these studies on healthy and diseased persons of various ages will allow more insight in the health effects of carotenoids in humans.This approach will allow the determination of the contribution of specific carotenoids in nutrition on maintaining the health of individuals and possible prevention of age related diseases and improvement of health by addition of carotenoids to the diet.

In this thesis general schemes are described that give access to ^{13}C-labeled carotenoids. The central part of carotenoids can now be labeled up to $^{13}C_{10}$. Besided ^{13}C-enriched β-carotene, now also zeaxanthin, canthaxanthin and astaxanthin can be prepared with ^{13}C labels at any position or combination of positions. All other nutritionally important carotenoids are accessible in less steps and reasonable yield by combining general synthetic methods with new conversions developed by Khachik.[16-19] ^{13}C isotopomers of carotenoids can be used for further exploration of carotenoproteins with isotope sensitive, non-invasive techniques, as has been discussed for the study of bathochromic shift of α- and β-crustacyanin in this thesis. Specific labeling of nutritionally important carotenoids will be essential to quantitatively elucidate the role of each carotenoid in maintaining health of man and animals, prevention of age-related diseases and possible improvement of health by medical therapy with carotenoids.

REFERENCES

[1] Cianci M, Rizkallah PJ, Olczak A, Raftery J, Chayen NE, Zagalsky PF, Helliwell JR, *Proc. Natl. Acad. Sci. U.S.A.* **2002**, *99(15)*, 9795-9800.
[2] Kihldahl-Andersen G, Lutnaes BF, Liaaen-Jensen S, *Org. Biomol. Chem.* **2004**, *2*, 489-498.
[3] Buchwald M, Jencks WP, *Biochemistry* **1968**, *7*, 844-859.
[4] Creemers AFL, Lugtenburg J, *J. Am. Chem. Soc.* **2002**, *124*, 6324-6334.
[5] McMurry JE, *Chem. Rev.* **1989**, *89*, 1513-1524.
[6] Li W-DZ, Li Y, Li Y, *Tetrahedron Letters* **1999**, *40*, 965-968.
[7] Gauthier S, Sancéau J-Y, Mailhot J, Caron B, Cloutier J, *Tetrahedron* **2000**, *56*, 703-709.
[8] Kukura P, McCamant DW, Davis PH, Mathies RA, *Chem. Phys Lett.* **2003**, *382*, 81-86.
[9] McCamant DW, Kukura P, Mathies RA, *J. Phys. Chem. A* **2003**, *107*, 8208-8214.
[10] McCamant DW, Kukura P, Mathies RA, *Appl. Spectroscopy* **2003**, *57*(11), 1317-1323.
[11] Touw SIE, de Groot HJM, Buda F, *J. Phys. Chem. B* **2004**, *108*, 13560-13572.
[12] Britton G, Liaaen-Jensen S, Pfander H in *Carotenoids, Volume 3: Biosynthesis and Metabolism*; Britton G, Liaaen-Jensen S, Pfander H; Eds. Birkhäuser Verlag: Basel, 1998.
[13] Wang Y, Xu X, Van Lieshout M, West CE, Lugtenburg J, Verhoeven MA, Creemers AFL, Muhilal, VanBreemen RB, *Anal. Chem.* **2000**, *72*, 4999-5003.
[14] Van Lieshout, West CE, Muhilal, Permaeshi D, Wang Y, Xu X, VanBreemen RB, Creemers AFL, Verhoeven MA, Lugtenburg J, *Am. J. Clin. Nutr.* **2001**, *73*, 949-958.
[15] Ramanauskaite RB, Segers Nolten IGMJ, De Grauw KJ, Sijtsema MN, Van der Maas L, Greve J, Otto C, Figdor CG, *Pure Appl. Chem.* **1997**, *69*(10), 2131-2134.
[16] Liaaen-Jensen S, *Acta Chem. Scand.* **1965**, *19*, 1166.
[17] Paust J in *Carotenoids, Volume 2:* Synthesis; Britton G, Liaaen-Jensen S, Pfander H; Eds. Birkhäuser Verlag: Basel, 1996, 267.
[18] Entschell R, Karrer P, *Helv. Chim. Acta* **1958**, *41*, 402.
[19] Khachik F, *J. Nat. Prod.* **2003**, *66*, 67-72.

SUMMARY

Carotenoids constitute a class of natural colorants, ranging from pale yellow to deep purple, with important biological functions. Besides being natural colorants, carotenoids have an essential function in plants by protecting the photosynthetic reaction centers against formation of destructive singlet oxygen. In humans carotenoids are converted to vitamin A, which is vital for vision. Recent research suggests that carotenoids reduce the risk of age-related macular degradation and cataract, the leading cause of blindness in the western world. Carotenoids in the human diet have a beneficial health effect, playing a role in the prevention of cardiovascular disease and cancer.

In nature, many carotenoids are bound to proteins, to form carotenoproteins. Often this binding to proteins is accompanied by a remarkable change in color. α-Crustacyanin is the carotenoprotein responsible for the dark blue color of lobsters. Upon heat treatment the dark blue protein denatures and the red carotenoid astaxanthin is released. In order to resolve the molecular basis of the coloration mechanism of α-crustacyanin we prepared >99% ^{13}C-enriched [6,6′,7,7′]-$^{13}C_4$ astaxanthin and [8,8′,9,9′,10,10′,11,11′,19,19′]-$^{13}C_{10}$ astaxanthin using a modular synthetic strategy, based on the C_{15}+C_{10}+C_{15} scheme commonly used for synthesis of carotenoids. The synthesis and ^{1}H NMR and ^{13}C NMR characterization of $^{13}C_4$- and $^{13}C_{10}$- astaxanthin are described in **Chapter 2**.

The ^{13}C-labeled astaxanthins were reconstituted with α-crustacyanin and the ^{13}C-enriched carotenoproteins were analyzed with solid-state ^{13}C NMR and resonance Raman spectroscopy. The experimental data were complemented with time-dependent density functional theory calculations on several models based on the structural information available for β-crustacyanin. The data rule out major changes and strong polarization effects in the ground-state electron density of astaxanthin upon binding to the protein. Conformational changes in the chromophore and hydrogen-bond interactions between the astaxanthin and the protein can account only for about one-third of the total bathochromic shift in α-crustacyanin. The exciton splitting due to the proximity of the astaxanthin chromophores is found to be large, supporting early suggestions that aggregation effects in the protein represent the primary source of the color change. This study of the bathochromic shift in α-crustacyanin is described in **Chapter 3**.

Information on which carotenoids are present in the human body, and in what amounts, is necessary to study the health effects of carotenoids. Resonance Raman spectroscopy can be used to determine the amounts of carotenoids in living human tissue and cells. When ^{13}C-labeled carotenoids are added to the food of individuals, resonance Raman spectroscopy

can be used to distinguish between different carotenoids and determine their presence and amounts in humans in vivo in a non-invasive way.

Recently a method was published to quantify, without perturbation, the nutritional status of β-carotene at the physiological level in individuals, via addition of $^{13}C_{10}$ β-carotene to their food. Using mass spectrometry the levels of the isotopically labeled $^{13}C_{10}$ β-carotene and its metabolites could be monitored. Extending the use of mass spectrometry and resonance Raman spectroscopy methods to other carotenoids that are present in our diet is now of utmost importance to be able to study the presence, quantity, bioconversion and bioavailability of carotenoids in individuals. Therefore, there is great need for ^{13}C-labeled carotenoids, and for an efficient synthetic strategy applicable to a range of carotenoids.

Chapter 4 describes an efficient synthetic scheme for ^{13}C-enrichment in the central part of carotenoids. Starting from acetic acid and methyl iodide ^{13}C-enriched C_{10}-dialdehyde can be prepared up to the $^{13}C_{10}$ level. The C_{10}-dialdehyde is a suitable building block for the central part in the synthesis of carotenoids via the $C_{15}+C_{10}+C_{15}$ scheme. Using a modular total organic synthetic strategy, now ^{13}C labels can be introduced at any position or combination of positions. By varying the end groups, a library of multifold ^{13}C-labeled carotenoids can easily be obtained.

In **Chapter 5** a modular synthetic scheme is described for the synthesis of ^{13}C-labeled naturally occurring visual pigment chromophores: 3,4-didehydroretinal, 3-hydroxyretinal and 4-hydroxyretinal. These compounds can now be made with >99% ^{13}C enrichment at any position or combination of positions. We used the common $C_{10}+C_5+C_5$ scheme for the synthesis of retinals, and by making variations in the C_{10} part we can now prepare the desired retinal derivatives with selective or uniform ^{13}C enrichment. The developed scheme also allows for the synthesis of ^{13}C-labeled carotenoids with functionalized end groups via the common $C_{15}+C_{10}+C_{15}$ modular strategy. The alternative $C_{20}+C_{20}$ McMurry reaction was successfully applied to obtain zeaxanthin directly by dimerization of 3-hydroxyretinal, and 3,4,3′,4′-didehydro-β-carotene from 3,4-didehydroretinal, showing potential as a complementary strategy for efficient synthesis of symmetric ^{13}C-labeled carotenoids with functional groups in the six-membered rings.

The impact of the work described in this thesis and prospects for further research are discussed in **Chapter 6**. The approach that was used for the study of the bathochromic shift of α-crustacyanin can be applied to other natural systems. Combining this strategy with available analytical and theoretical techniques that give structural information of both the ground state and electronically excited-state can be used to study photochemical processes at the atomic level. For these studies the access of various isotopomers is essential. These isotope-labeled systems are only accessible via total organic synthetic schemes.

The synthetic methods described in this thesis for preparation of isotopomers of carotenoids allow access to all nutritionally important carotenoids, which is a prerequisite for further exploration of the health effects of carotenoids with isotope-sensitive, non-invasive analytical techniques.

SAMENVATTING

Carotenoïden zijn een klasse van natuurlijke kleurstoffen, variërend van licht geel tot diep paars, met belangrijke biologische functies. Zo beschermen carotenoïden de fotosynthese Reactie Centra tegen de vorming van het schadelijke singlet zuurstof. In de mens worden carotenoïden omgezet tot vitamine A, wat essentieel is voor het zien. Verder blijkt uit recent onderzoek dat carotenoïden waarschijnlijk het risico verkleinen op cataract (staar) en macula degeneratie, de belangrijkste oorzaken van blindheid in de Westerse wereld. Daarnaast spelen carotenoïden in de voeding van mensen een rol in de preventie van kanker en hart- en vaatziekten.

In de natuur zijn carotenoïden vaak gebonden aan eiwitten, waarbij carotenoproteinen worden gevormd. Vaak gaat deze binding aan een eiwit gepaard met een opmerkelijke kleurverandering. α-Crustacyanine is het carotenoprotein dat verantwoordelijk is voor de donkerblauwe kleur van de schaal van de levende kreeft. Tijdens het koken van de kreeft denatureert het eiwit en het rode carotenoïde astaxanthine komt vrij, wat de kreeft de karakteristieke rode kleur geeft. Om het moleculaire mechanisme van de kleurverandering van de kreeft te doorgronden, zijn >99% ^{13}C-verrijkt [6,6′,7,7′]-$^{13}C_4$ astaxanthine en [8,8′,9,9′,10,10,11,11′,19,19′]-$^{13}C_{10}$ astaxanthine gesynthetiseerd via een modulaire strategie, gebaseerd op het C_{15}+C_{10}+C_{15} schema dat algemeen wordt gebruikt voor de synthese van C_{40}-carotenoiden. De synthese en ^{1}H NMR en ^{13}C NMR karakterisatie van $^{13}C_4$ astaxanthine en $^{13}C_{10}$ astaxanthine is beschreven in **Hoofdstuk 2**.

De ^{13}C-gelabelde astaxanthines zijn uitgewisseld tegen natuurlijk astaxanthine in α-crustacyanine en de verkregen ^{13}C-verrijkte carotenoproteinen zijn vervolgens geanalyseerd met vaste-stof ^{13}C NMR en resonantie Raman spectroscopie. De experimenteel verkregen gegevens zijn aangevuld met theoretische berekeningen van verschillende modellen die gebaseerd zijn op de structurele informatie van β-crustacyanine. De verkregen gegevens sluiten de eerdere hypothese uit dat een sterk ladingseffect optreedt bij binding van astaxanthine aan het eiwit. Verandering van conformatie van de chromofoor en waterstofbrug-vorming tussen astaxanthine en het eiwit verklaren ongeveer een derde van de totale kleurverandering. Een grote exciton splitsing als gevolg van de nabijheid van de astaxanthines in het eiwit treedt op, wat eerdere aanwijzingen bevestigt dat aggregatie effecten in het eiwit de voornaamste oorzaak zijn van de kleurverschuiving. Het onderzoek aan de kleurverschuiving van α-crustacyanine is beschreven in **Hoofdstuk 3**.

Meer gegevens over het gehalte aan verschillende carotenoïden in het menselijk lichaam en de organen tot op cellulair niveau is van groot belang om de gezondheidseffecten van carotenoïden te onderzoeken. Resonantie Raman spectroscopie kan worden gebruikt om het gehalte

aan carotenoïden te bepalen in cellen of in levend menselijk weefsel, bijvoorbeeld van de huid of het netvlies. Wanneer ^{13}C-gelabelde carotenoïden worden toegevoegd aan de voeding van personen, kan met resonantie Raman spectroscopie onderscheid worden gemaakt tussen verschillende carotenoïden, en het gehalte hiervan worden bepaald op niet-invasieve wijze. Recent is een methode gepubliceerd waarmee het metabolisme van β-caroteen in personen kan worden gevolgd tot op fysiologisch niveau, door het toevoegen van $^{13}C_{10}$ β-caroteen aan hun voeding. Via massa spectrometrie kan het gehalte aan isotoop-verrijkt $^{13}C_{10}$ β-caroteen en de daaruit gevormde metabolieten worden bepaald. Toepassing van massa spectrometrie en resonantie Raman spectroscopie voor onderzoek aan andere carotenoïden in ons dagelijks voedsel is van groot belang om de aanwezigheid, het gehalte, de bioconversie en de biobeschikbaarheid van carotenoïden in het menselijk lichaam te bepalen. Hiervoor is dringend behoefte aan ^{13}C-gelabelde carotenoïden, en efficiënte synthetische methoden voor ^{13}C labeling van een scala aan carotenoïden.

Hoofdstuk 4 beschrijft een efficiënt synthetisch schema voor ^{13}C verrijking van het centrale deel van carotenoïden. Het C_{10}-dialdehyde dat wordt gebruikt als bouwsteen voor het centrale deel van carotenoïden via het $C_{15}+C_{10}+C_{15}$ schema kan, uitgaande van ^{13}C-gelabeld azijnzuur en ^{13}C-gelabeld methyl jodide, worden verrijkt tot 10 ^{13}C labels. Gebruik makend van een modulaire organische synthese kunnen ^{13}C labels specifiek worden geïntroduceerd op iedere positie en combinatie van posities. Door variatie van de C_{15} eindgroepen kan een scala aan meervoudig ^{13}C-gelabelde carotenoïden worden verkregen.

In **Hoofdstuk 5** is een modulair synthetisch schema beschreven voor de synthese van ^{13}C-gelabelde natuurlijk voorkomende visuele chromoforen; 3,4-didehydroretinal, 3-hydroxyretinal en 4-hydroxyretinal. Deze verbindingen kunnen nu worden gemaakt met >99% ^{13}C verrijking op iedere positie of combinatie van posities. Het algemene $C_{10}+C_5+C_5$ schema is gebruikt voor de synthese van deze retinallen, en door variaties in de C_{10} eindgroep kunnen nu de gewenste retinal derivaten worden gesynthetiseerd met selectieve of uniforme ^{13}C verrijking. Het ontwikkelde schema kan ook worden gebruikt voor de synthese van ^{13}C-gelabelde carotenoïden met functionele groepen aan de ring via de $C_{15}+C_{10}+C_{15}$ strategie. De alternatieve $C_{20}+C_{20}$ McMurry reactie was succesvol voor de synthese van zeaxanthine en 3,3',4,4'-didehydrocaroteen via dimerizatie van respectievelijk 3-hydroxyretinal en 3,4-dehydroretinal. Dit geeft aan dat deze methode kan dienen als alternatieve strategie voor de synthese van ^{13}C-gelabelde carotenoïden met functionele groepen in de 6-ring.

Het werk beschreven in dit proefschrift wordt in een breder kader geplaatst in **Hoofdstuk 6**, waar tevens wordt ingegaan op de mogelijkheden die dit werk biedt voor toekomstig onderzoek. De aanpak die is gebruikt voor het onderzoek naar de kleurverschuiving van α-crustacyanine kan ook worden toegepast op andere natuurlijke systemen. Een combinatie van deze aanpak met beschikbare analytische en theoretische technieken die inzicht geven in de structuur van zowel de grondtoestand als de aangeslagen toestand kan worden gebruikt om fotochemische processen te onderzoeken op atomair niveau. Voor dit onderzoek is de beschikbaarheid van

diverse isotopomeren essentieel. De methoden beschreven in dit proefschrift maken de synthese van isotopomeren van alle carotenoïden in onze voeding mogelijk, wat van groot nut is voor verder onderzoek naar de gezondheidseffecten van carotenoïden met isotoopgevoelige, niet-invasieve analysetechnieken.

CURRICULUM VITAE

Na afronding van het VWO aan de Scholengemeenschap Lelystad (SGL) ben ik in september 1993 begonnen met de studie Scheikunde aan de Universiteit Utrecht. Het propedeuse diploma werd behaald in augustus 1994 (*cum laude*). Na een stage Milieukunde heb ik van juli 1996 tot december 1996 aan de Universiteit Stockholm gewerkt aan de synthese van koolhydraten die mogelijk een rol spelen bij de activering van de insulineproductie in het menselijk lichaam. Het afstudeeronderzoek werd uitgevoerd bij de vakgroep Bio-Organische Chemie van prof. dr. J.F.G. Vliegenthart en prof. dr. J.P. Kamerling. Onder begeleiding van dr. C.T.M. Fransen werd structuuranalyse verricht aan melksuikers die van belang zijn voor een goede balans van de darmflora. Het doctoraaldiploma werd behaald in 1998, waarna ik aan de Universiteit Leiden onder begeleiding van prof. dr. J. Lugtenburg en prof. dr. H.J.M. de Groot ben begonnen als assistent-in-opleiding aan het promotieonderzoek zoals beschreven in dit proefschrift. Poster-presentaties van de resultaten van dit onderzoek zijn verzorgd tijdens de *12th International Carotenoid Symposium* te Cairns (1999) en enkele SON-bijeenkomsten in Lunteren. Daarnaast zijn de resultaten gepresenteerd in voordrachten bij het HRSMC Symposium 2001 te Amsterdam, het *13th International Carotenoid Symposium* te Hawaï (2002) en bij *This Weeks Discoveries* te Leiden (2004).

Van februari 2003 tot maart 2004 ben ik werkzaam geweest als consultant bij de afdeling Milieu van het Nederlands Normalisatie Instituut (NEN) te Delft. Sinds maart 2004 werk ik als post-doc aan de Universiteit Leiden in de vakgroep Industriële Fermentatieve Chemie van prof. dr. ir. A.P.G. Kieboom aan de cross-linking van melkeiwitten via enzymatische oxidatie van koolhydraten.

LIST OF PUBLICATIONS

α-D-Glc*p*-(1↔1)-β-D-Gal*p*-containing oligosaccharides, novel products from lactose by the action of β-galactosidase

C.T.M. Fransen, K.M.J. van Laere, A.A.C. van Wijk, L.P. Brull, M. Dignum, J.E. Thomas-Oates, J. Haverkamp, H.A. Schols, A.G.J. Voragen, J.P. Kamerling, J.F.G. Vliegenthart

Carbohydrate Research, 314(1-2), 101-114 (1998)

Synthesis of ^{13}C-labeled carotenoids and retinoids

J. Lugtenburg, A.F.L. Creemers, M.A. Verhoeven, A.A.C. van Wijk, P.J.E. Verdegem, M.C.F. Monnee, F.J.H.M. Jansen

Pure and Applied Chemistry, 71(12), 2245-2251 (1999)

Synthetic scheme for the preparation of ^{13}C-labeled 2,7-dimethylocta-2,4,6-triene-1,8-dial, the central part of carotenoids

A.A.C. van Wijk, J. Lugtenburg

European Journal of Organic Chemistry, 24, 4217-4224 (2002)

Synthetic scheme for the preparation of ^{13}C-labeled 3,4-didehydro-retinal, 3-hydroxyretinal and 4-hydroxyretinal up to uniform ^{13}C-enrichment

A.A.C. van Wijk, M.B. van de Weerd, J. Lugtenburg

European Journal of Organic Chemistry, 5, 863-868 (2003)

Spectroscopy and quantum chemical modelling reveal a predominant contribution of excitonic interactions to the bathochromic shift in α-crustacyanin, the blue carotenoid pigment in the carapace of the lobster *Homarus Gammarus*

A.A.C. van Wijk, A. Spaans, N. Uzunbajakava, C. Otto, H.J.M. de Groot, J. Lugtenburg, F. Buda

Journal of the American Chemical Society, 127, 1438-1445 (2005)

NAWOORD

Dit proefschrift betekent de afronding van mijn promotieonderzoek, en graag wil ik dit afsluiten met het noemen van diegenen die een belangrijke bijdrage hebben geleverd bij het werk. Bij de uiteindelijke oplossing van de kleurverandering van de kreeft hebben vooral Franco Buda, maar ook Cees Otto en Natallia Uzunbajakava een belangrijke bijdrage geleverd. Johan Hollander, Kees Erkelens en Fons Lefeber ben ik erkentelijk voor hun hulp bij het opnemen en uitwerken van de vloeistof en vaste-stof NMR spectra.

Bij het synthetisch werk hebben Arnold Spaans, Michiel vd Weerd en Poerya Partovi tijdens hun stage nuttig werk geleverd, waarvan een groot deel uiteindelijk ook in dit proefschrift is beschreven. Naast de extra hulp die jullie gaven bij het 'koken en braden', heb ik ook veel plezier beleefd aan en geleerd van jullie stages.

Dan wil ik natuurlijk de collega's noemen die de sfeer bij het werk hebben verhoogd, altijd beschikbaar waren voor nuttige discussies of een luisterend oor wanneer zich problemen voordeden. In dit geval zijn het letterlijk te veel mensen om op te noemen, maar Alain en Els, Robin, Michiel, Rob, Richard, Niels en Sylvia mogen hier niet onvermeld blijven als collega's waar ik ook buiten het werk zeer plezierige avonden heb doorgebracht.

Een bijzondere vermelding verdienen Arjan en Ineke, waar ik altijd lief en leed mee kon delen, en die zorgden voor de welkome afleiding bij het kolommen en de afwas.

Tot slot wil ik Kees en Petra bedanken voor de steun, en jullie begrip voor de soms lastige situaties die het promotieonderzoek met zich meebracht. De mogelijkheden en ruimte die jullie mij hebben gegeven hebben er voor een belangrijk deel aan bijgedragen dat ik dit proefschrift en de bijbehorende promotie heb kunnen voltooien.